EVOLUTIONARY CONSERVATION OF GENES INVOLVED IN SECONDARY WALL BIOSYNTHESIS

By

MARZIYEH HAGHIGHAT
(Under the Direction of Zheng-Hua Ye)

ABSTARCT

Vascular plants appeared on land about 430 million years ago; one of the pivotal steps for the evolution of vascular plants was the acquisition of the mechanisms for making secondary walls-reinforced xylem conducting tissues. Dissecting the mechanisms controlling secondary wall biosynthesis may not only provide molecular tools for genetic modification of secondary wall-enriched biomass but also have implications in better understanding the evolution of vascular plants. In my dissertation, I used *Selaginella moellendorffii*, a model seedless vascular plant, and *Physcomitrella patens*, a model non-vascular plant, to investigate genes involved in secondary wall biosynthesis. It was found that *S. moellendorffii* xylan, one of the major secondary wall components, is substituted with methylated glucuronic acid, and xylans from both *S. moellendorffii* and *P. patens* are acetylated. Because gymnosperm xylans are non-acetylated, the finding that xylans from *S. moellendorffii* and *P. patens* are acetylated implies that the ability to acetylate xylans was acquired when land plants evolved, but this ability may be lost in the lineage of gymnosperms. There exist one DUF579 gene in *P. patens* and two DUF579 genes in *S. moellendorffii*, but only *S. moellendorffii* gene was found to encode a methyltransferase catalyzing

xylan methylation, indicating that vascular plants recruited ancestral DUF579 genes as methyltransferases for xylan methylation. Complementation analysis of GT43 genes from *P. patens* and *S. moellendorffii* has revealed that the two GT43 genes in *S. moellendorffii*, *SmGT43A* and *SmGT43B*, are functional orthologs of Arabidopsis IRX9 and IRX14, respectively. This finding indicates that the involvement of two functionally non-redundant groups of GT43 proteins in xylan biosynthesis is evolutionarily conserved in both seedless vascular plants and seed plants. To investigate the evolutionary conservation of roles of secondary wall-associated NAC (SWN) transcription factors in secondary wall biosynthesis, functions of SWN genes from *S. moellendorffii* and *P. patens* were investigated through complementation and overexpression analyses. *SmSWN* and *PpSWN* genes were found to be functional orthologs of *Arabidopsis* NAC transcription factors and capable of activating the secondary wall biosynthetic pathway, indicating that SWN-mediated transcriptional regulation of secondary wall formation evolved as early as vascular land plants appeared.

INDEX WORDS: glucuronoxylan methyltransferase; GT43 family; moss; *Selaginella*; xylan; xylan acetylation; NAC transcription factors

EVOLUTIONARY CONSERVATION OF GENES INVOLVED IN SECONDARY WALL BIOSYNTHESIS

By

MARZIYEH HAGHIGHAT

B.Sc., Tarbiat-Moallem University, Iran, 2005

M.Sc., University of Tehran, Iran, 2008

A Dissertation Submitted to the Graduate Faculty of The University of Georgia in Partial Fulfillment of the Requirements for the Degree

DOCTOR OF PHILOSOPHY

ATHENS, GEORGIA

2016

EVOLUTIONARY CONSERVATION OF GENES INVOLVED IN SECONDARY WALL

BIOSYNTHESIS

By

MARZIYEH HAGHIGHAT

Major Professor: Zheng-Hua Ye

Committee: Carl M. Deom
Wolfgang Lukowitz
Xiaoyu Zhang
Chang Hyun Khang

Electronic Version Approved:

Suzanne Barbour
Dean of the Graduate School
The University of Georgia
August 2016

DEDICATION

In memory of my mother, who always believed in me and taught me the sky's the limit.

To my husband, Yasser, and my father and sister whose love and support has always kept me moving towards my goals and fulfilling my dreams.

ACKNOWLEDGMENTS

I would like to express my sincere gratitude to my advisor Dr. Zheng-Hua Ye for the continuous support of my PhD study, for his patience, guidance, motivation, and immense knowledge. I could not have imagined having a better advisor and mentor for my PhD study. I cannot express enough thanks to the rest of my thesis committee: Dr. Carl M. Deom, Dr. Wolfgang Lukowitz, Dr. Xiaoyu Zhang, and Dr. Chang Hyun Khang, for their continued support, insightful comments, and encouragement. My completion of this project could not have been accomplished without the help and support of current and former members in the Ye lab, especially Ruiqin Zhong whose expert advice with molecular techniques has immensely helped me. My sincere thanks also goes to Beth Richardson for teaching me the histology and microscopy techniques and to all departmental staff for their work, specially Susan Watkins. I would like to thank Dr. Brigitte Bruns and Dr. Kristen Miller who helped me to improve my teaching skills and provided me an opportunity to share my love of biology with future generations of students. I am very grateful to Michael Boyd and Kevin Tarner for taking good care of our plants at Plant Biology greenhouses. I also thank my friends, Nahal Hoghooghi, Jessica Stephens, Chelsea Cunard, Katie Putney, Caitlin Ishibashi, Dorothy Christopher and Lauren Eserman for their support and encouragement. Last but not the least, I would like to thank my family: my caring, loving, and supportive husband, Yasser, my parents and my sister for supporting me spiritually throughout this journey.

TABLE OF CONTENTS

Page

LIST OF TABLES

Page

LIST OF FIGURES

Page

CHAPTER 1

INTRODUCTION AND LITERAURE REVIEW

The migration of leafy aquatic plants onto dry land required several adaptations to help them to survive in their new terrestrial environment. One of these adaptations was the acquisition of the vascular tissue, which enabled plants to transport water and nutrients throughout their bodies. Vascular plants were able to evolve to larger sizes than non-vascular plants due to the formation of a lignified cell wall within these vascular tissues. Plant cell walls are divided into primary walls and secondary walls. Primary walls, mainly composed of cellulose, xyloglucan and pectin, are formed during cytokinesis and continuously modified during cell expansion, whereas secondary walls are deposited between the plasma membrane and the primary walls in some specialized cells including vessel elements and fiber cells. Secondary cell walls constitute the bulk of cellulosic biomass in the form of fibers and wood produced by vascular plants and represent an important raw material for many industrial uses, such as timber, pulping, papermaking, and textiles. Cellulosic biomass has been also considered an abundant, renewable source for biofuel production. The major components of secondary cell walls are the polysaccharides cellulose and hemicellulose together with the more complex lignin polymer composed of phenylpropanoid subunits. The presence of lignin and hemicellulose in the secondary cell wall blocks access to cellulose by degrading enzymes like cellulases and negatively affects the net energy yield from plant biomass (Wu et al., 2010).

Plants need a complex biosynthetic machinery to synthesize polysaccharides and control proper deposition and assembly of cell wall components in each cell type based on its functional role. Glycosyltransferases (GTs) are the key enzymes in the process of polysaccharide synthesis.

These enzymes make glycosidic bonds by attaching a sugar group of a donor substrate to a specific acceptor substrate (Scheible and Pauly, 2004). *Arabidopsis* genome contains 466 GTs classified into 42 different families based on their amino acid sequence similarity (CAZy; www.cazy.org/). The biological activity and biochemical characteristics of only a few of these putative GTs have been demonstrated. Forward/reverse genetic studies have revealed functional roles of some GTs in secondary wall biosynthesis (Scheible and Pauly, 2004). Deciphering the molecular and biochemical mechanisms controlling secondary wall biosynthesis may help design novel strategies to genetically modify wall composition better suited for biofuel production.

CELLULOSE BIOSYNTHESIS

Cellulose is made of long parallel linear 1, 4-β-D-glucan chains that assemble into crystalline microfibrils by hydrogen bonding. Cellulose synthesis occurs at the plasma membrane where rosette-like structures composed of six hexagonally arranged subunits can be found (Reiter, 2002). The catalytic subunit of cellulose synthase is encoded by members of a multi-gene family of transmembrane proteins. The *Arabidopsis* genome possesses ten members of this gene family, *CELLULOSE SYNTHASE 1* (*CesA1*) through *CesA10*. All of *CesA* proteins contain eight transmembrane domains (TMDs), two amino-terminal (N-terminal) TMDs and six TMDs towards the carboxy-terminus (C-terminal) (Joshi et al., 2007). The N-terminal region has a zinc-binding domain required for protein-protein interactions and is followed by the first two hypervariable regions (HVRI) which is conserved among CesA orthologs. The cytoplasmic catalytic domain connecting TMD2 and TMD3 consists of two conserved sub-domains (A and B). These two sub-domains are separated by the second hypervariable region (HVRII) which is also known as the class-specific region (CSR). Domains A and B contain a specific motif of D,D,D,QxxRW (Joshi et al., 2007).

In addition to CesA proteins, cellulose biosynthesis occurs in the presence of additional gene products including *KORRIGAN* gene which encodes β-1, 4-glucanase; *CYT1* which is involved in the GDP-mannose biosynthesis; several *PEANUT* genes which encode enzymes involved in the biosynthesis of glycosylphosphatidylinositol (GPI) membrane anchors; *KOBITO1* which is a plant-specific gene involved in orientation of cellulose-microfibril deposition during cell elongation (Pagant et al., 2002) ; and *COBRA* which encodes a protein required for microfibril organization. It has been hypothesized that β-1, 4-glucanase encoded by *KOR* may be involved in trimming the growing glucan chain required for initiation of synthesis, or alternatively may trim the glucan chains to help crystallization and release newly synthesized microfibrils from the CESA complex (Marriott et al., 2015). *Arabidopsis* mutants with mutations in *AtCesA1* (*RSW1*), *AtCesA2, AtCesA3* (*IXR1/CEV1*), and *AtCesA6* (*PRC1/IXR2*) revealed that these genes are involved in the cellulose synthesis of primary cell walls and mutations of these genes lead to a reduction in cellulose synthesis which is associated with a decrease in cell elongation. *CesA4* (*IRX5*), *CesA7* (*IRX3*), and *CesA8* (*IRX1*) products are co-expressed in the same cells, and all three proteins are required for correct cellulose synthase complex (CSC) assembly (Scheible and Pauly, 2004). *IRX5, IRX3* and *IRX1* are involved in the synthesis of cellulose during secondary wall formation because the mutations of these genes caused severe reductions in cellulose content and secondary wall thickness (Lerouxel et al., 2006). However, the function of *CesA2*, *CesA5*, *CesA9* and *CesA10* are less clear. The loss of function of one of these four genes has minimal or no phenotype in comparison to the other six, suggesting functional redundancy (Scheible and Pauly, 2004).

Cellulose is synthesized at the plasma membrane of higher plants. The *CesA* complexes are assembled in the Golgi and then transported to the plasma membrane through exocytosis. The deposition of cellulose in primary cell wall is highly ordered and guided by cortical microtubules

(MT). Secondary cell wall formed inside of the primary cell wall is divided into three different layers, S_1, S_2 and S_3 which are made of cellulose microfibrils (MF). The S_1 layer is the thinnest of the S layers and located between the primary cell wall and the other two S layers (S_2 and S_3), while the S_2 layer is the thickest layer in the secondary cell wall and provides mechanical strength and support. The MF angles of deposition with regard to the cell axis are 60°-80° in S_1 layer and 5°-30° in S_2 layer. Microfibrils in S_3 layer, the innermost layer of the secondary cell wall, are ordered in a parallel arrangement with the MF angle of 60°-90° with regard to the cell axis (Plomion et al., 2001). The variation in the MF angles in these layers can be related to cell types and in response to environmental factors such as mechanical stress (wind). Therefore, in growing cells, the cellulose microfibrils are constantly deposited in parallel arrays horizontal to the direction of growth (Barnett and Bonham, 2004; Endler and Persson, 2011).

HEMICELLULOSE BIOSYNTHESIS

NDP-SUGAR BIOSYNTHESIS

Sugar precursors used in cell wall biosynthesis come from photosynthetic carbon fixation. In mature leaves, sucrose is synthesized in mesophyll cells and diffuses cell-to-cell through plasmodesmata toward the vein, a process known as phloem loading. Sucrose is loaded into the phloem either through the apoplasm using membrane embedded transporters or symplastically via plasmodesmata. Later, sucrose is unloaded into the ray cells in order to store the sucrose as well as transport to the developing xylem cells (Braun, 2012; Davidson et al., 2011; Fu et al., 2011).

In developing wood cells, sucrose is converted to nucleotide sugars which are activated sugar donors for glycan synthesis (Bar-Peled & O'Neill, 2011; Seifert, 2004). 30 different nucleotide sugars have been identified in plants. There are six basic metabolic and catabolic pathways in a plant cell to synthesize NDP sugars. Carbon derived from photosynthesis as

fructose-6-P and sucrose are main routes of UDP-Glc formation (Mohnen et al., 2008). A reversible phosphoglucose isomerase converts Frc-6-P to Glc-6-P. Phosphomutase then converts Glc-6-P to Glc-1-P which can be converted into UDP-Glc by UDP-Glc pyrophosphorylase (UGlcPP) in the presence of UTP. UDP-Glc is a key intermediate in nucleotide sugar interconversions and is the precursor for UDP-GlcA formation (Bar-Peled & O'Neill, 2011). Feingold (1982) showed that in vitro, UDP-GlcPPase is inhibited by UDP-Xylose which may lead to the regulation of the UDP-glucose pool and other NDP-sugars derived from UDP-Glc. Sucrose synthase (SuSy) catalyzes the reversible conversion of sucrose and UDP into UDP-Glc and fructose (Pontis, 1977). Epimerization is another route for formation of UDP-Glc in plants. The reversible interconversion of UDP-Glc and UDP-Gal is catalyzed by UDP-Gal 4-epimersae (UGE) (Feingold, 1982).

β-D-GlcA is present in rhamnogalacturonans I and II and in arabinogalactans, while the GlcA found in xylan is α-linked and often methylated at O-4 (Ebringerova et al., 2005). UDP-α-D-GlcA is a key intermediate in NDP-sugar metabolism. It is the precursor for UDP-D-xylose, UDP-L-Ara*p*, UDP-Api*f* and UDP-D-GalA. Two GlcA kinases (GlcAK) in the presence of Mg^{2+} phosphorylate GlcA to form GlcA-1-P (Pieslinger et al., 2010). GlcA-1-P then can be converted to UDP-GlcA by SLOPPY. UDP-GlcA can also be formed via UDP-Glc dehydrogenase (UDP-GlcDH) which catalyzes the oxidation of UDP-Glc to UDP-GlcA in the presence of NAD^+ (Klinghammer and Tenhaken, 2007; Bar-Peled & O'Neill, 2011). UDP-GlcDH is inhibited by UDP-xylose, and this feedback inhibition could regulate the flux of conversion of UDP-Glc to UDP-GlcA, UDP-Xyl, and other UDP-sugars in plants (Feingold, 1982; Stewart and Copeland, 1998; Harper and Bar-Peled, 2002). Another route to form UDP-GlcA is through the myo-inositol oxidation pathway. *Myo*-inositol-1-phospate synthase catalyzes the cyclization of Glc-6-P to form

myo-inositol-1-P which is then dephosphorylated by *myo*-inositol monophophatase (IMPase). Dephosphorylated *myo*-inositol is oxidized by inositol oxygenase (MIOX) to D-GlcA (Lorence et al., 2004; Bar-Peled & O'Neill, 2011). However, the amount of UDP-GlcA produced in this way is still unclear and could be tissue specific (Seitz et al., 2000). D-Xylose (Xyl), a major component of polysaccharides including xylan and xyloglucan, is found in both primary and secondary cell walls. UDP-Xyl biosynthesis occurs both in the cytosol and in the Golgi apparatus. UDP-xylose is mainly formed by the decarboxylation of UDP-GlcA which is catalyzed by different membrane-bound and soluble UDP-GlcA decarboxylase/ UDP-Xylose synthase (UGlcA-DC/UXS) isoforms (Harper and Bar-Peled, 2002; Bar-Peled & O'Neill, 2011). When the NAD^+ is tightly bound to UXS, the oxidation of UDP-GlcA to the UDP-4-keto-hexose intermediate is catalyzed and followed by the decarboxylation reaction to form UDP-4-keto-pentose. The UDP-4-keto-pentose is then reduced to UDP-Xylose by the enzyme-bound NADH (Mohnen et al., 2008; Harper and Bar-Peled, 2002).

Six *UXS* genes have been identified in *Arabidopsis*. These UXS isoforms act only on UDP-GlcA (Harper and Bar-Peled, 2002). Dimerization of UXS is required for the conversion of UDP-GlcA to UDP-xylose which is inhibited by UDP-xylose (Harper and Bar-Peled, 2002; Bar-Peled & O'Neill, 2011). *Arabidopsis* UXS isoforms belong to three distinct clades including Type A, Type B and Type C. Type A and B UXS isoforms have an N-terminal signal resulting in proteins with higher molecular masses than those of the cytosolic Type C. Type A and B UXS isoforms are predicted to be type II membrane proteins with the catalytic domain facing the membrane lumen, while the three Type C isoforms are cytosolic (Pattathil et al., 2005; Bar-Peled & O'Neill, 2011).

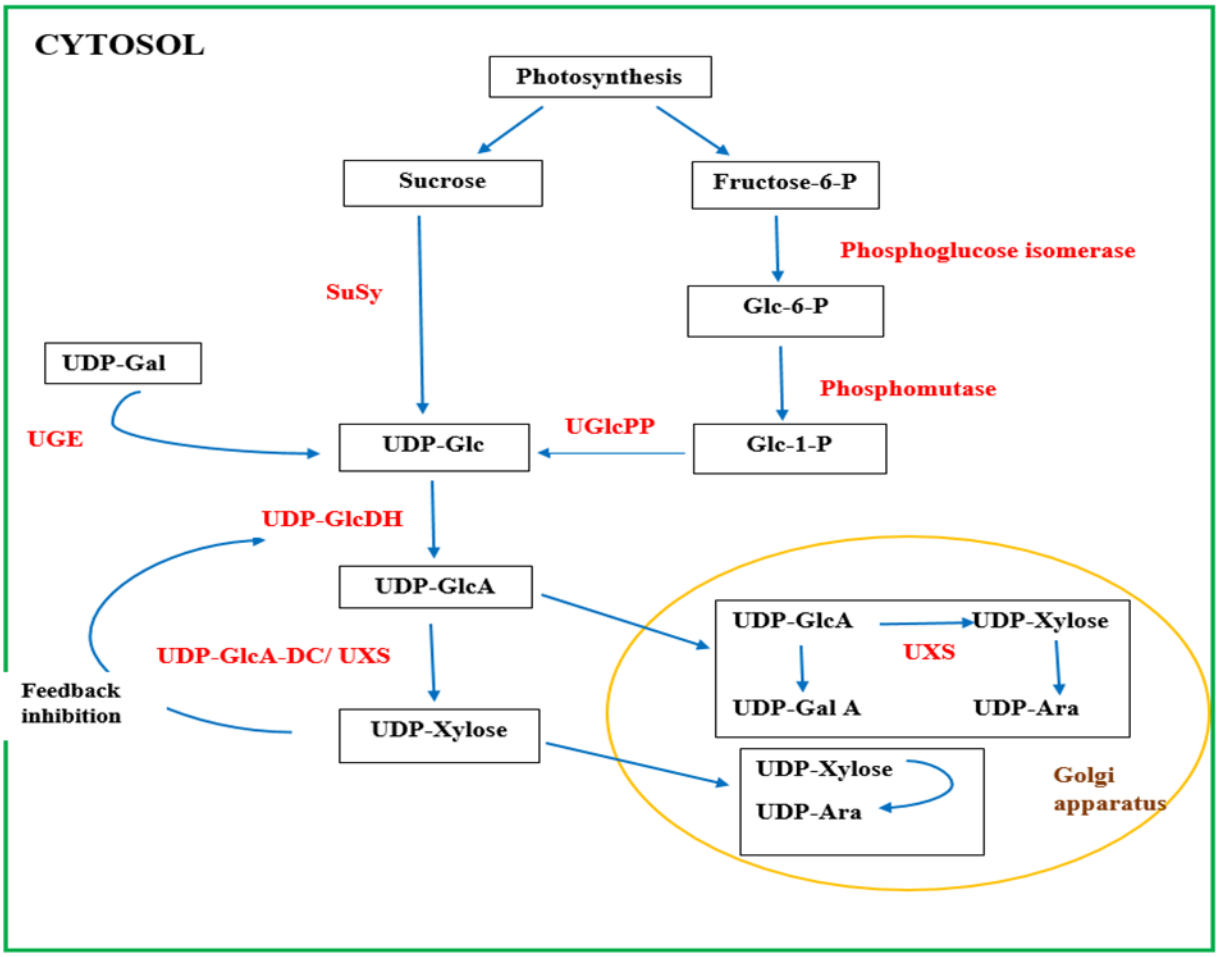

Figure 1.1- Metabolic routes involved in the synthesis of UDP-Xyl. Synthesis of UDP-Xyl occurs both in the cytosol and in membrane-bound compartments (M. Haghighat).

XYLAN BIOSYNTHESIS

Xylan, composed of a linear backbone of β-(1, 4)-linked xylosyl residues, is a predominant cell wall polymer in all higher plants as well as some algae. Homoxylans with β-(1, 3) glycosidic linkages have been found in green algae, while red seaweeds of Palmariales and Nemaliales contain homoxylans with mixed β-(1, 3 and 1, 4) glycosidic linkages (Ebringerová and Heinze, 2000). Xylan, as the main hemicellulose, cross-links with cellulose in the secondary cell walls of dicot plants to make the whole framework of cell walls much stronger. Xylan is also linked with

lignin, pectin and other hemicelluloses through formation of non-covalent linkages between xylan and α-carbon of the lignin monomers which results in the formation of hydrophobic microdomain (Barakat et al., 2007). It seems that xylan plays an important role in some of fundamental processes of adaptation and development due to its diverse structure among species and even in different tissues. Although most of the xylan found in plants share a backbone of β-(1, 4)-linked D-xylosyl (Xyl) residues, different distributions and compositions of side chains and any functional group substitution result in several various structures of xylan based on species (Ebringerová and Heinze, 2000). Xylan in primary cell walls is substituted with arabinose (Ara) and glucuronic acid (GlcA), while glucuronoxylan (GX), the predominant form of xylan in plant secondary cell walls, consists of the backbone of xylosyl residues substituted with α-(1, 2)-linked glucuronic acid (GlcA) and/or methylglucuronic acid (MeGlcA). The existence of side chains may prevent the xylan polymer from self-assembling. In addition, a unique tetrasaccharide sequence, β-D-Xyl*p*-(1→3)-α-L-Rha*p*-(1→2)-α-D-Gal*p*A-(1→4)-D-Xyl is found at the reducing end of the xylan chain. This conserved tetrasaccharide in a range of plant species suggests that it plays a critical role either in the synthesis or function of the xylan (Lee et al., 2007, 2010, and 2011).

The structure of xylan, the second most abundant plant cell wall polysaccharide, has been studied in the past few decades because of its biological importance for plant development and also its negative effect on converting cellulosic biomass into biofuels through blocking the accessibility of degrading enzymes like cellulases to cellulose (Lee et al., 2011; Wu et al., 2010). To identify the fine chemical structure, deacetylated xylan polymers can be isolated using an alkali solution such as NaOH or KOH. Then, a mild hydrolysis or xylanase treatment generates oligoxylosaccharides. Most of the acetyl groups attached to xylosyl residues at O-3 and/or O-2 are removed by an alkali treatment. In addition, other treatments such as steam, thermochemical and

microwave oven have been developed to successfully isolate acetylated xylan from plants especially some tree species (Vodenicˇarova´ et al., 2006; Ebringerová, 2000). Heteroxylans including the arabinoxylans (AX) and the (methyl) glucuronoarabinoxylans (M/GAX) are predominant in walls of the grasses. Arabinoxylans as the major noncellulosic polysaccharides can be found in walls of starchy endosperm and aleurone layer cells in cereal grains. AX is composed of a (1, 4)-β-D- xylan with the same conformation as a (1, 4)-β-D-glucan or cellulose. The β-D-xylopyranosyl (Xyl*p*) units of the xylan backbone are substituted with α-L-arabinofuranose units (Ara*f*) through α-(1, 3) and/or α-(1, 2) linkages in the ratio of 1:1.1-2 depending on the species and plant tissues/ wall type. Some of the Ara*f* units in the AX are esterified with some phenolic acids such as ferulic acid, the hydroxycinnamic acid, and its non-methoxylated analog *p*-coumaric acid (Fincher, 2009). The presence of the hydroxycinnamates, found at O-5 of some Ara*f* residues that are linked to the O-3 of the Xyl*p* units, suggested that it plays some potential roles in formation of covalent interactions between polysaccharides as well as polysaccharides and proteins. During the winter time, AX also inhibits intercellular ice formation by increasing the viscosity and the mechanical interference of the cell wall. M/GAX has been found in many tissues of monocot plants including straw, stems, stalk, and outer pericarp of grains as well as non-lignified tissues in dicot plants (Fincher, 2009). Xylan in the form of (methyl) glucuronoxylan (MGX) is only present in woody plants. In MGX, D-glucuronic acid (GlcA) and/or 4-O-methyl-a-D-glucuronic acid residues are attached at the O-2 of xylosyl residue. 30% of GlcA in not methylated in non-woody plants, while only methylated GlcA has been found in all tissues of woody plants which undergo secondary growth (Ebringerová and Heinze, 2000).

Xylan biosynthesis includes different enzymatic actions for the backbone initiation and elongation, side chain and functional group additions, transportation of the polymer to the cell wall

and finally assembly with other cell wall components (Ye et al., 2006). Radio-isotope labeling experiments revealed that xylan biosynthesis occurs in the Golgi complex, and the polymers synthesized in the Golgi are exported outside of the plasma membrane (Fry, 2004). Proteins responsible for backbone elongation and the side chain addition have been found in the Golgi fraction (Zeng et al., 2008).

Glycosyltransferases (GTs) are the key enzymes in the process of polysaccharide synthesis that catalyze the addition of carbohydrates onto acceptor substrates. Hemicelluloses are assembled by Golgi-membrane-bound glycosyltransferases in the Golgi lumen and then transported in secretory vesicles to the plasma membrane and integrated into the apoplastic cell wall network. In contrast, cellulose, made of long parallel linear 1, 4-β-D-glucan chains, is directly synthesized by plasma membrane-embedded glycosyltransferases and then released into the cell walls. GTs work with modifying enzymes and nucleotide sugar conversion enzymes and transporters in order to synthesize cell wall glycans in the Golgi apparatus. Most of GTs of plants show type II single-pass transmembrane protein with catalytic domain, stem region, transmembrane (TM) region, and cytosolic region. The N-terminal is on the cytosolic side while the C-terminal region with the catalytic domain locates in the Golgi lumen. Some of GTs are multi-pass transmembrane with catalytic site located on either the cytosolic or the luminal side of membrane (Oikawa et al., 2013). Forward and reverse genetics coupled with functional genomics, polysaccharide labeling experiments and immunocytochemistry, as well as in-vitro activity assay using membrane microsomes from actively xylan-synthesizing tissues revealed that the inner face of Golgi membrane is the site where the formation of xylan structure occurs, and several GTs have been identified to be involved in xylan biosynthesis. Moreover, all xylan-specific GTs in *Arabidopsis* with the exception of PARVUS are localized to the Golgi (Zhong et al., 2005; Pena et al., 2007;

Lee et al., 2007b; Wu et al., 2009). Like xyloglucan and pectin, xylan backbone polymerization and side chain addition take place at the Golgi complex. PARVUS, mostly localized to the endoplasmic reticulum (ER), is involved in an unknown initial step of xylan biosynthesis at the ER (Lee et al., 2007b). After xylan polymers are fully formed in the Golgi, they are then exported to the apoplast via vesicles (Taylor, 2008). Analyses of xylan-deficient mutants with stunted growth and thin secondary cell walls phenotypes have indicated that all the mutated genes encode type II-GT in the same or different GT family (Brown et al., 2007). Due to some similarities including glycosidic linkage (β-1, 4) in the backbone structure of xylan and cellulose, it has been predicted that one or more of cellulose-synthase like (CSL) enzymes might be involved in xylan xylosyltransferase (Lerouxel et al., 2006). However, Lee et al. (2007a) indicated that xylan synthase might be non-CSL proteins because there was no xylan xylosyltransferase activity when recombinant CSL proteins were heterologously expressed in *Drosophila* Schneider 2 cells.

Analysis of *Arabidopsis* mutants with collapsed xylem vessels in stem tissues has revealed a number of genes required for xylan synthesis. The identified genes encompass members of GT47 (FRA8/*IRX7* and *IRX10*), GT43 (*IRX9* and *IRX14*), and GT8 families (IRX8 and PARVUS) of glycosyltransferases. Analysis of mutants for each of these genes indicates that *IRX9*, *IRX10* and *IRX14* encode enzymes that act as xylosyltransferases in the synthesis of the β-1-4 xylan backbone, whereas FRA8, IRX8 and PARVUS are likely involved in synthesis of the reducing end tetrasaccharide structure. A complementation study has revealed that the poplar GT43, which is specifically expressed in the secondary xylem in wood, is a functional ortholog of the *ArabidopsisIRX9* and involved in the elongation of the xylan backbone (Lee et al., 2007, 2010, 2011; Wu et al., 2010). There are four known GT43 genes involved in xylan biosynthesis in *Arabidopsis.* Genetic studies have identified that the *Arabidopsis*GT43 members form two

functionally non-redundant groups, *IRX9*/I9H and *IRX14*/I14H, which are essential for the normal elongation of xylan backbone. Comprehensive molecular and genetic studies have indicated that *IRX9* and *I9H* are a pair of functional homologs and *IRX14* and *I14H* are another pair of functional homologs because they all are expressed in the same cell types that undergo secondary cell wall thickening and their encoded proteins are targeted to the Golgi, where GX is synthesized. Moreover, mutation of the *IRX9* and *IRX14* genes cause severe reduction in xylan xylosyltransferase activity and consequently a significant decrease in the GX chain length, GX amount and GX level (Lee et al., 2010). In addition, complementation studies have revealed that the GX defects in the *IRX9* mutant can be rescued by overexpression of I9H but not *IRX14*. Similarly, overexpression of I14H but not *IRX9* and I9H is able to complement the GX defects in *IRX14* mutant (Lee et al., 2010).

XYLOGLUCANS BIOSYNTHESIS

Xyloglucan (XyG) makes up 20-25% of the dicot primary cell walls. Xyloglucan plays an important role in cell wall structure through the cross-link with cellulose microfibrils and also by providing space in the XyG-network to avoid cellulose microfibrils aggregation (Thompson, 2005). Xyloglucan is composed of a β-(1, 4)-glucan backbone with 75% of the glucosyl residues substituted with a xylosyl residue. Some of these xylosyl residues are substituted with galactosyl or arabinosyl residues. Some of the galactosyl residues are also substituted with fucosyl residues. A minor part (2-5%) of the cell wall in grasses contains xyloglucan with less branching, no fucosyl or arabinosyl side chains and a small number of galactosyl residues (Vogel, 2008; Hsieh et al., 2009). Biosynthesis of xyloglugan occurs in the Golgi apparatus and several enzymes including β-(1, 4)-glucan synthase (AtCSLC4 from family GT2; Cocuron et al., 2007), α-fucosyltransferases (AtFUT1 from family GT34; Perrin et al., 2003), β-galactosyltransferases (AtMUR3 from family

GT47; Madson et al., 2003), and α-xylosyltransferases are involved in XyG biosynthesis. In *Arabidopsis* genome, there are seven genes from family GT34 that encode XyG xylosyltransferases (*XXT*s) including *XXT*1, *XXT*2, and *XXT*5 (Faik et al., 2002; Zabotina et al., 2008). Since *XXT1, XXT2,* and *XXT5* plants have the reduced amount of XyG in their structure, it seems these three genes are involved in xyloglucan biosynthesis. Plants with double mutation of *XXT1* and *XXT2* have a slower growth rate with severely shortened and abnormal root hair. These phonotypes could be rescued by expression of either *XXT*1 or *XXT*2 under the 35S promoter. Therefore, *XXT*1 and *XXT*2 encode active *XXT*s involved in XyG biosynthesis. However, the lack of XyG in the double mutants while *XXT*5 is being expressed suggested that the activity of *XXT*1 or *XXT*2 is required for the function of *XXT*5 due to an epistatic effect (Cavalier et al., 2008).

LIGNIN BIOSYNTHESIS

Lignin, a major component of plant cell wall, significantly contributes to the recalcitrance of the biomass. Lignin, mainly found in vessels and fibers, is a phenolic heteropolymer composed of monolignols that provide enhanced strength and waterproofing to the secondary cell wall. Synthesized by almost all land plants and some algae, lignin plays critical roles in mechanical support, stress responses, resistance to pests and disease, as well as water and nutrient transport. Common pretreatment methods used to reduce cell wall recalcitrance due to the presence of lignin either are very costly or need to be done in high temperatures. One approach to overcome these difficulties and increase the amount of biomass used for biofuel production is to alter the lignin content, composition and structure by changing the known lignin biosynthetic pathway (Simmons et.al 2010). In the cytoplasm, monolignols, including p-coumaryl alcohol, coniferyl alcohol, and sinapyl alcohol, are first synthesized from the amino acid phenylalanine through the phenylpropanoid pathway (Zhong et al. 2009). All of the enzymes involved in monolignol

biosynthesis have been identified: phenylalanine ammonia lyase (PAL), cinnamate 4-hydroxylase (C4H), 4-coumarate-CoA ligase (4CL), shikimate hydroxycinnamoyl transferase (HCT), coumarate 3-hydroxylase (C3H), caffeoyl-CoA 3-O-methyltransferase (CCoAOMT), cinnamoyl-CoA reductase (CCR), cinnamyl alcohol dehydrogenase (CAD), ferulate 5-hydroxylase (F5H) and caffeic acid/5-hydroxyferulic acid O-methyltransferase (COMT). Results from a comparative genomics and proteomic perspective evaluating the role of all of these enzymes involved in lignin biosynthesis suggest that there is functional redundancy at the transcript level for PAL, C4H, 4CL, HCT, CCoAOMT and F5H/CAId5H.

Synthesized lignin monomers are then exported through the plasma membrane into the cell walls by an ATP dependent membrane transporter in order to be oxidized by laccases or peroxidases and polymerized into lignin polymers within the secondary cell wall (Simmons et al. 2010; Vanholme et al. 2008). Previously, several mechanisms have been proposed in order to explain the mechanism of monolignol export from the cytosol to the apoplast,. One mechanism suggested that plasma membrane transporters may export free monolignols into the apoplast because no vesicular accumulation of labeled monolignols has been detected in lignifying cells fed by radiolabeled phenylalanine. It was also thought that other mechanisms such as free diffusion through the plasma membrane, glycosylated monolignol exporters and vesicular secretion might be responsible for the export of monolignols into the apoplast (Simmons et al. 2010). However, Alejandro et al. (2012) have found an ATP-binding cassette transporter acting as a *P*-coumaryl alcohol transporter in *Arabidopsis*. Expression analysis revealed that *AtABCG29* is expressed in both primary and secondary roots, the vascular tissues of the lower part of stem, rosette leaves and anthers. In addition, *Arabidopsis abcg29* mutants had fewer lignin subunits and were more sensitive to *P*-coumaryl alcohol. The co-expression analysis also indicated that *AtABCG29* showed

a high co-expression ratio with 4CL2 and 4CL5 (two 4-coumarate coenzyme A ligases) as well as one caffeoyl CoA-O-methyltransferase, which converts caffeoyl CoA into feruloyl CoA. Hence, *AtABCG29* can act as a transporter for monolignol export.

PECTIN BIOSYNTHESIS

Pectin is the most complex polysaccharide in plant cell walls and has functions in plant growth, development, morphology and defense. It is a component of all higher plant walls as well as pteridophytes, bryophytes Chara, a charophycean algae, and the closest extant relative of land plants. Pectins are made of galacturonic acid polysaccharides that are covalently linked together at the O-1 and the O-4 positions (Mohnen, 2008). Pectins are structurally divided into three subclasses including homogalacturonan (HG), rhamnogalacturonan I (RG-I) and rhamnogalacturonan II (RG-II). Homogalacturonan is a linear homopolymer of α-1, 4-linked galacturonic acid that is partially methylesterified at the C-6 carboxyl, O-acyetylated at O-2 or O-3. In addition to HG, there are other more complex pectic polysaccharides, such as the substituted HGs rhamnogalacturonan II (RG-II), xylogalacturonan (XGA), apiogalacturonan (AP) and also rhamnogalacturonan I with more variable structure. Rhamnogalacturonan II (RG-II) is composed of an HG backbone of at least 8 α-1, 4-linked galacturonic acid residues with side branches (a-d) containing 12 different types of sugars in over 20 different linkages. XGA, most predominant in reproductive tissues, contains a β-linked xylose at O-3 and occasionally an additional β-linked xylose at O-4. XGA may play a role in response to pathogen attack through making HG more resistant to degradation by endopolygalacturonases. The backbone of galacturonic acid residues can be substituted at O-2 and O-3 with D-apiofuraose (Harholt et al., 2010; Mohnen, 2008).

Biosynthesis of pectins occurs in Golgi apparatus, and it has been predicted that 67 different glycosyltransferases (GTs), methyltransferases, and acetyltransferases are required to

synthesize these pectic polysaccharides (Ridley et al., 2001). According to the CAZy database, the *GAUT* group of proteins belong to GT family 8 with 15 members in *Arabidopsis*. GALACTURONOSYLTRANSFERASE1 (*GAUT*1) is a type II membrane protein with a single N-terminal transmembrane helix and the main globular domain inside the Golgi domain and interact with *GAUT*7 to make a complex in vivo. *GAUT* 1 catalyzes the transfer of GalA from UDP-GalA onto HG acceptors. RGXT1 and RGXT2 from GT77 family are required for RG-II biosynthesis. A study of expression of these α-D-1,3-xylosyltransferases in insect cells indicated that both RGXT1 and RGXT2 transfer xylose from UDP-α-D- xyl onto fucose in an α-1,3-linkage (Mohnen, 2008). The *Arabidopsis* genome contains four members of RGXT family and three of them have shown similar biochemical function in vitro that may be a reason for the lack of clear differences in the structure of RG-II isolated from walls of RGXT1 and RGXT2 mutants compared with wild-type walls (Harholt et al., 2010).

WOOD FORMATION

Wood produced by vascular plants represents the world's most abundant form of biomass used for many industrial uses, such as timber, pulping, papermaking, and textiles as well as production of liquid biofuels. Wood in dicot species is composed of xylem fiber, vessel and ray parenchyma cells (Demura and Fukuda, 2007). The vascular tissue in stems, leaves, and roots is formed through cell division and differentiation from the meristematic procambium. During primary growth of stems and roots, procambium is generated by the shoot apical meristem and develops into primary xylem and primary phloem (Jung and Park, 2007); later during secondary growth of plants it produces a secondary meristem, vascular cambium which results in secondary xylem or wood and secondary phloem (Carlsbecker and Helariutta 2005). Primary xylem includes protoxylem followed by metaxylem that develops before secondary xylem. The vascular cambium

established with more asymmetric cell divisions is made of two cell types, fusiform cambial cells (FCCs) and ray cambial cells (RCCs). Adaxial and abaxial cell divisions of FCCs result in xylem and phloem mother cells, respectively. These cells differentiate into vessel and fibers before undergoing secondary cell wall formation followed by programmed cell death (Nieminen et al., 2004). Xylem ray parenchyma cells produced by RCCs differentiate into two types, contact cells and isolation cells. Contact cells make direct connections with adjacent vessel elements through pits to facilitate transport between vessel elements while isolation cells have no pit-mediated connections with adjacent vessel elements and may be more specialized for radial translocation than contact cells. Development of tyloses from only contact cells has suggested that contact cells may have a role in protection of living ray parenchyma cells from hydrolases that are released from dead vessel elements (Murakami et al., 1999).

Wood or secondary xylem, composed of fiber and vessels, is formed from vascular cambium. Fibers support the plant bodies, whereas tracheary elements including vessels and tracheids transport water and nutrients. The main function of the xylem is to transport water and soluble mineral nutrients from the root throughout the plant and to provide mechanical support to the plant body. Tracheary elements in the xylem undergo elongation before tubular conducting system is formed, necessitating expansion of the cellulose-hemicellulose network through cell wall loosening enzymes. Plant hormones such as brassinosteroids are also involved in the regulation of cell elongation. After elongation, tracheary elements undergo secondary wall thickening to create different patterns including scalariform, annular, and pitted. Mechanical strength provided by the thickened secondary walls is important for plants to bear the negative pressure produced through transpiration. Programmed Cell Death (PCD) is the last step of wood formation which produces mature xylem cells. Some hydrolytic enzymes including cysteine protease, serine proteases, and

nucleases are produced during wood formation (xylogenesis), and they are stored in vacuoles before autolysis initiates. PCD begins with destroying the vacuoles membrane and releasing these hydrolytic enzymes into cytosol. The enzymes degrade nuclear DNA and remove the cellular contents in order to create hollow tubular columns that are called vessels (Ye, 2002). Therefore, the formation of secondary cell walls or wood begins with the deposition of cellulose, followed by hemicellulose and finally by the initiation of lignification before PCD (Jones, 2001). All these steps of wood formation are tightly regulated by both transcription factors and hormonal signals.

TRANSCRIPTION FACTORS REGULATING SECONDARY CELL WALL BIOSYNTHESIS

Transcription factors are proteins binding to specific DNA sequences to control the expression of target genes quantitatively, temporally, and spatially. The NAC (for NAM, ATAF1/2 and CUC2) domain transcription factors acting as master transcriptional switches of the secondary cell wall biosynthesis are plant-specific transcription factors with a conserved NAC domain at the N-terminal region and a divergent C-terminal activation domain. The *Arabidopsis* genome contains 114 NACs that play important roles in plant growth and development as well as stress responses and plant defense (Pimrote et al., 2012; Zhong et al., 2010). A subgroup of phylogenetically, closely related NAC domain transcription factors including SECONDARY WALL ASSOCIATED NAC DOMAIN PROTEIN 1(SND1/NST3) and NST1 are specifically expressed in fibers, whereas VASCULAR-RELATED NAC-DOMAIN 1 (VND1) to VND7 are specifically expressed in vessels. Mutations of SND1 and NST1 simultaneously cause a loss of secondary walls in fibers, while dominant repression of VND6 and VND7 block secondary wall thickening in vessels. On the other hand, overexpression of any of these Secondary Wall NACs (SWNs) results in ectopic deposition of secondary walls in cells that are normally paranchymatous.

Hence, these NAC transcription factors are the first level of master transcriptional switches that activate secondary cell wall biosynthesis in fibers and vessels (Zhong et al., 2010).

The second level of master regulators in secondary cell wall biosynthesis is MYB proteins that belong to a large family of transcription factors that regulate plant metabolism and development. MYB proteins contain a highly conserved DNA-binding domain, the MYB domain composed of up to four imperfect amino acid sequence repeats (R) of about 52 amino acids. Each of these repeats form three α-helices. There are different classes of MYB proteins depending on the number of adjacent repeats in MYB domain. The *Arabidopsis* genome contains over 120 members of R2R3-MYB class which is one of the largest families of transcription factors in plants (Pimrote et al., 2012).

In *Arabidopsis*, several MYB proteins have been identified as the direct targets of secondary wall NACs master switches. Studies have shown MYB46 and its close homolog MYB83 are direct targets of the fiber- specific SND1 and NST1 as well as the vessel-specific VND6 and VND7. They are expressed in both fibers and vessels. Mutations of MYB46 and MYB83 at the same time lead to lack of secondary wall thickening in vessels, whereas overexpression of MYB46 or MYB83 causes activation of secondary wall biosynthetic genes for cellulose, xylan and lignin and also results in ectopic deposition of secondary walls in parenchymatous cells. Hence, MYB46 and MYB83 are the second-level master regulators that control the downstream genes in secondary wall formation (Zhong and Ye, 2012; Zhong et al. 2010; McCarthy et al., 2009). Among downstream transcription factors, SND3, MYB103, and KNAT7 (a Knotted1-like homeodomain protein) are direct targets of SND1 and its close homologs NST1, NST2, and vessel-specific VND6 and 7. Dominant repression of SND3 and MYB103 caused reduced secondary wall thickening in fiber cells, while overexpression of these

transcription factors resulted in an increase in secondary wall thickening in fibers and induced the expression of *CesA8*, a cellulose synthase. MYB58, MYB63 and MYB85 are involved in the lignin biosynthesis. Expression of MYB58 and MYB63 is regulated by the SND1 close homologs NST1, NST2, VND6 and VND7 as well as MYB46. They are expressed in lignifying cells, and overexpression of these transcription factors activate lignin biosynthetic genes by directly binding to the AC elements at the promoter regions (Demura and Ye, 2010; Zhong and Ye, 2009; Zhong et al., 2010).

Secondary Wall NACs (SWNs) may be up- or down-regulated by other transcription factors including MYB32, WRKY12 and SHN2. MYB32, a known target for regulation of SND1 and a downstream component of SWNs, is activated by MYB46. Based on the protein sequence, MYB32 is a transcriptional repressor that negatively regulates the expression of SND1 (Wang et al., 2011; Pimrote et al., 2012). Loss of function of WRKY12 in *Arabidopsis* results in ectopic deposition of secondary wall formation in pith cells. Mutation of AtWRKY12 up-regulates the expression of NST2 and other secondary cell wall-related transcription factors. The pith cells of double mutant of *wrky12-1* and *nst2* were restored to wild-type. Therefore, WRKY12 may negatively regulate SWNs and control the cell fate in pith cells (Wang et al., 2010; Pimrote et al., 2012). SHN2, a member of SHINE/WAX INDUCER (SHN/WIN) transcription factor, both negatively and positively regulates SWNs. SND1/NST1/2 and VND6, the first level master switches, are negatively regulated by SHN2. Lignin formation and cellulose synthesis are indirectly affected by SHN2 through negative regulation of the MYB58/63 and direct activation of MYB20/43 and other related transcription factors, respectively (Ambavaram et al., 2011; Pimrote et al., 2012). KNAT7, MYB75 and OFP4 are also negative regulators of the lignin biosynthesis in secondary wall formation. MYB75 or PRODUCTION OF ANTHOCYANIN

PIGMENT1 (PAP1) acts in the phenylpropanoid pathway in *Arabidopsis*. A loss-of-function mutation in MYB75 showed an increased cell wall thickness in the inflorescence stem through up-regulation of a group of genes involved in lignin biosynthesis. Therefore, MYB75 is a negative regulator of lignin biosynthesis and may form functional complexes with KNAT7 to contribute to the regulation of secondary cell wall deposition in inflorescence stems (Li et al, 2011; Pimrote et al., 2012). KNAT7, one of the direct targets of SND1 and MYB46, is a transcriptional repressor rather than activator in regulation of secondary cell wall formation (Zhong et al., 2008). KNAT7 loss-of-function mutants showed an increased cell wall thickness in interfascicular fibers, whereas over-expression of KNAT7 caused the opposite phenotype. Interactions between KNAT7 and OFP4, a member of Ovate Family Protein transcription co-regulators, enhance the transcriptional repressor activity of KNAT7. *Ofp4* mutant has the similar fiber cell wall phenotypes as *knat7*, and the phenotype of double mutant of *ofp4 knat7* was similar to phenotypes of the single mutants (Pimrote et al., 2012).

NAC transcription factors, VND6 and VND7 regulate formation of metaxylem and protoxylem in roots and leaves, respectively. VND-INTERACTING2 (VNI2), a NAC transcription factor, represses the expression of genes that are regulated by VND7, and has a negative effect on vessel formation. ASL20/LBD18 and ASL19/LBD30, two homologous ASYMMETRIC LEAVES2 (AS2)/LATERAL ORGAN OUNDARIES DOMAIN (LBD) family proteins, are up-regulated by VND6 and VND7 and are expressed in differentiating tracheary elements (Demura and Ye, 2010; Ohashi-Ito and Fukuda, 2010). Overexpression of these transcription factors causes the formation of tracheary element-like cells in mutant plants with ectopic expression of VND7 in ASL20/LBD18 over-expressing plants. Therefore, there is a

positive feedback loop for VND7 expression that is controlled by ASL20/LBD18 (Pimrote et al., 2012).

MYB26 plays a critical role in the development of secondary thickening walls in the anther endothecium. The NST1 and NST2 NAC transcription factors are turned on and off by MYB26 in the anther endothecium. The *nst1 nst2* double mutant showed the same phenotype as *myb26* mutant, and overexpression of MYB26 results in ectopic secondary thickening in both *Arabidopsis* and tobacco. Hence, MYB26 located upstream of SWNs in the anther endothecium and is an activator of secondary wall formation.

REFERENCES

Alejandro, S., Lee, Y., Tohge, T., Sudre, D., Osorio, S., Park, J., Bovet, L., Lee, Y., Geldner, N., Fernie, A.R and Martinoia, E. (2012). *AtABCG29* is a monolignol transporter involved in lignin biosynthesis. *Current Biology*, 22: 1207–1212.

Ambavaram, M.M., Krishnan, A., Trijatmiko, K.R., and Pereira, A. (2011). Coordinated activation of cellulose and repression of lignin biosynthesis pathways in rice. *Plant Physiology*, 155:916-931.

Barakat, A., Winter, H., Rondeau-Mouro, C., Saake, B., Chabbert, B., and Cathala, B. (2007). Studies of xylan interactions and cross-linking to synthetic lignins formed by bulk and end-wise polymerisation: a model study of lignin carbohydrate complex formation. *Planta*. 226:267–281.

Barnett, J.R. and Bonham, V.A. (2004) Cellulose microfibril angle in the cell wall of wood fibers. *Biology Review*, 79:461-472

Brown, D.M., Goubet, F., Wong, V.W., Goodacre, R., Stephens, E., Dupree, P., and Turner, S.R. (2007). Comparison of five xylan synthesis mutants reveals new insight into the mechanisms of xylan synthesis. *Plant Journal*, 52:1154-116.

Carlsbecker, A. and Helariutta, Y. (2005) Phloem and xylem specification: pieces of the puzzle emerge, *Current Opinion in Plant Biology*, 8: 512-517.

Cavalier, D. M., Lerouxel, O., Neumetzler, L.,Yamauchi, K., Reinecke, A., Freshour,G., Zabotina, O. A., Hahn, M. G., Burgert, I.,Pauly, M., Raikhel, N. V., & Keegstra, K.(2008). Disrupting two *Arabidopsis thaliana* xylosyltransferase genes results in plants deficient in xyloglucan, a major primary cell wall component. *Plant Cell, 20*, 1519-1537.

Cocuron, J.-C., Lerouxel, O., Drakakaki, G., Alonso, A. P., Liepman, A. H., Keegstra, K., Raikhel,N., & Wilkerson, C. G. (2007). A gene from the cellulose synthase-like C family

encodes a β-1,4 glucan synthase. *Proceedings of the National Academy of Science USA, 104*,8550-8555.

Demura, T. and Fukuda, H. (2007) Transcriptional regulation in wood formation, *TRENDS in Plant Sciences*, 12: 64-70.

Demura, T. and Ye, Z-H (2010) Regulation of plant biomass production, *Current Opinion in Plant Biology*, 13: 299-304.

Ebringerová, A., and Heinze, T. (2000). Xylan and xylan derivatives—Biopolymers with valuable properties. I. Naturally occurring xylans structures, isolation procedures and properties. *Macromol. Rapid Commun*. 21:542–556.

Ebringerová, A. (2006). Structural diversity and application potential of hemicelluloses. *Macromolecular Symposia*, 232:1–12.

Endler, A. and Persson, S. (2011) Cellulose Synthases and Synthesis in *Arabidopsis*. *Molecular plant*, 4 (2): 199-211.

Faik, A., Price, N. J., Raikhel, N. V., & Keegstra, K. (2002). An *Arabidopsis* gene encoding an α-xylosyltransferase involved in xyloglucanbiosynthesis. *Proceedings of the National Academy of Science USA, 99*, 7797-780

Fincher, G.B. (2009). Revolutionary times in our understanding of cell wall biosynthesis and remodeling in the grasses. *Plant Physiol.* 149:27–37.

Fry, S.C. (2004). Primary cell wall metabolism: tracking the careers of wall polymers in living plant cells. *New Phytology*, 161 (3):642-675.

Harholt, J., Suttangkakul, A., and Scheller, H., V. (2010) Biosynthesis of Pectin, *Plant Physiology*, 153: 384-395.

Hsieh, Y. S.-Y., & Harris, P. J. (2009). Xyloglucans of monocotyledons have diverse structures. *Molecular Plant, 2,* 943-965.

Jensen, J.K., Kim, H., Cocuron, J-C., Orler, R., Ralph, J., and Wilkerson, C.G. (2011) The DUF579 domain containing proteins *IRX15* and *IRX15*-L affect xylan synthesis in *Arabidopsis*. *Plant Journal*, 66: 387-400.

Jones, A. M. (2001) Programmed cell death in development and defense. *Plant Physiology*, 125: 94-97.

Joshi, C.P. and Mansfield, S.D. (2007) The cellulose paradox-simple molecule, complex biosynthesis. *Current Opinion in Plant Biology*, 10: 220-226.

Jung, J.H., Park, C.M. (2007). Vascular development in plants: specification of xylem and phloem tissues. *Journal of Plant Biology*, 50:301-305

Lee, C., O'Neill, M.A., Tsumuraya, Y., Darvill, A.G., and Ye, Z.-H (2007) The irregular xylem9 mutant is deficient in xylan xylosyltransferase activity, *Plant Cell Physiology*, 48: 1624-1634.

Lee, C., Teng, Q., Huang, W., Zhong, R. and Ye, Z.-H. (2010) The *Arabidopsis* family GT43 glycosyltransferases form two functionally nonredundant groups essential for the elongation of glucuronoxylan backbone. *Plant Physiology*, 153: 526–541.

Lee, C., Teng, Q., Zhong, R. and Ye, Z.-H. (2011a) Molecular dissection of xylan biosynthesis during wood formation in poplar. *Molecular Plant*, 4: 730–747.

Lee, C., Zhong, R. and Ye, Z.-H. (2012) *Arabidopsis* family GT43 members are xylan xylosyltransferases required for the elongation of the xylan backbone. *Plant Cell Physiology*, 53: 135-143.

Lerouxel, O., Cavalier, D.M., Liepman, A.H., and Keegstra, K. (2006). Biosynthesis of plant cell wall polysaccharides—A complex process. *Current Opinion in Plant Biology*, 9:621–630.

Madson, M., Dunand, C., Li, X., Verma, R., Vanzin, G. F., Caplan, J., Shoue, D. A., Carpita, N. C., & Reiter, W.-D. (2003). The *MUR3* gene of *Arabidopsis* encodes a xyloglucan galactosyltransferase that is evolutionarily related to animal exostosins. *Plant Cell*, *15*,1662-1670.

Marriott, P. E., Gomez, L. D. and McQueen-Mason, S. J. (2015) Unlocking the poteional of lignocellulosic biomass through plant science, *New Phytologist*, doi:10.1111/nph.13684.

McCarthy, R. L., Zhong, R., and Ye, Z.H. (2009) MYB83 is a direct target of SND1 and acts redundantly with MYB46 in the regulation of secondary wall biosynthesis in *Arabidopsis.* *Plant Cell Physiology*, 50:1950-1964.

Mohnen, D. (2008) Pectin structure and biosynthesis, *Current Opinion in Plant Biology*, 11:266-277.

Murakami, Y., Funada, R., Sano, Y., and Ohtani, J. (1999) The differentiation of contact cells and isolation cells in the xylem ray parenchyma of Populus maximowiczii. *Annuals Botany*, 84:429-435.

Nieminen, K. M., Kauppinen, L., and Helariutta, Y. (2004) A weed for wood? *Arabidopsis* as a genetic model for xylem development. *Plant Physiology*, 135:653-659.

Ohashi-Ito, K. and Fukuda H. (2010) Transcriptional regulation of vascular cell fates, *Current Opinion in Plant Biology*, 13: 670-676.

Oikawa, A., Have Lund, C., Sakuragi, Y., and Scheller, H. V. (2013) Golgi-localized enzyme complexes for plant cell wall biosynthesis. *TRENDS in Plant Science*, 18: 49-58.

Pagant, S., Bichet, A., Sugimoto, K., Lerouxel, O., Desprez, T., McCann, M., Lerouge, P., Vernhettes, S., and Hofte, H. (2002) *KOBITO1* encodes a novel plasma membrane protein necessary for normal synthesis of cellulose during cell expansion in *Arabidopsis*. *Plant Cell*, 14:2001-2013.

Pauly, M. and Keegstra, K. (2010) Plant cell wall polymers as precursors for biofuels, *Current Opinion in Plant Biology*, 13: 305-312.

Peña, M.J., Zhong, R., Zhou, G.-K., Richardson, E.A., O'Neill, M.A., and Darvill, A.G. (2007) *Arabidopsis* irregular xylem8 and irregular xylem9: implications for the complexity of glucuronoxylan biosynthesis. *Plant Cell*. 19: 549–563.

Pimrote, K., Tian, Y., and Lu, X. (2012). Transcriptional regulatory network controlling secondary cell wall biosynthesis and biomass production in vascular plants. *African J. Biotechnol*. 11: 13928–13937.

Plomion, C., Leprovost, G., and Stokes, A. (2001). Wood formation in trees. *Plant Physiology*, 127:1513-1523.

Ridley, B.L., O'Neill, M.A., and Mohnen, D. (2001) Pectins: structure, biosynthesis, and oligogalacturonide-related signaling. *Phytochemistry*, 57: 929-967.

Reiter, W-D. (2002) Biosynthesis and properties of the plant cell wall. *Current Opinion in Plant Biology*, 5: 536-542.

Simmons, B.A., Loque´, D., and Ralph, J. (2010) Advances in modifying lignin for enhanced biofuel production. *Current Opinion in Plant Biology*, 13: 313-320.

Taylor, N.G. (2008). Cellulose biosynthesis and deposition in higher plants. *New Phytologist*, 178:239–252.

Thompson, D.S. (2005). How do cell walls regulate plant growth? J. Exp. Bot. 56: 2275–2285.

Vanholme, R., Morreel, K., Ralph, J., and Boerjan, W. (2008) Lignin engineering. *Current Opinion in Plant Biology*, 11: 278-285.

Vodenicˇarova´, M., Drimalova´, G., Hroma´dkova´, Z., Malovikova´, A., and Ebringerova´, A. (2006) Xyloglucan degradation using different radiation sources: A comparative study. *Ultrasonics Sonochemistry*, 13: 157-164.

Vogel, J. (2008) Unique aspects of the grass cell wall. *Current Opinion in Plant Biology*, 11:301-307.

Wang, H., Avci, U., Nakashima, J., Hahn, M.G., Chen, F., and Dixon, R.A. (2010). Mutation of WRKY transcription factors initiates pith secondary wall formation and increases stem biomass in dicotyledonous plants. *Proceedings of the National Academy of Science USA*, 107:22338-22343.

Wang, H., Zhao, Q., Chen, F., Wang, M., and Dixon, R.A. (2011). NAC domain function and transcriptional control of a secondary cell wall master switch. *Plant Journal*, 68:1104-1114.

Wang, H.Z. and Dixon, R.A. (2012). On-Off switches for secondary cell wall biosynthesis. *Molecular Plant*, 5:297-303.

Wu, A-M, Rihouey, C., Seveno, M., Ho¨rnblad, E., Singh, S.K., Matsunaga, T., Ishii, T., Lerouge, P., and Marchant, A. (2009) The *Arabidopsis IRX10* and *IRX10*-LIKE glycosyltransferases are critical for glucuronoxylan biosynthesis during secondary cell wall formation. *Plant Journal*, 57: 718-731.

Wu, A-M., Ho¨rnblad, E., Voxeur, A., Gerber, L., Rihouey, C., and Lerouge, P. (2010a) Analysis of the *Arabidopsis IRX9*/*IRX9*-L and *IRX14*/ *IRX14*-L pairs of glycosyltransferase genes

reveals critical contributions to biosynthesis of the hemicellulose glucuronoxylan. *Plant Physiology*, 153: 542–554.

Ye, Z-H (2002) Vascular tissue differentiation and pattern formation in plants, *Annual Review in Plant Biology*, 53: 183-202.

Ye, Z.H., York, W.S., and Darvill, A.G. (2006). Important new players in secondary wall synthesis. *TRENDS in Plant Sciences*. 11:162–164.

Zabotina, O. A., van de Ven, W. T. G., Freshour, G., Drakakaki, G., Cavalier, D., Mouille, G., Hahn, M. G., Keegstra, K., & Raikhel, N. V. (2008). *Arabidopsis XXT5* gene encodes a putative α-1,6-xylosyltransferase that is involved in xyloglucan biosynthesis. *Plant Journal, 56,* 101-115.

Zeng, W., Chatterjee, M., and Faik, A. (2008). UDP-xylose-stimulated glucuronyltransferase activity in wheat microsomal membranes: characterization and role in glucurono(arabino)xylan biosynthesis. *Plant Physiology*, 147:78–91.

Zeng, W., Jiang, N., Nadella, R., Killen, T.L., Nadella, V., and Faik, A. (2010) A glucurono (arabino) xylan synthase complex from wheat contains members of the GT43, GT47, and GT75 families and functions cooperatively. *Plant Physiology*, 154: 78-97.

Zhang, J., Elo, A., and Helariutta, Y. (2011) *Arabidopsis* as a model for wood formation, *Current Opinion in Biotechnology*, 22: 293-299.

Zhong, R., Taylor, J.J., and Ye, Z-H (1997) Disruption of interfascicular fiber differentiation in an *Arabidopsis* mutant. *Plant Cell* 9:2159-2170.

Zhong, R., Peña, M.J., Zhou, G.-K., Nairn, C.J., Wood-Jones, A., Richardson, E.A., Morrison, W.H., Darvill, A.G., York, W.S. and Ye, Z.-H. (2005) *Arabidopsis* Fragile Fiber8, which

encodes a putative glucuronyltransferase, is essential for normal secondary wall synthesis. *Plant Cell* 17: 3390–3408.

Zhong, R., Demura, T., and Ye, Z-H (2006) SND1, a NAC domain transcription factor, is a key regulator of secondary wall synthesis in fibers of *Arabidopsis*. *Plant Cell* 18:3158-3170.

Zhong, R., Richardson, E.A., and Ye, Z-H (2007) Two NAC domain transcription factors, SND1 and NST1, function redundantly in regulation of secondary wall synthesis in fibers of *Arabidopsis*. *Planta*, 225: 1603-1611.

Zhong, R. and Ye, Z-H (2009) Secondary cell walls, *Encyclopedia of Life Sciences (ELS)*, pp. 1-9.

Zhong, R., Lee, C., and Ye, Z-H (2010) Evolutionary conservation of the transcriptional network regulating secondary cell wall biosynthesis, *TRENDS in Plant Sciences*, 15: 625-632.

Zhong, R. and Ye, Z.H. (2012) MYB46 and MYB83 bind to the SMRE sites and directly activate a suite of transcription factors and secondary wall biosynthetic genes. *Plant Cell Physiology*, 53: 368-380.

CHAPTER 2

XYLAN STRUCTURE AND BIOSYNTHETIC GENES IN SELAGINELLA MOELLENDORFFII, A MODEL SEEDLESS VASCULAR PLANT[1]

[1]Haghighat, M., Teng, Q., Zhong, R., and Ye, Z.H. Accepted by Plant Cell Physiology (2016). Reprinted here with permission of publisher.

ABSTRACT

Xylan is a major cross-linking hemicellulose in secondary walls of vascular tissues in vascular plants. It has been suggested that the recruitment of xylan as a secondary wall component was a pivotal event for the evolution of vascular tissues. To decipher the evolution of xylan structure and xylan biosynthetic genes, we analyzed xylan substitution patterns and characterized genes mediating methylation of glucuronic acid (GlcA) side chains in xylan of the model seedless vascular plant, *Selaginella moellendorffii*, and xylan acetylation in the model non-vascular plant, *Physcomitrella patens*. Using nuclear magnetic resonance (NMR) spectroscopy, we have demonstrated that *S. moellendorffii* xylan consists of β-1,4-linked xylosyl residues substituted solely with methylated GlcA residues and that xylans from *S. moellendorffii* and *P. patens* are acetylated at *O*-2 and *O*-3. The finding that xylans from both *S. moellendorffii* and *P. patens* are acetylated indicates that the ability to acetylate xylans was acquired when land pants appeared. To investigate genes responsible for GlcA methylation of xylan, we identified two DUF579 genes in the *S. moellendorffii* genome and showed that one of them, *SmGXM,* encodes a glucuronoxylan methyltransferase capable of adding the methyl group onto the GlcA side chain of xylooligomers. This finding indicates that vascular plants recruited ancestral DUF579 genes as methyltransferases for xylan methylation.

INTRODUCTION

One of the most important events in the history of life was the colonization of land by the ancestral green algae (Mikkelsen et al., 2014). Since the terrestrial organisms are exposed to the stress of drought and gravity, invasion from water to land has required some innovations including the coticule layer to protect the body of land plants from drought and microbe infection as well as the presence of lignin as a major compound of the secondary wall of conductive and supporting cells in vascular plants. Living under a strong stress of gravity, land plants develop vascular tissues for water and nutrient conduction due to presence of secondary cell wall biosynthetic pathways (Kato, 2010).

The bulk of plant biomass is cell walls that are mainly made of cellulose, hemicelluloses and lignin. The complex structure of xylan includes the backbone consisting of a linear chain of β-(1,4)-linked xylosyl residues that are often substituted to various degrees with glucuronic acid (GlcA), methylglucuronic acid (MeGlcA), and arabinose depending on the plant species (Zhong and Ye 2015). *Arabidopsis* xylan is substituted with both GlcA and MetGlcA, while dicot wood xylan is decorated predominantly with MetGlcA, and xylan from grasses and gymnosperms has arabinose residues and GlcA/MetGlcA. The addition of side chains may prevent the xylan polymer from self-assembling. A unique tetrasaccharide sequence, β-D-Xyl*p*-(1→3)-α-L-Rha*p*-(1→2)-α-D-Gal*p*A-(1→4)-D-Xyl, at the reducing end of the xylan chain is conserved in a range of plant species. This conservation suggests that it plays a critical role in the synthesis or function of the xylan (Lee et al., 2007, 2010, and 2011). Based on the complex structure of xylan, it is estimated that at least 8 enzymes are needed to be involved in biosynthesis of the reducing end tetrassaccharide sequence (GT8 families including IRX8 and PARVUS), the elongation of the xylan backbone (GT43 families including *IRX9* and *IRX14*; GT47 families including FRA8 and

IRX10), and the addition and modification of side chains (including GUX1/2/3; GXM1/2/3; RWA1/2/3/4). The *Arabidopsis* genome harbors many members of family GT8 of which two, GUX1 and GUX2, are required for xylan glucuronylation. It has been shown that the expression of GUX1 and GUX2 is regulated by *SND1*, a secondary wall NAC master switch, and they are expressed predominantly in both interfascicular and xylem cells, while the expression of *GUX3*, an additional homolog, is only observed in xylem cells of stem. Mutations of two *Arabidopsis* GT8 genes, *GUX1* and *GUX2*, affect the addition of GlcA and MeGlcA side chains to xylan, and simultaneous mutations of *GUX1/2/3* cause a complete loss of GlcA and MeGlcA side chains on xylan, leading to the reduced secondary wall thickening and altered plant growth (Lee et al., 2012a). This indicates that all three GUX proteins are glucuronyltransferases and function redundantly in the GlcA substitution of xylan, but the expression of all three GUX genes is required for the normal addition of GlcA side chains onto xylan. In spite of its biological importance for plant development, xylan is one of the factors contributing to biomass recalcitrance not only through blocking the accessibility of degrading enzymes to cellulose but also through the negative impact of the various substitutions in xylan on the digestion of xylan by xylanolytic enzymes.

Xylan acetylation can occur at O-2 or O-3 of different xylosyl residues, and at O-3 of xylosyl residues substituted at O-2 with GlcA/MeGlcA (monoacetylation), and at both O-2 and O-3 of the same xylosyl residue (diacetylation). There exist four *RWA* (reduced wall acetylation) genes in the *Arabidopsis* genome that are known to affect xylan acetylation. Lee et al. (2011b) demonstrated that simultaneous mutations of these four *Arabidopsis RWA* genes cause a reduction in all acetyl groups at different positions of xylosyl residues. This finding indicates that *rwa* mutations affect a general process of xylan acetylation at different positions. RWA proteins like their CAS1 homolog from *Cryptococcus neoformans* have multiple transmembrane domains but

they lack a large loop of putative acetyltransferase domain. It has been proposed that RWAs are putative transporters to transport acetyl CoA from the cytoplasm to the Golgi lumen (Yuan et al., 2013). Therefore, a defect in the acetyl CoA transportation could cause a reduction in the supply of acetyl CoA in the Golgi leading to a uniform reduction of acetyl substitutions at different positions of the xylosyl residues in the *rwa 1/2/3/4* quadruple mutant.

About 60% of xylosyl residues in *Arabidopsis* xylan are acetylated. Yuan et al. (2013) found that another *SND1*-activated gene, *ESKIMO1* (*ESK1*) a DUF231 domain-containing protein, plays a critical role in the acetylation of xylan during secondary wall biosynthesis. The *ESK1* gene is specifically expressed in xylem and interfascicular fibers, and its encoded protein is localized in the Golgi where the biosynthesis of xylan occurs. While the mutation of *esk1* in *Arabidopsis* causes a reduction in secondary wall thickness and stem strength with no effect on xylan content, the *esk1* mutation causes specific reduction in the degree of xylan 2-O or 3-O-monoacetylation and in the activity of xylan acetyltransferase but no specific defect in 2,3-di-O-acetylation or 3-O-acetylation of xylosyl residues substituted at O-2 with GlcA. The analysis of *esk1* xylan revealed a 70% increase in GlcA/MeGlcA substitution compared to the wild type. Since the addition of GlcA/MeGlcA side chains occurs at O-2 of xylosyl residues where acetyl groups are also added, the reduction in acetylation at O-2 of xylosyl residues in *esk1* mutants may provide more O-2 positions available for GlcA substitutions. It has been also demonstrated that the relative amount of the overall acetyl groups in xylan isolated from the *gux1/2/3* mutant with no GlcA/MeGlcA side chains was increased by 23% compared with the wild-type xylan (Lee et al., 2014). Hence, it seems that xylan acetyltransferases and glucuronyltransferases compete with each other for xylosyl residues for their acetylation or GlcA substitutions.

Presence of xylan in the structure of *Selaginella moellendorffii,* a seedless vascular plant, and *Physcomitrella patens,* a non-vascular plant, has been detected by comprehensive microarray polymer profiling (CoMPP) analyses. *Selaginella moellendorffii* is a member of the lycopsid lineage, which diverged from the Euphyllophyta, ferns and seed plants, about 400 million years ago (Harholt et al., 2012). Lycopsids have typical features of vascular plants including a true vascular system for water and assimilate transport, which separate them from the mosses. CoMPP analysis of *S. moellendorffii* detected many of the polysaccharides found in higher plants including *Arabidopsis*. In *S. moellendorffii,* there is only one vascular bundle located in the middle of stem. The cortex contains cells with very thick secondary walls due to the presence of both xylan and lignin (Figure 2.1 and 2.2). Both cortical sclerenchyma and xylem cells have been shown to be positively immunostained with xylan monoclonal antibody LM10 (Harholt et al., 2012).

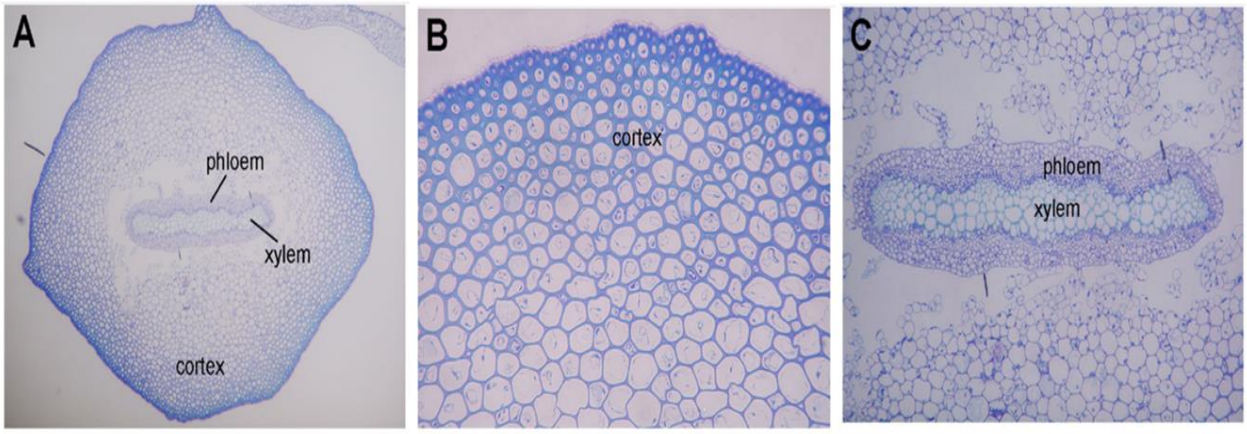

Figure 2.1- Structure of vascular system in *S. moellendorffii. S. moellendorffii* stem was fixed, embedded, sectioned, and examined under a light microscope for anatomy.

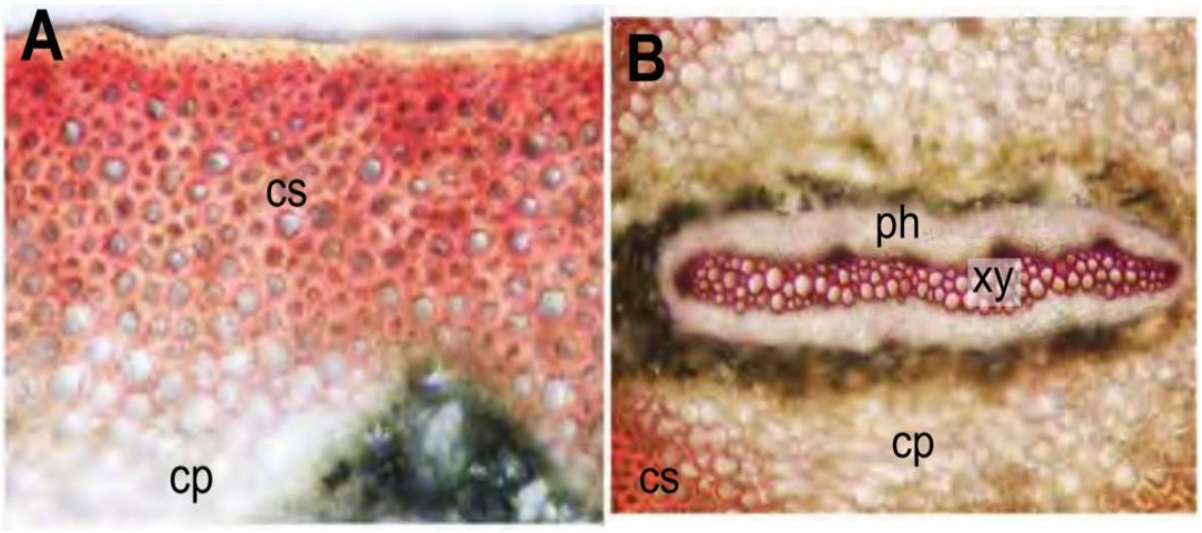

Figure 2.2- (A) and (B) Cross sections of stems of *S. moellendorffii* showing the thick-walled cortical sclerenchyma cells (A) and xylem cells (B). The sections were stained for lignin by phloroglucinol-HCl. cp, cortical parenchyma; cs, cortical sclerenchyma; ph, phloem; xy, xylem.

Physcomitrella patens, a member of the Funariales, resides in a phylogenetic position at the base of the true mosses, and has diverged from land plants before the acquisition of well-developed vasculature. *P. patens* can be found in moist soils where it tolerates dehydration but not desiccation, so it represents a "primitive moss ecology" (Roberts et. al, 2012). Cell wall polysaccharide composition has been investigated in *P. patens* using comprehensive microarray polymer profiling (CoMPP) as a complement to biochemical methods to examine the distribution of polysaccharides (Roberts et al., 2012). Moller et al. (2007) have presented evidence for the presence of xylan in *P. patens* chloronemal filament cell walls. Immunolabeling of leafy gametophore cross-sections with several monoclonal antibodies such as LM11, CCRC-M147, CCRC-M154 and CCRC-M160 detected diverse and distinct xylan epitopes. The linear and substituted xylan in the walls of cells known as axillary hair cells was detected by LM11. Axillary

hair cell walls and leaf cell walls were labeled by CCRC-M137 which binds to a xylan epitope distinct from the ones recognized by other xylan-directed antibodies. Unsubstituted xylan detected by LM10 was not evident in the axillary hair cell walls and very weak labeling was detected in the leaf cell walls. Shoot axis cells were not labeled by any of these xylan-directed monoclonal antibodies, indicating very low abundance of xylan epitopes in the protonemal filament (Kullkarni et al. 2012). The presence of xylan in the axillary hair cells may be related to its biological function and different pattern of gene expression in the axillary hair cells than in other *P. patens* cells and tissues (Hiwatashi et al., 2001). Deposition of glucuronoxylan in vascular plant cell walls are required for the mechanical support and water transport capabilities to enable these plants to survive in the terrestrial environment. Medina et al. (2011) have suggested that axillary hair cells of mosses secrete mucilage to protect newly formed tissues from desiccation. Although glucuronoxylan in *P. patens* has a similar structure to glucumoroxylans in the secondary cell walls of vascular plants, it lacks the unique tetrasaccharide sequence found at the reducing end of the xylan chains in vascular plants. A detailed structural analysis has indicated that O-methylation of glucosyluronic acid evolved after divergence of mosses and vascular plants because glucuronoxylan in *P. patens* is made of a 1,4-linked β-D-xylan backbone and α-D-glucosyluronic acid side chains, but no 4-O-methyl- α-D-glucosyluronic acid side chains are present (Roberts et al., 2012). Xyloglucan detected in *P. patens* has an XXGGG branching pattern, and having pairs of side chains separated by a single xylosyl and possibly an unidentified pentosyl residue make the structure of xylan unusual. Putative homologs of the *Arabidopsis* xyloglucan xylosyltransferases XXT1 and XXT2, and galactosyltransferases MUR3 and GT18 haven been found in the *P. patens* genome. However, it was suggested that the *P. patens* homologs differ from MUR3/GT18 in substrate specificity because xylopyranosyl residues of *P. patens* xyloglucan are

substituted with galactosyluronic acid or arabinopyranosyl residues instead of galactopyranosyl residues (Pena et.al, 2008). Members of GT43 (*IRX9*, *IRX9L*, *IRX14*, *IRX14L*) and GT47 (*RX10*, *I10L*) are involved in xylan backbone synthesis in *Arabidopsis*. *P. patens* sequences have been found as a component of the major clades containing the GT43 and GT47 members and their putative seed plant orthologs (Kulkarni et al., 2012).

Because the fine chemical structure of xylan in *S. moellendorffii* has not been previously studied, 1H-nuclear magnetic resonance (NMR) spectroscopy was employed in this study to analyze the structure of xylan in *S. moellendorffii* and the distribution pattern of acetyl groups in both *S. moellendorffii* and *P. patens.*

RESULTS

Structure of *Selaginella moellendorffii* xylan

To investigate the biochemical mechanism controlling xylan biosynthesis in *S. moellendorffii*, xylan was isolated from *S. moellendorffii* stems and subjected to structural analysis. KOH-extracted xylan was first digested with β-1, 4-endoxylanse and its structure was subsequently analyzed using nuclear magnetic resonance (NMR) spectroscopy. *S. moellendorffii* xylan displayed similar resonances attributed to the backbone xylosyl residues and the GlcA side chain of *Arabidopsis* xylan. It had similar NMR signals for the backbone [branched (4.62 ppm) and unbranched (4.46 ppm) xylosyl residues] and methylated GlcA (5.29 ppm) as *Arabidopsis* xylan, and it exhibited little signals for unmethylated GlcA (5.31 ppm). The signals for a unique tetrasaccharide sequence, β-D-Xyl-(1→3)-α-L-Rha-(1→2)-α-D-GalA-(1→4)-D-Xyl found at the reducing end of xylan chains in *Arabidopsis* were not evident in *S. moellendorffii* xylan (Figure 2.3).

S. moellendorffii and *P. patens* xylans were extracted with Dimethyl Sulfoxide (DMSO) to study the acetylation pattern. ^{1}H NMR analysis of DMSO-extracted xylan has revealed the presence of the characteristic resonances for acetyl groups around 2.2 ppm (Figure 2.4). Integration analysis of acetyl and carbohydrate signals showed that the average degree of acetyl substitution of xylosyl residues (DS_{AC}) in *S. moellendorffii* and *P. patens* xylans were 0.42 and 0.21, which were lower than that of *Arabidopsis* xylan (DS_{AC} = 0.60).

Similar to *Arabidopsis* xylan, *S. moellendorffii* and *P. patens* xylans exhibited NMR signals for 2-*O*- and 3-*O*-monoacetylated, 2,3-di-*O*-acetylated, and 3-*O*-acetylated 2-*O*-GlcA-substituted xylosyl residues (Figure 2. 5). Integration analysis showed that both *S. moellendorffii* and *P. patens* xylans had a very low level of 3-*O*-monoacetylation compared with *Arabidopsis* xylan (Table 2.1). Unlike *Arabidopsis* xylan, *S. moellendorffii* xylan appeared to have a higher level of GlcA/MeGlcA substitutions (Table 2.1). Together, these structural analyses have demonstrated that *S. moellendorffii* xylan is composed of a backbone of β-1, 4-xylosyl residues substituted with MeGlcA and acetylated at *O*-2 and *O*-3.

P. patens xylan has a 1,4-linked β-D-xylan substituted with only GlcA side chains and also acetylated at O-2 and O-3. It has been shown that the acetylation of xylan in *Arabidopsis* is catalyzed by the *SND1*-activated gene, ESK1 and its close homologs that belong to the DUF231 protein family (Yuan et al., 2013 and 2016). The *S. moellendorffii* and *P. patens* genomes contain 16 and 17 DUF231 genes, respectively. Since they are not phylogenetically grouped with *ESK1* (Figure 2. 6), it will be interesting to study whether any of *S. moellendorffii* DUF 231 genes are involved in xylan acetylation.

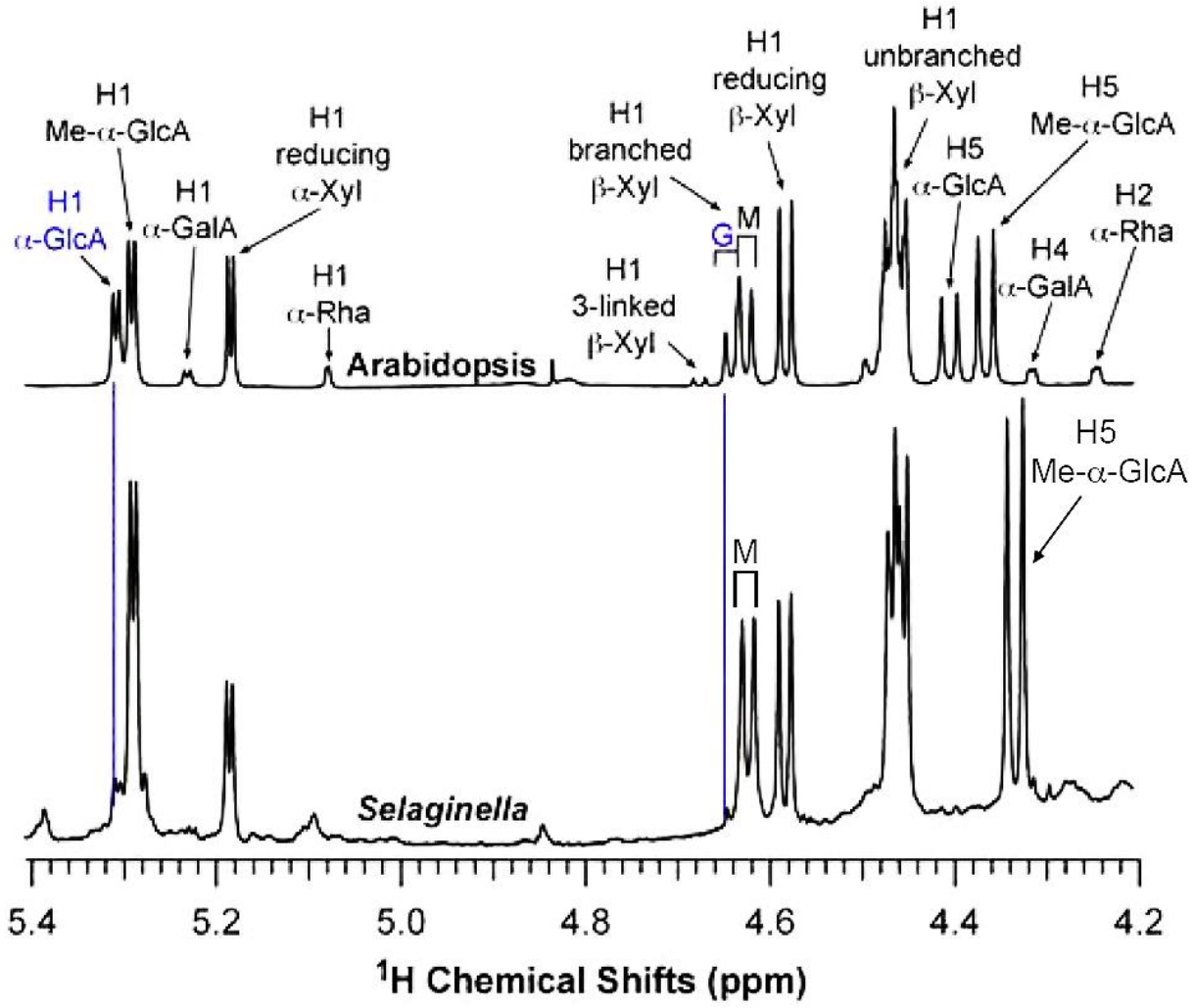

Figure 2.3- NMR spectrum of xylan from *S. moellendorffii* in comparison with that from *Arabidopsis*. KOH-extracted xylan was digested with xylanase and the released xylooligomers were subject to ^{1}H-NMR analysis. The proton resonances are labeled with the identity of the sugar residues. G denotes GlcA-substituted xylosyl residues and M denotes MeGlcA-substituted xylosyl residues. Note the predominance of methylated GlcA residues in xylan from *S. moellendorffii*.

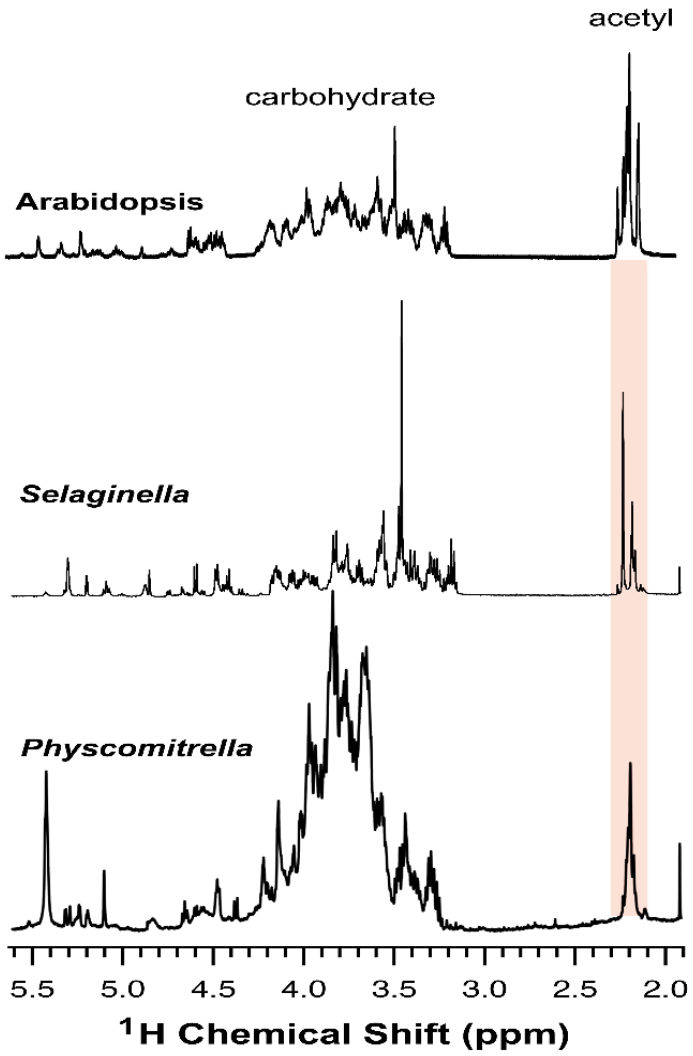

Fig. 2.4- ^{1}H-NMR analysis of acetyl substitutions of *S. moellendorffii* and *P. patens* xylans. Xylan was extracted with DMSO to preserve acetyl groups, which was subsequently subject to ^{1}H-NMR analysis. DMSO-extracted xylan from *Arabidopsis* was included for comparison of the acetyl substitutions.^{1}H-NMR spectra of xylans from *Arabidopsis*, *S. moellendorffii*, and *P. patens* showing the resonance regions for acetyl groups and carbohydrate.

Table2.1. Substitution patterns of acetyl groups in xylans from *Arabidopsis, S. moellendorffii* and *P. patens*

Structural fragment	Relative Abundance (mol%)		
	Arabidopsis	***S. moellendorffii***	***P. patens***
Non-acetylated xylose (Xyl)	43	60	79
2-O-Acetylated xylose (Xyl-2Ac)	15	13	9
3-O-Acetylated xylose (Xyl-3Ac)	18	2	2
2,3-di-O-Acetylated xylose (Xyl-2,3Ac)	17	13	5
3-O-Acetylated, 2-O-GlcA-substituted xylose (Xyl-3Ac-2GlcA)	7	12	5
GlcA/MeGlcA	9	25	11

Non-acetylated and 2-O-monoacetylated xylosyl residues are integrated based on their anomeric proton resonances, and 3-O-monoacetylated, 2,3-di-O-acetylated and 3-O-acetylated 2-O- GlcA/MeGlcA-substituted xylosyl residues are integrated based on their H3 resonances (Figure 2.5). The total balance of acetyl groups was verified by integration of acetyl signals at 2.2 ppm (Figure 2.4).

Biochemical characterization of a glucuronoxylan methyltransferase from *S. moellendorffii*

Finding that all the GlcA side chains were methylated in *S. moellendorffii* xylan inspired us to identify and biochemically characterize *S. moellendorffii* gene(s) involved in glucuronoxylan methylation. *S. moellendorffii* genome contains close homologs of *Arabidopsis IRX9, IRX14, IRX10, FRA8, GUXs, GXMs,* and *RWAs,* but not those of *IRX8, PARVUS, ESK1,* and *IRX15*. The same true for the moss *P. patens* (Table 2.2 and Figure 2.10). Based on the reverse transcription

PCR analysis, all of these *S. moellendorffii and P. patens* homologs of xylan biosynthetic genes except *SmGUX3, PpGUX1* and *PpRWA3* were transcribed, indicating that these genes are expressed and most likely are functional (Figure 2.7). To functionally characterize genes involved in glucuronoxylan methylation, *S. moellendorffii* and *P. patens* homologs of *Arabidopsis* GXMs which are members of DUF579 family, were used for further analysis. A total of two DUF579 genes in *S. moellendorffii* and one DUF579 gene in *P. patens*, all of which are phylogenetically grouped with each other more closely than with the *GXM* group and the *IRX15* group in *Arabidopsis* (Figure 2.8).

To investigate whether their encoded proteins possess methyltransferase activities, we fused the *S. moellendorffii* and *P. patens* DUF579 cDNAs with that of the maltose-binding protein (MBP) and expressed in *E. coli* for purification of their recombinant proteins. When recombinant proteins were incubated with S-[^{14}C-methyl] adenosylmethionine (SAM) and GlcA-substituted xylotetraose [(GlcA)Xyl$_4$], a high level incorporation of radioactivity into the (GlcA)Xyl$_4$ oligosaccharides was detected for SmGXM but not for SmDUF579 and PpDUF579, indicating that SmGXM was able to transfer methyl groups from the methyl donor (SAM) onto the (GlcA)Xyl$_4$ acceptors (Figure 2.9 A and B).

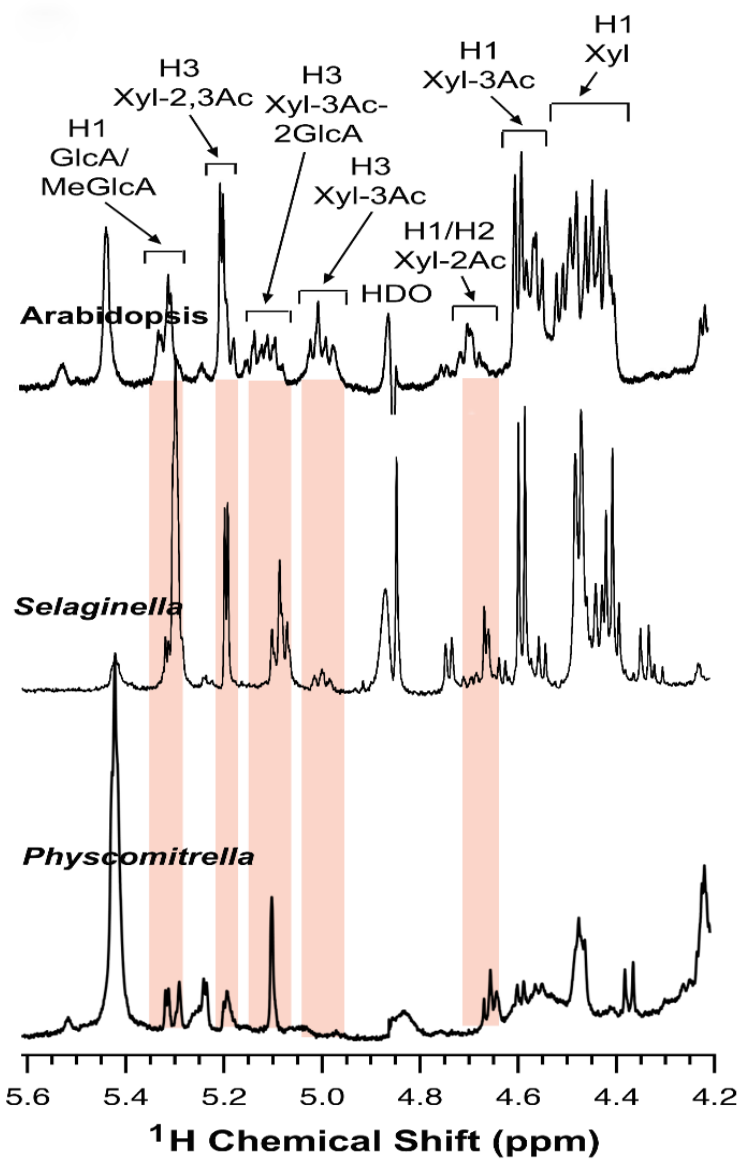

Figure 2.5: The fingerprint regions of ^{1}H-NMR spectra of xylans from *Arabidopsis*, *S. moellendorffii* and *P. patens* showing the resonances corresponding to various acetylated xylose residues including 2-*O*-acetylated (Xyl-2Ac), 3-*O*-acetylated (Xyl-3Ac), 2,3-di-*O*-acetylated (Xyl-2,3Ac), and 3-*O*-acetylated 2-*O*-GlcA/MeGlcA-substituted (Xyl-3Ac-2GlcA). The resonances for non-acetylated xylosyl residues (Xyl) and GlcA/MeGlcA side chains are also identified. HDO, hydrogen deuterium oxide.

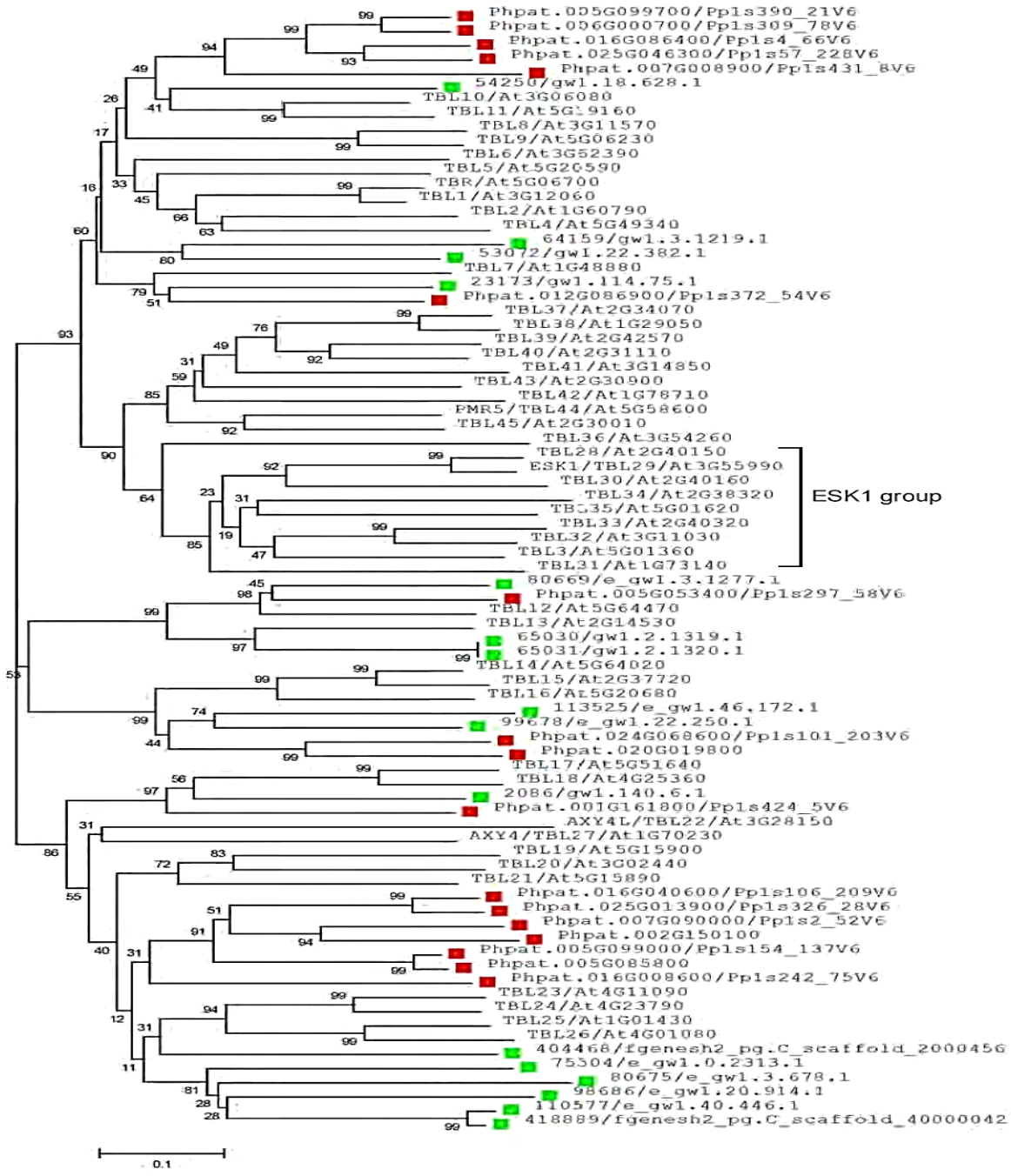

Figure 2.6: Phylogenetic relationship of DUF231 genes from *Arabidopsis thaliana*, *Physcomitrella patens* (marked with red squares) and *Selaginella moellendorffii* (marked with green squares). The phylogenetic tree was constructed with the neighbor-joining algorithm and bootstrap values resulted from 1,000 replicates are shown as percentages at the node. The 0.1 scale denotes 10% change.

Table 2.2: List of close homologs of *Arabidopsis* xylan biosynthetic genes in *S. moellendorffii* and *P. patens*.

***Arabidopsis* genes**	***S. moellendorffii* homologs (gene and locus names)**	***P. patens* homologs (gene and locus name)**
RX9/ *IRX9*L	SmGT43A (e_gw1.2.345.1)	PpGT43A (Pp1s52_108V6) PpGT43B (Pp1s1_540V6)
IRX14/*IRX14*L	SmGT43B (gw1.32.71.1)	PpGT43C (Pp1s78_128V6) PpGT43D (Pp1s248_13V6) PpGT43E (Pp1s19_221V6)
IRX10/IRX10L	SmGT47D1 (estExt_fgenesh2_pg.C_210321)	PpGT47A (Pp1s7_455V6)
FRA8/F8H	SmGT47D2 (estExt_fgenesh2_pg.C_260194)	PpGT47B (Pp1s13_216V6) PpGT47C (Pp1s217_58V6) PpGT47D (Pp1s315_20V6)
GUX1/2/3	SmGUX1 (e_gw1.0.1122.1) SmGUX2 (gw1.0.66.1) SmGUX3 (e_gw1.105.51.1)	PpGUX1 (Pp1s223_30V6) PpGUX2 (Phpat.003G104500) PpGUX3 (Pp1s21_381V6)
GXM1/2/3	SmGXM (gw1.38.480.1) SmDUF579 (gw1.59.411.1)	PpDUF579 (Pp1s15_437V6)
RWA1/2/3/4	SmRWA (estExt_Genewise1.C_130194)	PpRWA1 (Pp1s5_239V6) PpRWA2 (Pp1s74_21V6) PpRWA3 (Pp1s357_34V6)

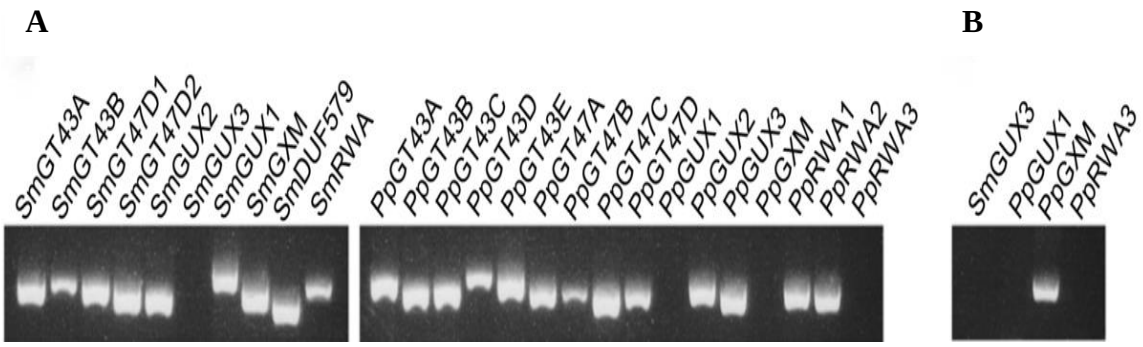

Figure 2.7: Reverse-transcription PCR detection of transcripts of close homologs of *Arabidopsis* xylan biosynthetic genes in *S. moellendorffii* and *P. patens*. Total RNAs from the stems of *S. moellendorffii* and gametophytes/sporophytes of *P. patens* were first treated with DNase and then converted into first-strand cDNAs. A total of 40 ng of cDNAs in each PCR reaction were used as templates for detection of transcripts. **(A)** PCR products of *S. moellendorffii* and *P. patens* genes after 35 cycles of PCR reactions. Note the presence of transcripts of most of the genes except *SmGUX3*, *PpGUX1*, *PpDUF579* and *PpRWA3*. **(B)** RT-PCR products of *SmGUX3, PpGUX1, PpDUF579* and *PpRWA3* after 45 cycles of PCR reactions. Note the presence of the transcript of *PpDUF579*.

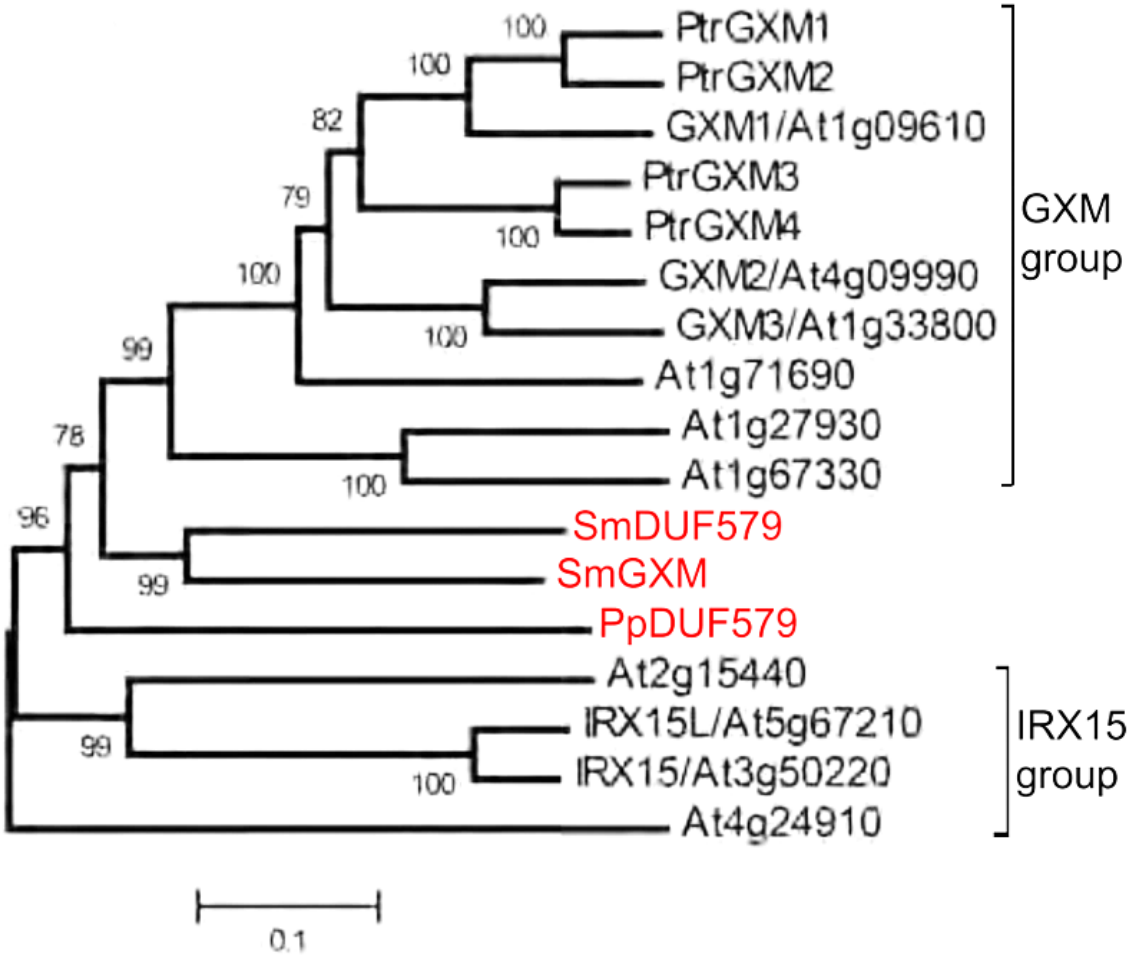

Figure 2.8: Phylogenetic relationship of DUF579 proteins from *S. moellendorffii* (Sm), *P. patens* (Pp), and *Arabidopsis*. GXMs from poplar (Ptr) are also included. The phylogenetic tree was generated with the neighbor-joining algorithm using the neighbor-joining method in MEGA5.2 (Tamura et al., 2011). Numbers at the nodes are percentage bootstrap values from 1000 replicates. The 0.1 scale indicates 10% change.

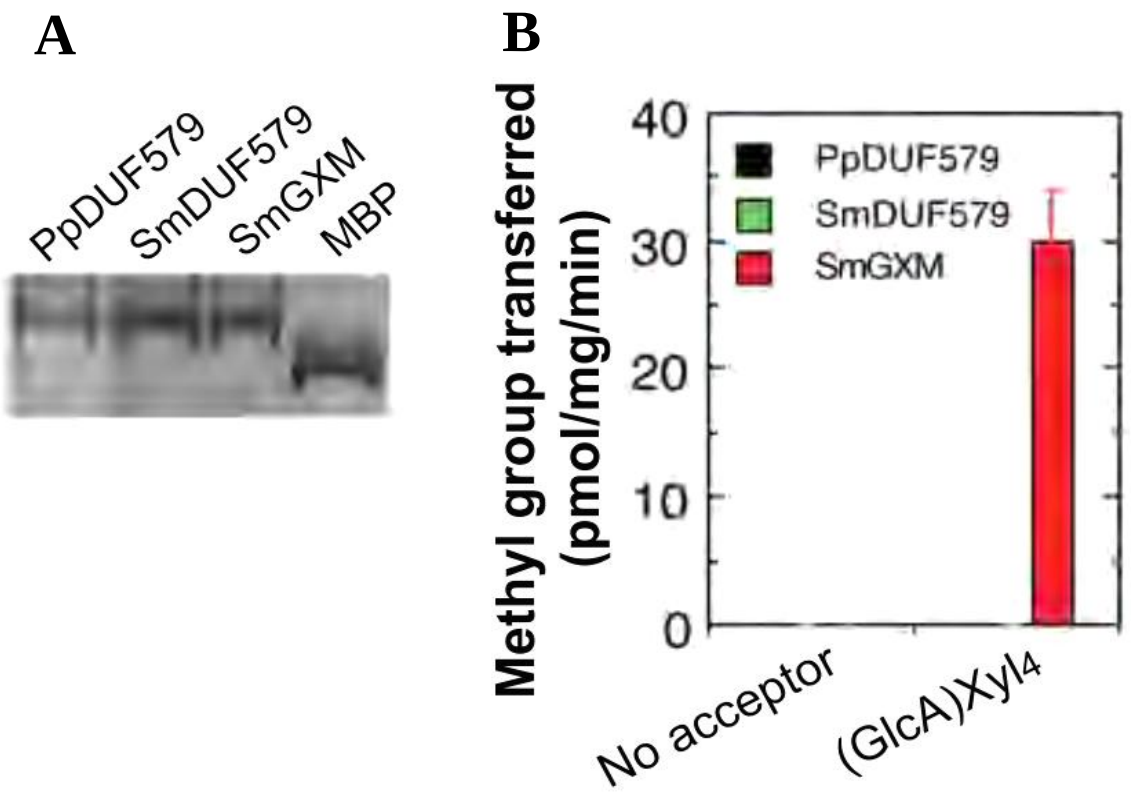

Figure 2.9: Identification of a *S. moellendorffii* DUF579 protein as glucuronoxylan methyltransferase. **(A)** SDS-polyacrylamide gel electrophoresis detection of recombinant MBP-fused DUF579 proteins (PpDUF579, SmDUF579 and SmGXM). Proteins were purified on the maltose-conjugated resins and 5 μg of purified proteins were loaded in each lane. MBP alone was included as a control. **(B)** Methyltransferase activity detection of MBP-fused DUF579 proteins. The proteins were incubated with ^{14}C-labeled methyl donor (^{14}C-SAM) in the presence or absence of the methyl acceptor [(GlcA)Xyl$_4$]. After incubation, the reaction products, ^{14}C-methylated (GlcA)Xyl$_4$, were separated from ^{14}C-SAM on the AG1-X4 resin and counted for the amount of radioactivity. The data were the averages of activities from three separate assays.

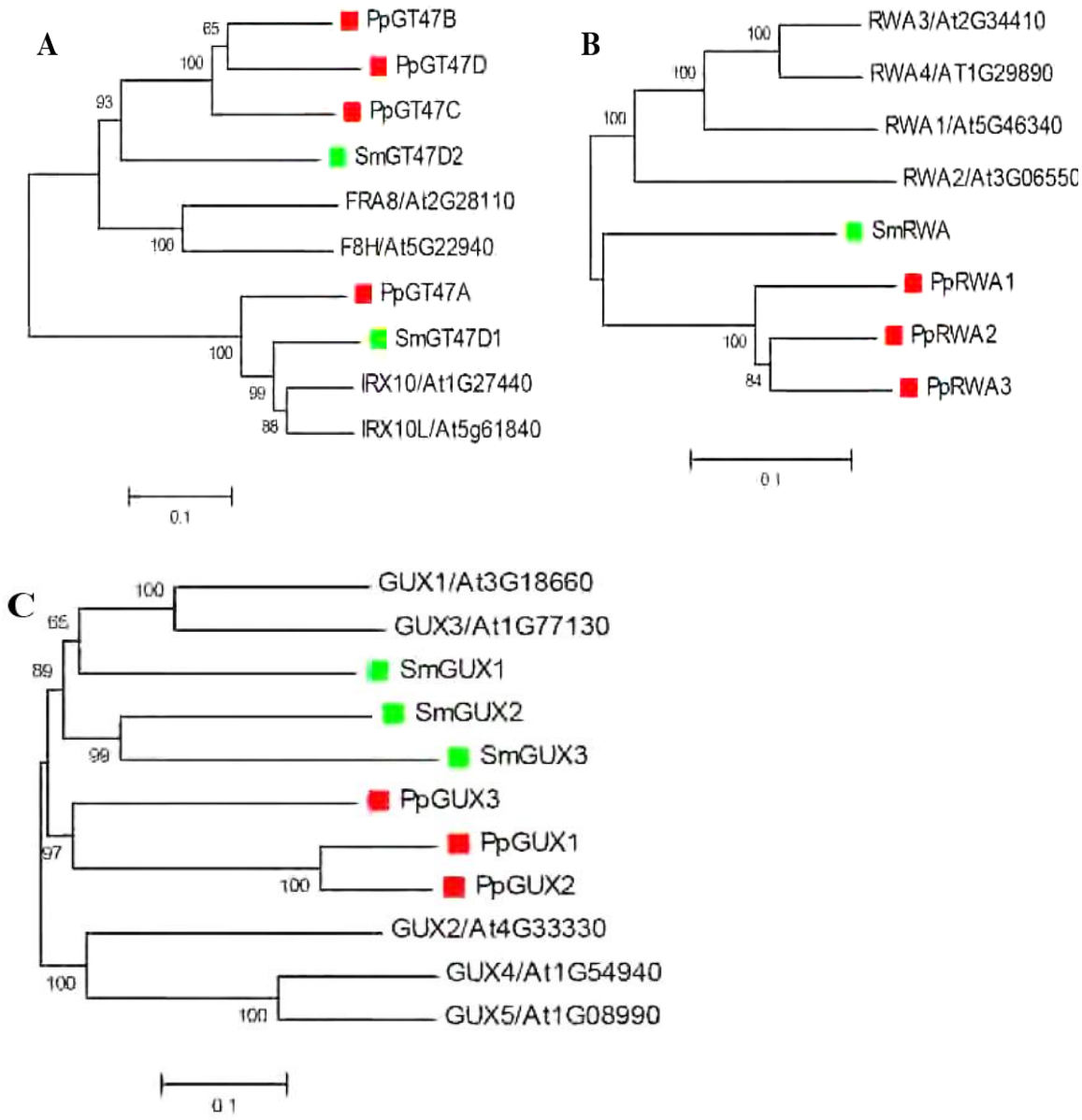

Figure 2.10: Phylogenetic relationship of *Arabidopsis FRA8/F8H* genes **(A)**, *RWA* genes **(B)**, *GUX* genes **(C)** and their close homologs in *Physcomitrella patens* (marked with red squares) and *Selaginella moellendorffii* (marked with green squares). The phylogenetic tree was constructed with the neighbor-joining algorithm and the bootstrap values resulted from 1,000 replicates are shown as percentages at the nodes. The 0.1 scale denotes 10% change.

The MALDI-TOF-MS analysis of the SmGXM-catalyzed reaction products showed appearance of a new ion peak at m/z 759 corresponding to (MeGlcA)Xyl4 in addition to the ion peak at m/z 745 corresponding to the (GlcA)Xyl4 acceptor (Figure 2.11). These results indicate that SmGXM is a glucuronoxylan methyltransferase mediating methylation of the GlcA side chains of xylan in *S. moellendorffii*. Further kinetic analysis revealed that the SmGXM methyltransferase activity is acceptor concentration-dependent with a K_m value of 0.58 mM and a Vmax of 350 pmol/min/mg protein (Figure 2.12).

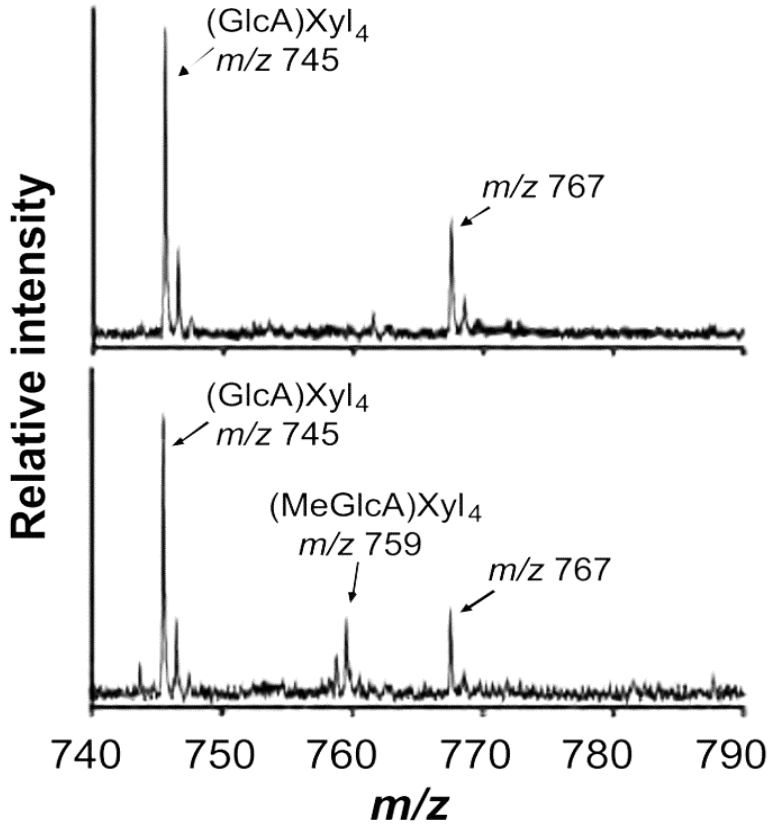

Figure 2.11: MALDI identification of the reaction products catalyzed by SmGXM. The (GlcA)Xyl_4 acceptor has the molecular mass at *m/z* 745 and the methylated (GlcA)Xyl_4 reaction product has the molecular mass at *m/z* 759. Note the presence of the ion at *m/z* 759 in SmGXM-catalyzed reaction products but not in the control (MBP). The ion at *m/z* 767 represent doubly sodiated species of (GlcA)Xyl_4.

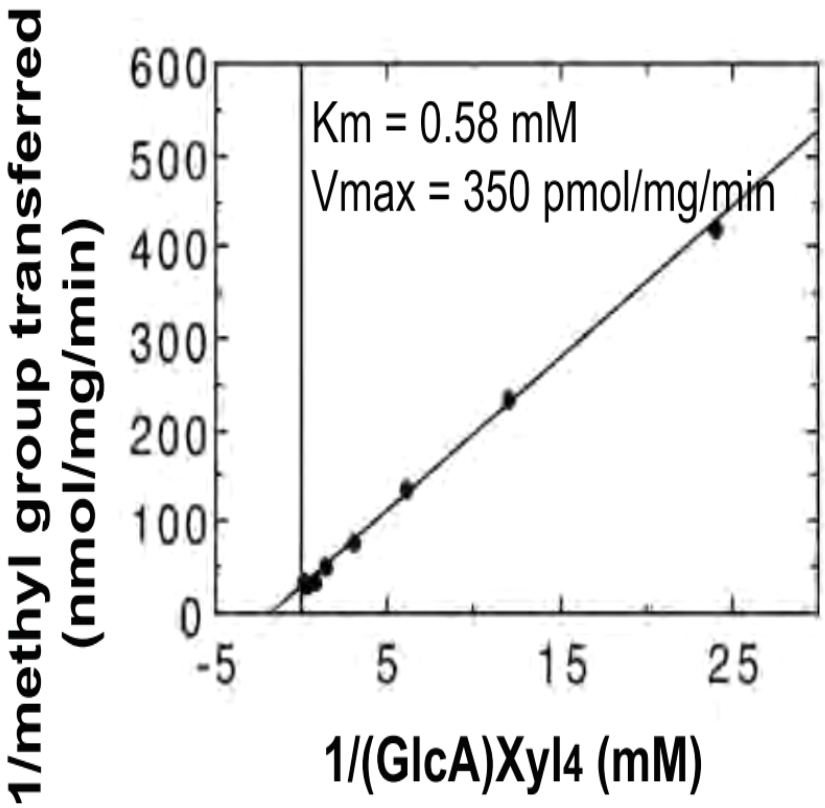

Figure 2.12: Kinetic analysis of the methyltransferase activity of SmGXM. Various concentrations of the methyl acceptor [(GlcA)Xyl_4] were used to assay the methyltransferase activity of SmGXM, and the data were analyzed by the Lineweaver-Burk plot to calculate the K_m and V_{max} values.

DISCUSSION

Our structural analysis of *S. moellendorffii* xylan has shown that its GlcA side chains are almost completely methylated, which differs from *Arabidopsis* xylan in which about 60% of the GlcA side chains are methylated (Lee et al. 2012b). The difference in the degree of GlcA methylation in xylan could be attributed to different enzymatic properties and activities of glucuronoxylan methyltransferases. We have demonstrated that *SmGXM*, one of the two DUF579 genes, in *S. moellendorffii* encodes a protein possessing glucuronoxylan methyltransferase activity

with a K_m value of 0.58 mM toward the (GlcA)Xyl_4 acceptors, which is 6.6 times lower than that of *Arabidopsis* GXM3/GXMT1 (3.85 mM) (Urbanowicz et al. 2012). This indicates that SmGXM has a much higher substrate binding affinity than *Arabidopsis* GXM, which may contribute to the complete methylation of GlcA side chains in *S. moellendorffii* xylan. In agreement with this scenario is the demonstration that the high substrate binding affinity of poplar GXMs correlates with the complete methylation of the GlcA side chains of poplar xylan (Yuan et al. 2014b). The ratio of the relative amount of xylan to the glucuronoxylan methyltransferase activities could also affect the degree of its methylation. It has been shown that a reduction in the total amount of xylan in several *Arabidopsis* xylan mutants results in methylation of all the xylan GlcA side chains (Zhong et al. 2005, Brown et al. 2007, Pena et al. 2007), which is likely attributed to the availability of methyltransferase activities that are sufficient to methylate all of the remaining GlcA side chains in the mutant xylan.

Although there exists a DUF579 gene in *P. patens*, we were unable to detect any glucuronoxylan methyltransferase activity of its encoded protein. This result is consistent with the previous observation that the GlcA side chains of *P. patens* xylan is not methylated (Kulkarni et al. 2012). Because glucuronoxylan methyltransferases from both seedless vascular plants (*S. moellendorffii*) and seed plants (poplar and *Arabidopsis*) are DUF579-containing proteins, it is tempting to propose that early vascular plants might have co-opted ancestral DUF579 genes, through gene duplication and functional diversification, to function as glucuronoxylan methyltransferase. It should be pointed out that two *Arabidopsis* DUF579 proteins, IRX15 and IRX15-L, which do not exhibit glucuronoxylan methyltransferase activity, are also required for normal xylan biosynthesis (Brown et al. 2011, Jensen et al. 2011). Since *SmDUF579* is the only other DUF579 gene beside *SmGXM* in *S. moellendorffii* and PpDUF579 is the only DUF579 gene

in *P. patens*, it will be interesting to investigate whether they perform similar functions as *IRX15* and *IRX15-L* in xylan biosynthesis.

We have demonstrated that *S. moellendorffii* and *P. patens* xylans have an acetyl distribution pattern similar to that of xylan from seed plants (Teleman et al. 2000 and 2002, Evtuguin et al. 2003, Gonçalves et al. 2008, Naran et al. 2009, Marques et al. 2010, Prozil et al. 2012, Yuan et al. 2013). *S. moellendorffii* and *P patens* xylans are monoacetylated at *O*-2 or *O*-3, diacetylated at *O*-2 and *O*-3, and monoacetylated at *O*-3 of xylosyl residues substituted with 2-*O*-MeGlcA. Compared with the acetyl distribution pattern of *Arabidopsis* xylan in which the acetyl groups are abundant at both *O*-2 and *O*-3, *S. moellendorffii* and *P. patens* xylans appear to have fewer acetyl groups at *O*-3. It is interesting to note that *S. moellendorffii* xylan has a lower degree of acetylation than *Arabidopsis* xylan, which coincides with the relative higher amount of GlcA/MeGlcA side chains compared with Arabidopsis xylan. It is possible that the degree of xylan acetylation might affect the addition of GlcA/MeGlcA side chains and vice versa.

The finding that *S. moellendorffii* and *P. patens* xylans are acetylated may have important implications in understanding the evolution of xylan acetylation. It has been shown that xylans from gymnosperms are non-acetylated (Timell 1967), and it is currently unknown in which taxa land plants evolved the ability to acetylate xylans. Because *S. moellendorffii* and *P. patens* xylans contain acetyl substituents, it is tempting to propose that the ability to acetylate xylans evolved as early as land plants appeared and that this ability might have been lost in the lineage of gymnosperms. The acetylation of xylan in *Arabidopsis* has been shown to be catalyzed by ESK1 and its close homologs that belong to the DUF231 protein family (Yuan et al. 2013 and 2016). The *S. moellendorffii* and *P. patens* genomes harbor 16 and 17 DUF231 genes, respectively, but

phylogenetically they are not grouped together with ESK1. It will be interesting to study whether any of *S. moellendorffii* and *P. patens* DUF231 genes are involved in xylan acetylation.

MATERIALS AND METHODS

Xylan isolation and ^{1}H-NMR spectroscopy

Stems of *S. moellendorffii* and *Arabidopsis* were ground into powders in a mortar and pestle and subsequently extracted in acetone and ethanol. The resulting alcohol-insoluble cell wall residues were dried and used for xylan isolation. Xylan was extracted from alcohol-insoluble cell wall residues by incubating with 1N KOH or dimethyl sulfoxide (DMSO). The isolated xylan was digested with endo-1,4-β-xylanase M6 (Megazyme) to generate xylooligosaccharides (Zhong et al. 2005). Xylooligosaccharides were subjected to acquisition of NMR spectra on a Varian Inova 600 MHz spectrometer using a 5 mm cryogenic triple resonance probe (Teng et al. 2012). The NMR spectra of samples were collected with 64 transients using a spectral width of 6,000 Hz and an acquisition time of 5-seconds. The proton positions and residue identities in NMR spectra were assigned based on the NMR spectra data for xylans from Arabidopsis and aspen (Teleman et al., 2000; Peña et al., 2007;Yuan et al., 2013). Xylans isolated from three separate pools of samples were examined and identical NMR spectra were obtained.

Gene expression analysis

Total RNAs were isolated from stems of *S. moellendorffii* and gametophytes/sporophytes of *P. patens* with a Qiagen RNA isolation kit (Qiagen). Total RNAs were first treated with DNase I and then converted into first strand cDNAs, which were used as a template for PCR detection of transcripts of interest. The PCR primers for *SmGT47D1* were 5'-gtgatcctcaagaagcaacggctg-3' and 5'-ctaccatggtttcaagtctccagg-3', those for *SmGT47D2* were 5'-gacgtgcacaagctggacaggatc-3' and 5'-tcacgccacttttatccggga-3', those for *SmGUX1* were 5'-gagttcacgacagcatgagcaaga-3' and 5'-tcaggtggtgaccacagcagcagc-3', those for *SmGUX2* were 5'-atgccggcggagctccagaagttt-3' and 5'-tcaatcttccagcaatctcctcct-3', those for *SmGUX3* were 5'-accggctgtccatcaggtttgttc-3' and 5'-

ttacccctcttggtgatgatccta-3', those for *SmDUF579* were 5'-caggagccggaagaatggaacgac-3' and 5'-tcagcaaaagcttttggaggaact-3', those for *SmGXM* were 5'-gagccgcaagactgggaatgggac-3' and 5'-cacacgagctcaattggcgggaga-3', those for *SmRWA* were 5'-cttgtcattcataccggactaccc-3' and 5'-tcatactgaaggcgtggatttctc-3', those for *PpGT47A* were 5'-gactactggctaacccagccatga-3' and 5'-ttacaaatcattgccccaaggata-3', those for *PpGT47B* were 5'-taaacttgataaaatccttctcaa-3' and 5'-tcagtgcttgataaacgatctttc-3', those for *PpGT47C* were 5'-gaaactcgacaagattctcatcgg-3' and 5'-tcactgatttgcaaacgatctgtc-3', those for *PpGT47D* were 5'-aaactttacaaaattcttctcaac-3' and 5'-tcagaagttttcgtgcttgacaaa-3', those for *PpGUX1* were 5'-cagagaatctgcagaaacattgcg-3' and 5'-ctatttccggataaactgggttct-3', those for *PpGUX2* were 5'-cggagaatctgcagaagttttgtt-3' and 5'-tcaggcaagcactgaactcgagga-3', those for *PpGUX3* were 5'-cttcaacggcagtgttggctcagg-3' and 5'-tcaaagagcttgcggtggtggttc-3', those for *PpDUF579* were 5'-cttctgcggttgtagcgcacacaa-3' and 5'-tcaatgggttttatctgaacaaaatcg-3', those for *PpRWA1* were 5'-cctcttctcaactttatgggaact-3' and 5'-ctagaaagccagaagcatcgggag-3', those for *PpRWA2* were 5'-ccacttcttaacttcatggcaaca-3' and 5'-tcagagacccaagagggttgggag-3', and those for *PpRWA3* were 5'-tatccattgctcaacttcatgttg-3' and 5'-ctacaaaaatagactaatatgaag-3',

Production of recombinant fusion proteins

PpDUF579, SmDUF579 and SmGXM cDNAs, excluding the sequences encoding the N-terminal transmembrane domain, were PCR-amplified and ligated in frame with the maltose binding protein (MBP) in the bacterial expression vector pMAL (New England BioLabs). The primers for *PpDUF579* were 5'-ctggctacgtggaatcccgctgcg-3' and 5'-tcaatgggttttatctgaacaaaatcg-3', those for *SmDUF579* were 5'-ctgtgcattctccgggacaccact-3' and 5'-tcagcaaaagcttttggaggaact-3', those for *SmGXM* were 5'-ttactcttccgcgacgctagcaat-3' and 5'-cacacgagctcaattggcgggaga-3'. The recombinant fusion proteins were purified by binding to amylose resin and verified by SDS

polyacrylamide gel electrophoresis. The predicted molecular masses of MBP, PpDUF579-MBP, SmDUF579-MBP and SmGXM-MBP are 42.5 kD, 73.2 kD, 71.6 kD and 73.9 kD, respectively.

Assay of glucuronoxylan methyltransferase activity

Recombinant fusion proteins (20 μg) were incubated with a reaction mixture (50 μl) containing 50 mM HEPES-KOH, pH 7.0, 1 mM $CoCl_2$, 0.2 mg GlcA-substituted Xyl_4 [(GlcA)Xyl_4] and *S*-[^{14}C-methyl] adenosylmethionine (^{14}C-SAM, 0.1 μCi; American Radiolabeled Chemical). After 1-hr incubation at 37 ^{o}C, the reaction products were separated from ^{14}C-SAM by passing through AG1-X4 anion exchange resin (Lee et al. 2012b) and counted for radioactivity with a PerkinElmer scintillation counter. For determination of the substrate binding properties of SmGXM, different concentrations of (GlcA)-Xyl_4 were used for the assay and the resulting activity data were analyzed by Lineweaver-Burk plot to calculate the K_m and V_{max} values. For MALDI-TOF MS analysis of the methyltransferase reaction products, ^{14}C-SAM was replaced with 1 mM non-radiolabeled SAM in the reaction mixture as described above.

MALDI-TOF MS

The samples were mixed with 0.2 M 2,5-dihydroxybenzoic acid (1:1, v/v), dried on a stainless steel target plate and subjected to MALDI-TOF MS analysis as described (Zhong et al. 2005). Spectra are the average of 250 laser shots.

REFERENCES

Brown, D.M., Goubet, F., Wong, V. W., Goodacre, R., Stephens, E., Dupree, P. et al. (2007) Comparison of five xylan synthesis mutants reveals new insight into the mechanisms of xylan synthesis. *Plant J.* 52: 1154-1168.

Brown, D.M., Wightman, R., Zhang, Z., Gomez, L.D., Atanassov, I., Bukowski, J.P. et al. (2011) Arabidopsis genes *IRREGULAR XYLEM* (*IRX15*) and *IRX15L* encode DUF579-containing proteins that are essential for normal xylan deposition in the secondary cell wall. *Plant J.* 66: 401-413.

Evtuguin, D.V., Tomás, J.L., Silva, A.M. and Neto, C.P. (2003) Characterization of an acetylated heteroxylan from Eucalyptus globulus Labill. *Carbohydr. Res.* 338: 597-604.

Gonçalves, V.M., Evtuguin, D.V. and Domingues, M.R. (2008) Structural characterization of the acetylated heteroxylan from the natural hybrid Paulownia elongata/Paulownia fortunei. *Carbohydr. Res.* 343: 256-266.

Harholt, J., Sørensen, I., Fangel, J., Roberts, A., Willats, W.G., Scheller, H.V. et al. (2012) The glycosyltransferase repertoire of the spikemoss *Selaginella moellendorffii* and a comparative study of its cell wall. *PLoS One* 7: e35846.

Hiwatashi, Y., Nishiyama, T., Fujita, T., and Hasebe, M. (2001) Establishment of gene-trap and enhancer-trap systems in the moss Physcomitrella patens. Plant Journal 28, 105- 116.

Jensen, J.K., Kim, H., Cocuron, J.C., Orler, R., Ralph, J. and Wilkerson, C.G. (2011) The DUF579 domain containing proteins IRX15 and IRX15-L affect xylan synthesis in Arabidopsis. *Plant J.* 66: 387-400.

Kato, M. (2010) Evolution of primitive land plants: A review. *Bull. Natl. Mus. Nat. Sci., Ser. B*, 36(1), pp. 1–11.

Kulkarni, A.R., Pena, M.J., Avci, U., Mazumder, K., Urbanowicz, B.R., Pattathil, S. et al. (2012) The ability of land plants to synthesize glucuronoxylans predates the evolution of tracheophytes. *Glycobiology* 22: 439-451.

Lee, C., Zhong, R., Richardson, E.A., Himmelsbach, D.S., McPhail, B.T. and Ye, Z.-H. (2007) The *PARVUS* gene is expressed in cells undergoing secondary wall thickening and is essential for glucuronoxylan biosynthesis. *Plant Cell Physiol.* 48: 1659-1672.

Lee, C., Teng, Q., Huang, W., Zhong, R. and Ye, Z.-H. (2010) The Arabidopsis family GT43 glycosyltransferases form two functionally nonredundant groups essential for the elongation of glucuronoxylan backbone. *Plant Physiol.* 153: 526-541.

Lee, C., Teng, Q., Zhong, R. and Ye, Z.-H. (2011b) Molecular dissection of xylan biosynthesis during wood formation in poplar. *Mol. Plant* 4: 730-747.

Lee, C., Teng, Q., Zhong, R. and Ye, Z.-H. (2012a) Arabidopsis GUX proteins are glucuronyltransferases responsible for the addition of glucuronic acid side chains onto xylan. *Plant Cell Physiol.* 53: 1204-1216.

Lee, C., Teng, Q., Zhong, R., Yuan, Y., Haghighat, M. and Ye, Z.-H. (2012b) Three Arabidopsis DUF579 domain-containing GXM proteins are methyltransferases catalyzing 4-*O*-methylation of glucuronic acid on xylan. *Plant Cell Physiol.* 53: 1934-1949.

Lee, C., Teng, Q., Zhong, R., Yuan, Y. and Ye, Z.-H. (2014) Functional roles of rice glycosyltransferase family GT43 in xylan biosynthesis. *Plant Signal Behav.* 9: e27809.

Marques, G., Gutierrez, A., Del Rio, J.C. and Evtuguin, D.V. (2010) Acetylated heteroxylan from Agave sisalana and its behavior in alkaline pulping and TCF/ECF bleaching. *Carbohydr. Polymers* 81: 517-523.

Mikkelsen, M. D., Harholt, J., Ulvskov, P., Johansen, I. E., Fangel, J. U., Doblin, M. S., Bacic, A. and Willats, W. G. T. (2014). Evidence for land plant cell wall biosynthetic mechanisms in charophyte green algae. *Annals of Botany,114*(6), 1217–1236.

Moller,I., Sørensen,I., Bernal,A.J., Blaukopf,C.,Lee,K.,Øbro,J.,Pet- tolino,F., Roberts,A., Mikkelsen,J. D.,Knox,J.P.,Bacic,A.,andWillats, W.G.T.(2007).High-throughput mapping of cell-wall polymers within and between plants using novel microarrays. *PlantJ.* 50, 1118–1128.

Naran, R., Black, S., Decker, S.R. and Azadi, P. (2009) Extraction and characterization of native heteroxylans from delignified corn stover and aspen. *Cellulose* 16: 661-675.

Pena, M.J., Zhong, R., Zhou, G.-K., Richardson, E.A., O'Neill, M.A., Darvill, A.G., et al. (2007) Arabidopsis irregular xylem8 and irregular xylem9: Implications for the complexity of glucuronoxylan biosynthesis. *Plant Cell* 19: 549-563.

Prozil, S.O., Costa, E.V., Evtuguin, D.V., Lopes, L.P. and Domingues, M.R. (2012) Structural characterization of polysaccharides isolated from grape stalks of Vitis vinifera L. *Carbohydr. Res.* 356: 252-259.

Roberts, A.W., Roberts, E.M. and Haigler, C.H. (2012) Moss cell walls: structure and biosynthesis. *Front. Plant Sci.* 3: 166.

Teleman, A., Lundqvist, J., Tjerneld, F., Stålbrand, H. and Dahlman, O. (2000) Characterization of acetylated 4-O-methylglucuronoxylan isolated from aspen employing 1H and 13C NMR spectroscopy. *Carbohydr. Res.* 329: 807-815.

Teleman, A., Tenkanen, M., Jacobs, A. and Dahlman O. (2002) Characterization of O-acetyl-(4-O-methylglucuronoxylan isolated from birch and beech. *Carbohydr. Res.* 337: 373-377.

Timell, T.E. (1967) Recent progress in the chemistry of wood hemicelluloses. *Wood Sci. Technol.* 1: 45-70.

Urbanowicz, B.R., Peña, M.J., Ratnaparkhe, S., Avci, U., Backe, J., Steet, H.F. et al. (2012) 4-O-methylation of glucuronic acid in Arabidopsis glucuronoxylan is catalyzed by a domain of unknown function family 579 protein. *Proc. Natl. Acad. Sci. USA* 109: 14253-14258.

Yuan, Y., Teng, Q., Zhong, R. and Ye, Z.-H. (2013) The Arabidopsis DUF231 domain-containing protein ESK1 mediates 2-*O*- and 3-*O*-acetylation of xylosyl residues in xylan. *Plant Cell Physiol.* 54: 1186-1199.

Yuan, Y., Teng, Q., Lee, C., Zhong, R. and Ye, Z.-H. (2014a) Modification of the degree of 4-O-methylation of secondary wall glucuronoxylan. *Plant Sci.* 219-220: 42-50.

Yuan, Y., Teng, Q., Zhong, R. and Ye, Z.-H. (2014b) Identification and biochemical characterization of four wood-associated glucuronoxylan methyltransferases in *Populus*. *PLoS One* 9: e87370.

Yuan, Y., Teng, Q., Zhong, R. and Ye, Z.-H. (2016) TBL3 and TBL31, two Arabidopsis DUF231 domain proteins, are required for 3-*O*-monoacetylation of xylan. *Plant Cell Physiol.* doi:10.1093/pcp/pcv172.

Zhong, R. and Ye, Z.-H. (2015) Secondary cell walls: biosynthesis, patterned deposition and transcriptional regulation. *Plant Cell Physiol.* 56: 195-214.

Zhong, R., Peña, M.J., Zhou, G.-K., Nairn, C.J., Wood-Jones, A., Richardson, E.A. et al. (2005) Arabidopsis *Fragile Fiber8*, which encodes a putative glucuronyltransferase, is essential for normal secondary wall synthesis. *Plant Cell* 17: 3390-3408.

CHAPTER 3

EVOLUTIONARY CONSERVATION OF ROLES OF GT43 GENES IN XYLAN BIOSYNTHESIS IN *SELAGINELLA MOELLENDORFFII* AND *PHYSCOMITRELLA PATENS*[2]

[2] Haghighat, M., Teng, Q., Zhong, R., and Ye, Z.H. Accepted by Plant Cell Physiology (2016). Reprinted here with permission of publisher.

ABSTRACT

Xylan, consisting of a linear chain of β-(1,4)-linked xylosyl residues, is the second most abundant polysaccharide in dicot wood and one of the factors contributing to biomass recalcitrance for biofuel production. Xylan polysaccharides have been detected in both nonvascular and vascular plants. To understand the evolution of xylan biosynthetic genes, we investigated GT43 genes from the model seedless vascular plant, *Selaginella moellendorffii* and the model nonvascular plant, *Physcomitrella patens*, for their roles in xylan biosynthesis. We have revealed that the two GT43 genes in *Selaginella moellendorffii*, *SmGT43A* and *SmGT43B*, are functional orthologs of the *Arabidopsis* xylan backbone biosynthetic genes *IRX9* and *IRX14*, respectively, indicating the evolutionary conservation of the involvement of two functionally non-redundant groups of GT43 genes in xylan backbone biosynthesis between seedless and seed vascular plants. Among the five GT43 genes in *Physcomitrella patens*, *PpGT43A* was found to be a functional ortholog of Arabidopsis *IRX9*, suggesting that the recruitment of GT43 genes in xylan backbone biosynthesis occurred when nonvascular plants appeared on land.

INTRODUCTION

Xylan, composed of a linear backbone of β-(1, 4)-linked xylosyl residues, is the main hemicellulose that cross-links with cellulose in the secondary cell walls of dicot plants. Xylan has recently attracted much attention because it might provide an important source of sugars from higher plants that can be used for biofuel production, and also its complex structure negatively impacts the digestion of plant cell walls throughout the process of biofuel production. Glucuronoxylan (GX), the predominant form of xylan in plant secondary cell walls, consists of the backbone of xylosyl residues substituted with α-(1, 2)-linked glucuronic acid (GlcA) and/or methylglucuronic acid (MeGlcA). In addition, a unique tetra-saccharide sequence, β-D-Xyl*p*-(1→3)-α-L-Rha*p*-(1→2)-α-D-Gal*p*A-(1→4)-D-Xyl is found at the reducing end of the xylan chain. This conserved tetra-saccharide may play a critical role in the synthesis or function of the xylan (Lee et al., 2007, 2010, and 2011). Analysis of *Arabidopsis* mutants has revealed a number of genes required for xylan synthesis. The identified genes encompass members of GT47 (*FRA8/IRX7* and *IRX10*), GT43 (*IRX9* and *IRX14*), and GT8 families (*IRX8* and *PARVUS*) of glycosyltransferases. Analysis of mutants for each of these genes indicates that *IRX9*, *IRX10* and *IRX14* encode enzymes that act as xylosyltransferases in the synthesis of the β-1-4 xylan backbone, whereas *FRA8*, *IRX8* and *PARVUS* are likely involved in synthesis of the reducing end tetra-saccharide structure. A complementation study has revealed that the poplar GT43, which is specifically expressed in the secondary xylem in wood, is a functional ortholog of the *Arabidopsis IRX9* and involved in the elongation of the xylan backbone (Lee et al., 2007, 2010, 2011; Wu et al., 2010).

There are four known GT43 genes involved in xylan biosynthesis in *Arabidopsis*. Genetic studies have identified that the *Arabidopsis* GT43 members form two functionally non-redundant groups, *IRX9/IRX9-L* and *IRX14/IRX14-L*, which are essential for the normal elongation of xylan

backbone. Comprehensive molecular and genetic studies have indicated that *IRX9* and *IRX9-L* are a pair of functional homologs, and *IRX14* and *IRX14-L* are another pair of functional homologs. They all are expressed in the same cell types that undergo secondary cell wall thickening, and their encoded proteins are targeted to the Golgi, where GX is synthesized. In addition, mutation of the *IRX9* gene leads to a severe reduction in xylan xylosyltransferase activity and consequently a significant decrease in the GX chain length and GX amount (Lee et al., 2010). Mutation of the *IRX14* gene causes a reduction in the GX level and the xylosyltransferase activity (Lee et al., 2010). Complementation studies have revealed that the GX defects in the *irx9* mutant can be rescued by overexpression of *IRX9-L* but not *IRX14*. Similarly, overexpression of *IRX14-L* but not *IRX9* and *IRX9-L* is able to complement the GX defects in *irx14* mutant (Lee et al., 2010).

Xylan polysaccharides have been detected in non-vascular plants, such as mosses, and vascular plants; however, it is still unknown whether xylan biosynthetic genes are functionally conserved across non-vascular and vascular plants. The genomes of both *Physcomitrella patens*, a non-vascular plant and *Selaginella moellendorffii*, a seedless vascular plant contain a number of GTs that are close homologs of *Arabidopsis* xylan biosynthetic genes. It has been shown that *P. patens GT47A* was able to partially complement the growth defect of *Arabidopsis irx10 irx10-L* mutant and exhibited xylosyltransferase activity, suggesting that *PpGT47A* is a functional orthologs of *Arabidopsis IRX10*. Based on a previous study, both *P. patens* and *S. moellendorffii* have putative orthologs of *IRX14* but lack direct orthologs of *IRX9*, and therefore, it is uncertain whether any of these PpGT43 and SmGT43 genes are functional orthologs of *Arabidopsis IRX9* and *IRX14*. Considering the possibility that some GT families in *P. patens* and *S. moellendorffii* may retain ancestral genes that were lost in seed plants and some may have undergone independent diversification (Harholt et al., 2012), functional characterization of GTs in *P. patens* and *S.*

moellendorffii will be important to understand the evolutionary relationship in different taxa of xylan biosynthetic genes.

RESULTS

Family GT43 glycosyltransferases in *P. patens* and *S. moellendorffii*

The *S. moellendorffii* genome has only two GT43 genes including one *IRX9* close homolog (*SmGT43A*) and one *IRX14* close homolog (*SmGT43B*). The *P. patens* genome contains five GT43 genes including two *IRX9* close homologs (*PpGT43A* and *PpGT43B*) and three *IRX14* close homologs (*PpGT43C, PpGT43D,* and *PpGT43E*). Full-length *IRX9* and *IRX14* sequences from both *P. patens* and *S. moellendorffii* were used to conduct a BlastP search against the *Arabidopsis* protein database. A phylogenetic tree including sequences from *P. patens*, *S. moellendorffii*, and *Arabidopsis* places *IRX14* and *IRX14*-L together in a sub-branch separate from *IRX9* and *IRX9*-L (Figure 3.1).

Functional complementation of *Arabidopsis irx9* and *irx14* mutants by GT43 genes from *P. patens* and *S. moellendorffii*

To investigate whether GT43 genes from *S. moellendorffii* and *P. patens* were functionally conserved with those in *Arabidopsis*, we performed complementation analysis in the *Arabidopsis irx9* and *irx14* mutants. For complementation analysis, the full-length cDNAs of *P. patens* and *S. moellendorffii* GT43 genes were expressed under the CaMV 35S promoter in the *Arabidopsis irx9* and *irx14* mutants. At least 120 transgenic plants were generated and used for cell wall analysis for each complementation. Since the amino acid sequence of PpGT43D shares 80% similarity with that of PpGT43C, PpGT43D was not included in the complementation analysis. Expression of *SmGT43* and *PpGT43* genes in the *irx9* mutant demonstrated that the *P. patens* and *S. moellendorffii IRX9* homologs, including *PpGT43A*, *PpGT43B*, and *SmGT43A*, were able to

restore the rosette size and stem height of *irx9* plants nearly to the wild-type level (Figure 3.2). Furthermore, the mechanical strength of stems of *irx9* expressing *PpGT43A* and *SmGT43A* was comparable to that of the wild type, whereas *PpGT43B* only partially rescued the stem strength phenotype (Figure 3.3). Consistent with the restored stem strength, the collapsed xylem vessel phenotype in *irx9* was rescued by *PpGT43A* and *SmGT43A* (Figure 3.4 A-H).

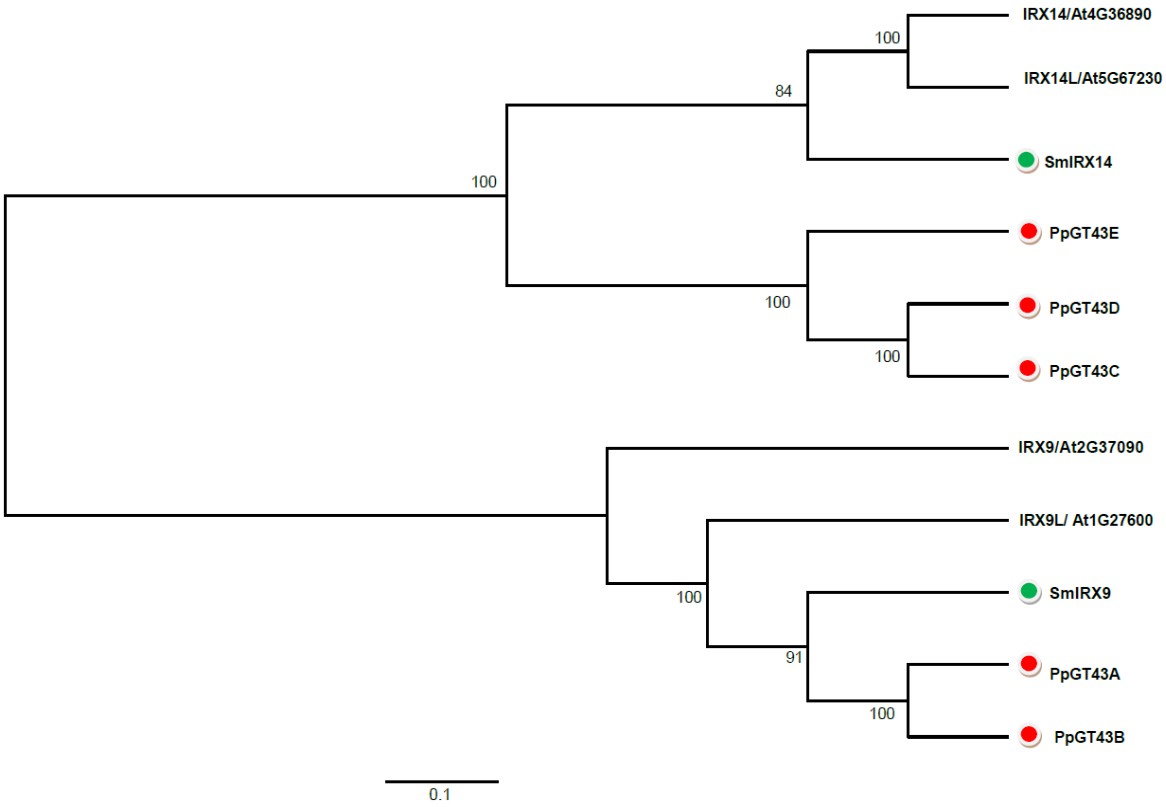

Figure 3.1: Phylogenetic relationship of GT43 genes in *Arabidopsis Thaliana*, *Physcomitrella patens* (marked with red circles), and *Selaginella moellendorffii* (marked with green circles). The phylogenetic tree was constructed with the neighbor-joining algorithm and bootstrap values resulted from 1,000 replicates are shown as percentages at the node. The 0.1 scale denotes 10% change.

Figure 3.2: Complementation analysis of GT43 genes from *P. patens* (*PpGT43*) and *S. moellendorffii* (*SmGT43*) by their expression in the *Arabidopsis irx9* and *irx14* mutants. (A) and (B) Morphology of 4-week-old **(A)** and 7-week-old **(B)** plants of wild type, *irx9,* and *irx9* expressing *PpGT43* and *SmGT43* genes. Note the restoration of plant morphology to that of the wild type in *irx9* expressing *PpGT43A*, *PpGT43B*, and *SmGT43A*.

The *Arabidopsis irx14* mutant did not display any defects in rosette size and stem growth, therefore, we only examined the stem mechanical strength and vessel phenotype in the complementation analysis of *irx14*. Expression of *SmGT43* and *PpGT43* genes in the *irx14* mutant revealed that only the *S. moellendorffii IRX14* homolog *SmGT43B* restored the stem mechanical strength and rescued the collapsed vessel phenotype of *irx14* (Figures 3.3 and 3.4 I-P), whereas the *P. patens IRX14* homologs *PpGT43C* and *PpGT43E* were unable to rescue the *irx14* mutant

phenotypes (Figures 3.3 and 3.4 I-P). In addition, expression of the *P. patens* and *S. moellendorffii IRX9* homologs could not complement *irx14* and likewise, expression of the *P. patens* and *S. moellendorffii IRX14* homologs could not complement *irx9* (Figures 3.2, 3.3 and 3.4).

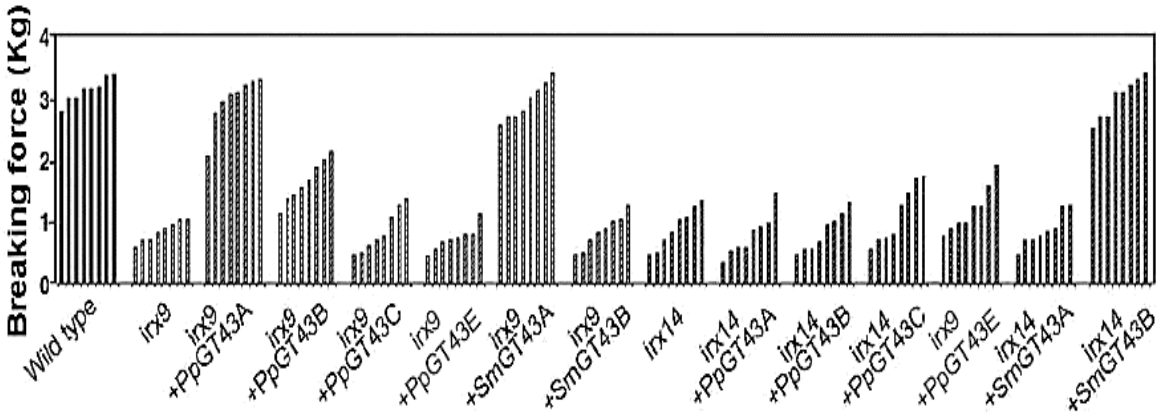

Figure 3.3: Breaking force measurement of stems of 9-week-old wild type, *irx9*, and *irx9* expressing *PpGT43* and *SmGT43* genes. The bottom segments of stems of 8 independent transgenic plants for each gene were measured for the force to break stems apart (shown as individual bars). Note the restoration of the stem strength to the wild type level in *irx9* expressing *PpGT43A* and *SmGT43A*, and in *irx14* expressing *SmGT43B*.

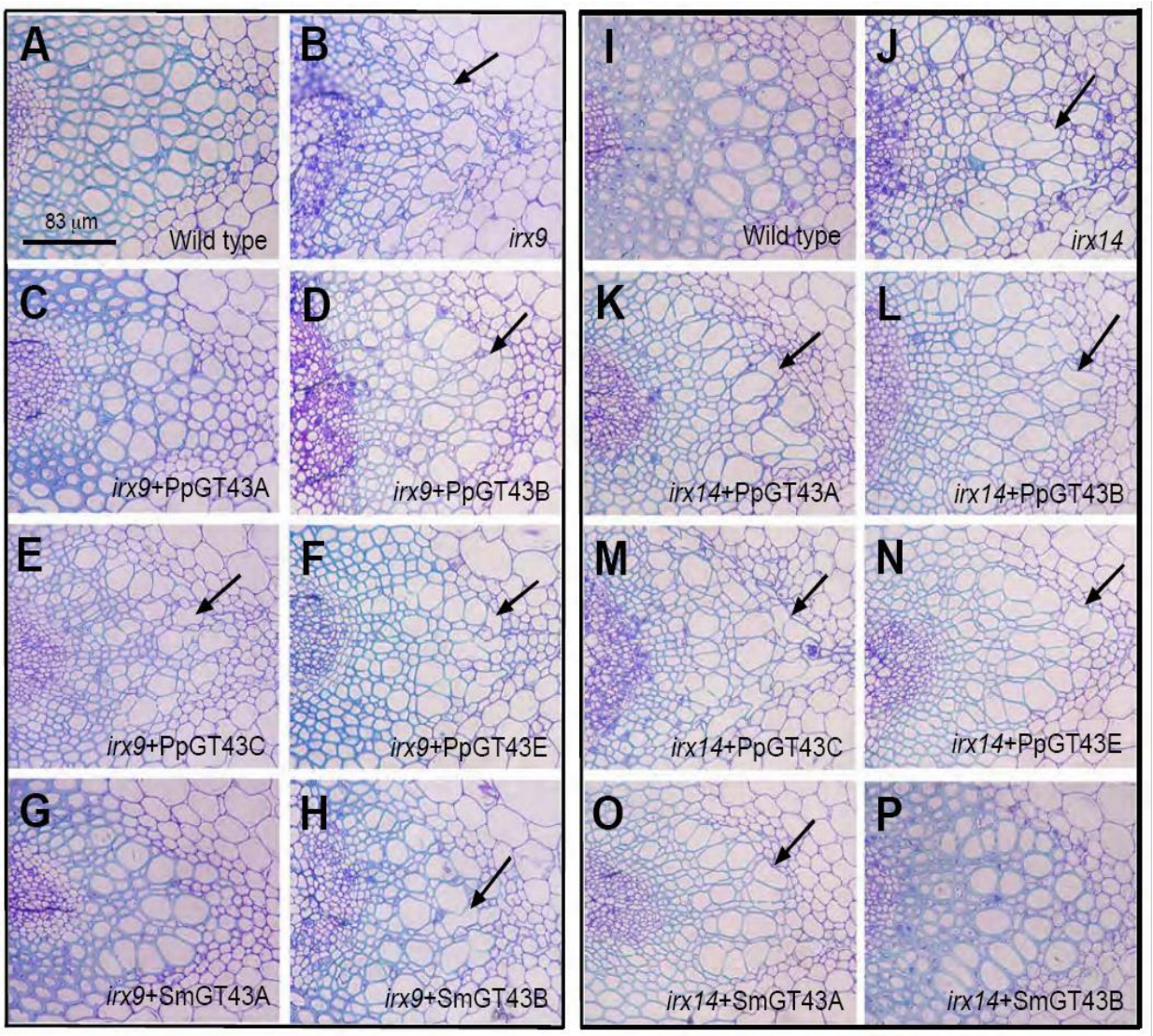

Fig.3.4: Examination of xylem vessel morphology in stems of *irx9* and *irx14* expressing *PpGT43* and *SmGT43* genes. The bottom segments of 9-week-old stems were sectioned and stained with toluidine blue for observation of the xylem bundles. (A) to (H) Xylem bundles of wild type (A), *irx9* (B), and *irx9* expressing *PpGT43* and *SmGT43* genes (C-H). Note the restoration of xylem vessel morphology in *irx9* expressing *PpGT43A* (C) and *SmGT43A* (G). (I) to (P) xylem bundles of wild type (I), *irx14* (J), and *irx14* expressing *PpGT43* and *SmGT43* genes (K-P). Note the restoration of xylem vessel morphology in *irx14* expressing *SmGT43B.* Arrows indicate deformed vessels. Scale bar in (A) = 83 µm for (A) to (P).

It has been shown that although *P. patens GT47A* could partially complement the growth defect of *Arabidopsis irx10 irx10-L* mutant, it was not able to rescue the xylan defect (Hörnblad et al. 2013). To find out whether the restoration of *irx9* and *irx14* mutant phenotypes by the expression of *PpGT43* and *SmGT43* genes was accompanied by the restoration of normal xylan biosynthesis, we analyzed cell wall composition and xylan structure. It was found that expression of *PpGT43A, PpGT43B,* and *SmGT43A* in *irx9* led to a partial restoration of the xylose content in the stem cell walls (Figure 3.5 A). In addition, their expression reduced the elevation of several cell wall sugars, including mannose, galactose, and arabinose, that was observed in the *irx9* mutant (Figure 3.5 A). Similarly, expression of *SmGT43B* in *irx14* restored the xylose content to the wild-type level and eliminated the elevation of mannose, galactose, and arabinose observed in the *irx14* mutants (Figure 3.5 B). In congruent with the restored xylose content in the stem cell walls, assays of xylosyltransferase activity in stem microsomes revealed that expression of *PpGT43A* and *SmGT43A* in *irx9* and expression of *SmGT43B* in *irx14* restored the xylan xylosyltransferase activity to the wild-type level (Figure 3.6).

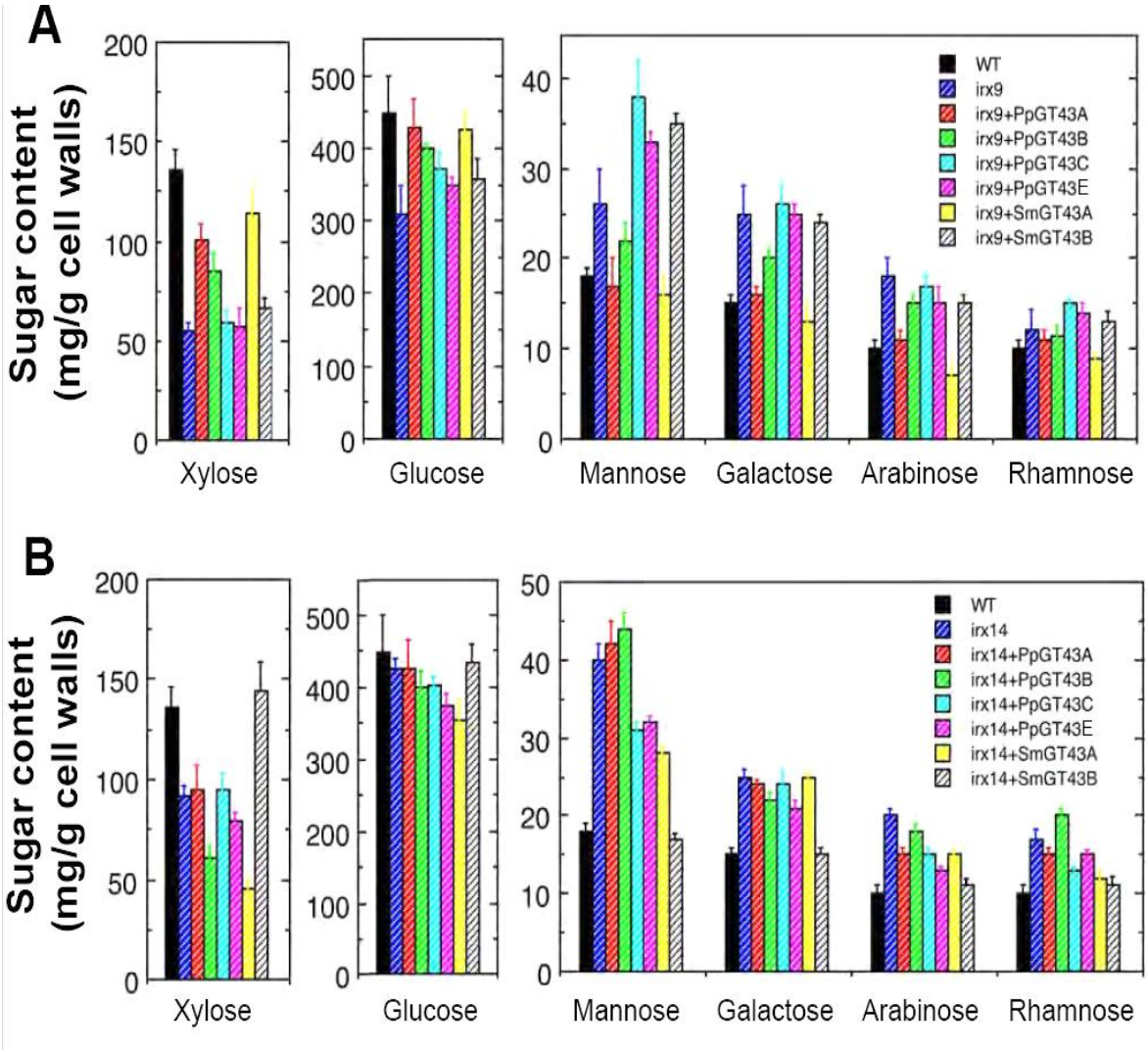

Fig. 3.5: Cell wall sugar composition analysis of stems of *irx9* expressing *PpGT43* and *SmGT43* genes (A) and *irx14* expressing *PpGT43* and *SmGT43* genes (B). Stems of 9-week-old plants were extracted for alcohol-insoluble cell wall residues, which were subsequently analyzed for sugar composition. Error bars represent the SD of three biological replicates. Note that the xylose content was significantly elevated in *irx9* expressing *PpGT43A, PpGT43B,* and *SmGT43B* compared with *irx9*, and in *irx14* expressing *SmGT43B* compared with *irx14*.

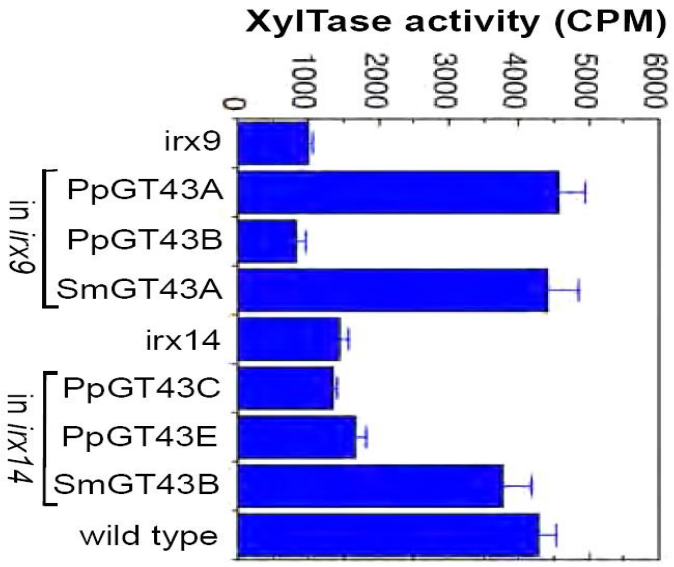

Figure 3.6: Measurement of xylosyltransferase activity in stems of *irx9* expressing *PpGT43A/B* and *SmGT43A* and in stems of *irx14* expressing *PpGT43C/E* and *SmGT43B*. Microsomes were isolated from stems of 7-week-old plants and assayed for xylosyltransferase activity using ^{14}C-labeled UDP-xylose as the xylosyl donor and Xyl_4 as the acceptor. The incorporation of ^{14}C-xylosyl residues onto the Xyl_4 acceptor was determined by counting the amount of radioactivity in the reaction products. Error bars denote the SD of three biological replicates.

Analysis of xylan structure in complemented plants

We next examined the xylan structure of the complemented *irx9* and *irx14* lines. Xylan was extracted with KOH from stem cell walls and then digested with endoxylanase to release xylooligomers for structural analysis. It has previously been shown that the GlcA side chains of xylans from *irx9* and *irx14* are all methylated (Brown et al. 2007; Pena et al. 2007), which was proposed to be attributed to the reduced xylan content in the mutants, thus leaving all of the GlcA

side chains to be methylated by methyltransferases (Yuan et al. 2014a). MALDI-TOF-MS showed that while xylooligomers from xylanase-digested wild-type xylan exhibited two major ion peaks at *m/z* 745 and 759 that correspond to GlcA-substituted Xyl_4 and MeGlcA-substituted Xyl_4, respectively (Figure 3.7), those from *irx9* and *irx14* xylan were devoid of the ion peak at *m/z* 745 for GlcA-substituted Xyl_4. The *m/z* 745 ion peak was restored in *irx9* expressing *PpGT43*A and *SmGT43A* and in *irx14* expressing *SmGT43B* (Figure 3.7). NMR spectroscopy confirmed the restoration of resonances for α-GlcA (5.3 ppm) and β-xylosyl residues branched with GlcA (4.63 ppm) in *irx9* expressing *PpGT43A* and *SmGT43A* and in *irx14* expressing *SmGT43B* (Figure 3.8). Together, these results demonstrated that *PpGT43A* and *SmGT43A* functionally complemented the xylan defects in *irx9* and that *SmGT43B* functionally complemented the xylan defects in *irx14*.

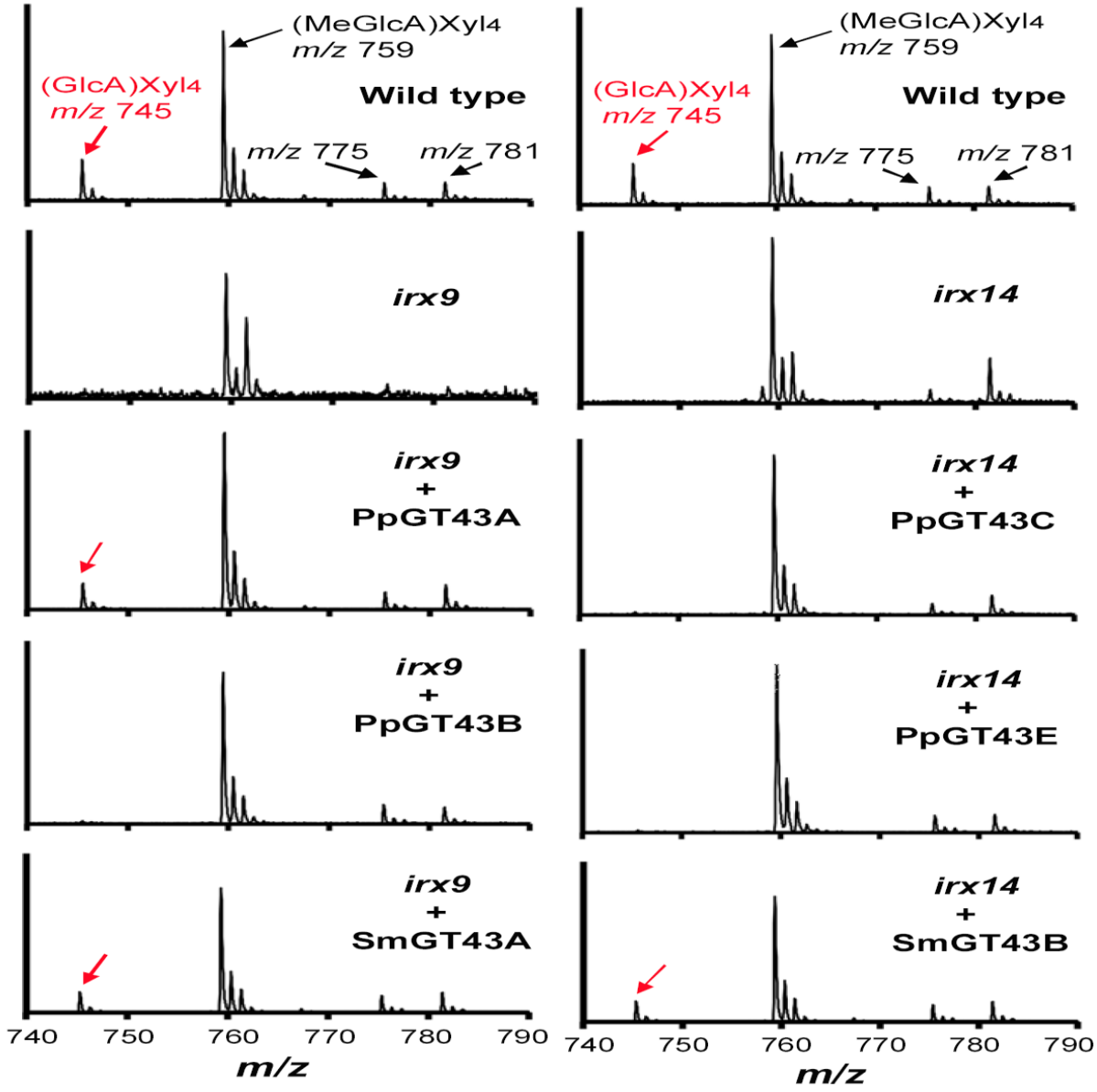

Figure 3.7: MALDI analysis of xylooligomers released from xylanase digestion of xylans from stems of *irx9* expressing *PpGT43A/B* and *SmGT43A* and stems of *irx14* expressing *PpGT43C/E* and *SmGT43B*. The ions at *m/z* 745 and 759 correspond to (GlcA)Xyl_4 and (MeGlcA) Xyl_4, respectively, and those at *m/z* 775 and 781 are doubly sodiated species of (GlcA)Xyl_4 and (MeGlcA)Xyl_4, respectively. Note the restoration of the ion at *m/z* 745 in *irx9* expressing *PpGT43A* and *SmGT43A* and in *irx14* expressing *SmGT43B*.

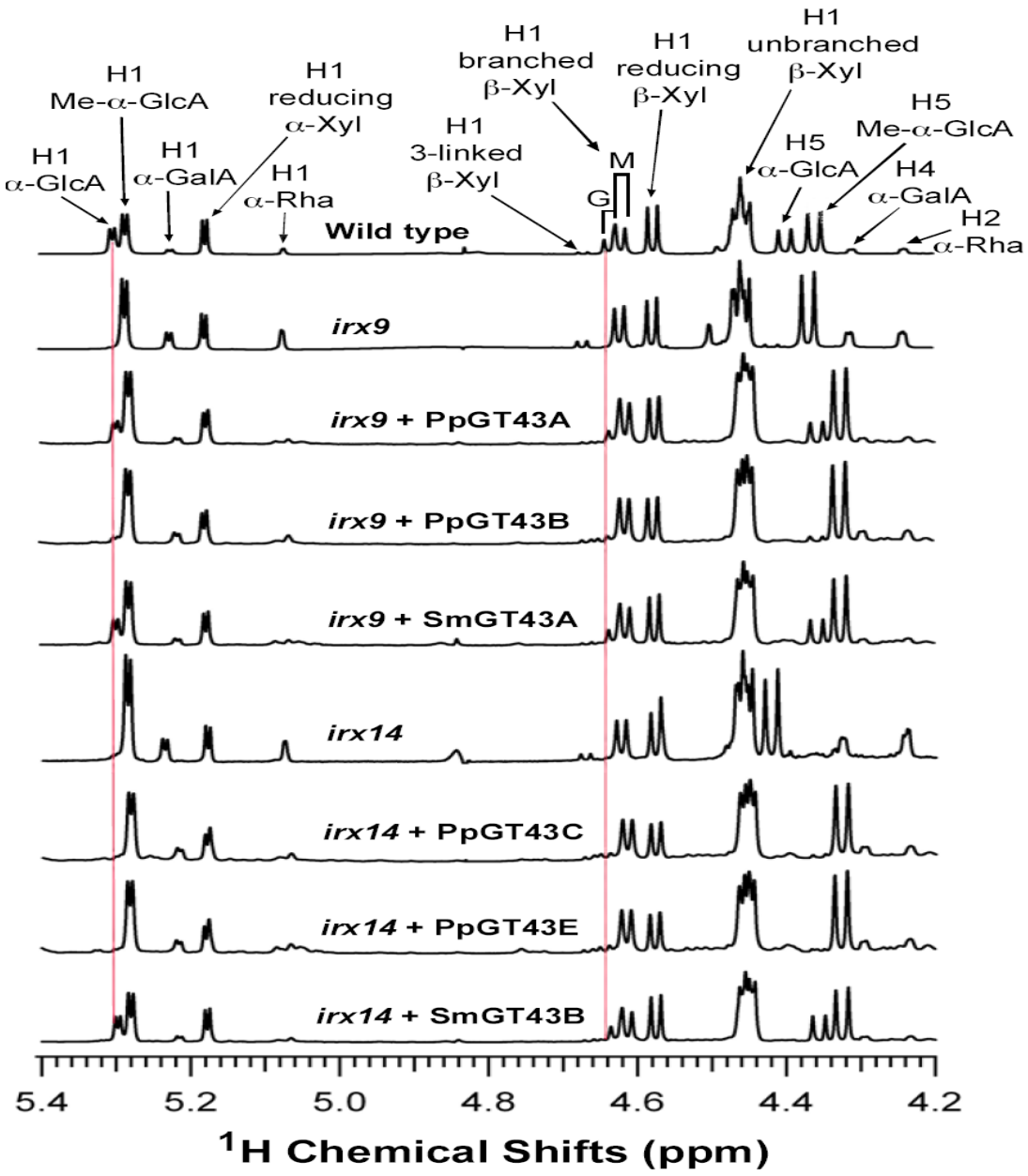

Figure 3.8: ^{1}H-NMR determination of the structure of xylans from stems of *irx9* expressing *PpGT43A/B* and *SmGT43A* and stems of *irx14* expressing *PpGT43C/E* and *SmGT43B*. The resonance peaks in the wild-type xylan are labeled with the identity of structural elements and the position of the assigned protons. Note the restoration of the resonances corresponding to H1 α-GlcA in *irx9* expressing *PpGT43A* and *SmGT43A* and in *irx14* expressing *SmGT43B*.

DISCUSSION

The *Arabidopsis* IRX9 and IRX14 are two functionally non-redundant groups of GT43 proteins and are required for normal elongation of xylan backbone. (Lee et al., 2010). Comprehensive molecular and genetic studies have indicated that *IRX9/IRX9L* and *IRX14/IRX14L* all are expressed in the same cell types that undergo secondary cell wall thickening and their encoded proteins are targeted to the Golgi, where GX is synthesized. Mutation of the *IRX9* and *IRX14* genes cause severe reduction in xylan xylosyltransferase activity and consequently a significant decrease in the GX chain length, GX amount and GX level (Lee et al., 2010).

Our complementation analysis has provided genetic evidence that the two GT43 genes in *S. moellendorffii*, *SmGT43A* and *SmGT43B*, are functional orthologs of *Arabidopsis IRX9* and *IRX14*, respectively. This finding indicates that the involvement of two functionally non-redundant groups of GT43 proteins in xylan biosynthesis is evolutionarily conserved in both seedless vascular plants and seed plants. In contrast to *S. moellendorffii*, there exist five GT43 gens in *P. patens*, two of which are phylogenetically *IRX9* close homologs (*PpGT43A/B*) and the other three are *IRX14* close homologs (*PpGT43C/D/E*). Complementation analysis has demonstrated that *PpGT43A* is a functional orthologs of *IRX9*, and *PpGT43B* could partially complement some aspects of the mutant phenotypes of *irx9*. However, the *IRX14* homologs *PpGT43C/E* were not able to complement the xylan defects conferred by the *IRX14* mutation in *Arabidopsis*. One possible explanation is that the *P. patens IRX14* homologs possess functions different from *Arabidopsis IRX14* and that the recruitment of *IRX14* and its homologs in xylan biosynthesis may have occurred later during the evolution of vascular plants. Another possible explanation is that *P. patens IRX14* homologs may perform similar functions as *IRX14* in xylan biosynthesis in *P. patens*, but their sequences may have diverged to such a degree that they could not form a functional complex with other *Arabidopsis* proteins involved in xylan biosynthesis. The latter possibility is congruent with

the observation that although the *P. patens IRX10* close homolog *PpGT47A* was not able to restore the xylose content in the secondary walls of the *irx10 irx10-l* mutant, it exhibits xylosyltransferase activity capable of transferring xylosyl residues from the UDP-Xyl donor to the xylooligomer acceptor (Hörnblad et al. 2013, Jensen et al. 2014). Together with our demonstration that *PpGT43A* is a functional ortholog of *IRX9*, these findings indicate the evolutionary conservation of the involvement of both GT47 and GT43 proteins in xylan backbone elongation in non-vascular plants.

MATERIALS AND METHODS

Xylan isolation and ^{1}H-NMR spectroscopy

Stems of *Arabidopsis* plants expressing PpGT43 and SmGT43 genes were ground into powders in a mortar and pestle and subsequently extracted in acetone and ethanol. The resulting alcohol-insoluble cell wall residues were dried and used for xylan isolation. Xylan was extracted from alcohol-insoluble cell wall residues by incubating with 1N KOH. The isolated xylan was digested with endo-1,4-β-xylanase M6 (Megazyme) to generate xylooligosaccharides (Zhong et al. 2005). Xylooligosaccharides were subjected to acquisition of NMR spectra on a Varian Inova 600 MHz spectrometer using a 5 mm cryogenic triple resonance probe (Teng et al. 2012). The NMR spectra of samples were collected with 64 transients using a spectral width of 6,000 Hz and an acquisition time of 5-seconds. The proton positions and residue identities in NMR spectra were assigned based on the NMR spectra data for xylans from Arabidopsis and aspen (Teleman et al., 2000; Peña et al., 2007;Yuan et al., 2013). Xylans isolated from three separate pools of samples were examined and identical NMR spectra were obtained.

Gene expression analysis

Total RNAs were isolated from stems of *S. moellendorffii* and gametophytes/sporophytes of *P. patens* with a Qiagen RNA isolation kit (Qiagen). Total RNAs were first treated with DNase I and then converted into first strand cDNAs, which were used as a template for PCR detection of transcripts of interest. The PCR primers for *SmGT43A* were 5'- accagttcgtcagctcgacactgt-3' and 5'-ctacaagtgaatcacaggctccaa-3', those for *SmGT43B* were 5'-ttgtggagactgaatccacaggag-3' and 5'-actttatgaaagtttctgatgacc-3', those for *PpGT43A* were 5'-atccggcatcgagacaccatcaga-3' and 5'-ttagtcatccttgtgcagaggcat-3', those for *PpGT43B* were 5'-aacctcgtttattgagcagctcgt-3' and 5'-ttatagctgtactaagttggcttt-3', those for *PpGT43C* were 5'-cgaagaaaacaccgtggccagaca-3' and 5'-

ctacgtatttttagtggcaatggt-3', those for *PpGT43D* were 5'-gtgagagtcaagcctataacggtt-3' and 5'-actttcgtggaccctctgaatggg-3', those for *PpGT43E* were 5'-gacgaaactcatgtagagccgctt-3' and 5'-tcatactgaaggcgtggatttctc-3'.

MALDI-TOF MS

The samples were mixed with 0.2 M 2,5-dihydroxybenzoic acid (1:1, v/v), dried on a stainless steel target plate and subjected to MALDI-TOF MS analysis as described (Zhong et al. 2005). Spectra are the average of 250 laser shots.

Complementation analysis

PpGT43 and SmGT43 full-length cDNAs were ligated into the XbaI site between the cauliflower mosaic virus (CaMV) 35S promoter and the nopaline synthase terminator in the pGPTV binary vector. The resulting constructs were transformed into agrobacterium, which was further used to transform the Arabidopsis *irx9* or *irx14* mutants. The first generation of transgenic plants was examined for their morphology, anatomical structure and cell wall chemistry. A pool of stems from at least 15 transgenic plants (10 weeks old) was collected for cell wall composition and xylan structural analyses for each biological replicate. For stem breaking force measurement, basal segments (2 cm) of main stems from 10-week-old plants were measured for the force to break apart the segment using a digital force/length tester (Zhong et al. 1997).

Histology

Basal segments (1 cm) of main stems from 10-week-old plants were fixed in 1.5% formaldehyde and embedded in LR White (Electron Microscopy Sciences) (Burk et al., 2006). The embedded tissues were cut into 1-μm-thick sections and stained with toluidine blue for light microscopy. Stems of 10 independent transgenic plants were sectioned and representative data were shown.

Cell wall composition analysis

Alcohol-insoluble cell wall residues isolated from a pool of stems of at least 30 plants were analyzed for their sugar composition following the procedure described by Hoebler et al. (1989). The alditol acetates of sugars were separated and quantitated on a PerkinElmer Clarus 500 gas-liquid chromatography equipped with a silica capillary column DB 225 (30 m x 0.25 mm).

Microsome isolation and xylosyltransferase activity assay

Stems of 7-week-old wild type, *irx9, irx14* and their complemented lines were isolated for microsomes according to Kuroyama and Tsumuraya (2001). For each biological replicate, a pool of stems from 10 independent plants was used. For xylosyltransferase activity assay, microsomes (200 μg) were incubated with a reaction mixture (50 μl) containing 50 mM HEPES-KOH (pH 7.0), 5 mM $MnCl_2$, 0.5% Triton X-100, 1 mM dithiothritol, 0.1 mM UDP-Xyl (CarboSource Service), 0.2 μg/μl Xyl_6 (Megazyme) and UDP-[^{14}C]Xyl (0.1 μCi; American Radiolabeled Chemical). After 1-hr incubation at 22 ^{o}C, the reaction products were subjected to paper chromatography for separation of radiolabeled xylooligomers from UDP-[^{14}C]Xyl according to Ishikawa et al. (2000). The amount of radioactivity in the radiolabeled xylooligomers was counted with a PerkinElmer scintillation counter.

Statistical analysis

The data of cell wall composition and xylosyltransferase activities were examined for statistical significance using the Student's *t* test program.

(http://www.graphpad.com/quickcalcs/ttest1.cfm)

REFERENCES

Bechtold, N. and Bouchez, D. (1989) In planta Agrobacterium-mediated transformation of adult Arabidopsis thaliana plants by vacuum infiltration. In: Potrykus I, Spangenberg, editors. Gene Transfer to Plants. Berlin: *Springer-Verlag*; 1994. p. 19-23.

Brown, D.M., Goubet, F., Wong, V. W., Goodacre, R., Stephens, E., Dupree, P. et al. (2007) Comparison of five xylan synthesis mutants reveals new insight into the mechanisms of xylan synthesis. *Plant J.* 52: 1154-1168.

Burk, D.H., Zhong, R, Morrison, W.H.III and Ye, Z.-H. (2006) Disruption of cortical microtubules by overexpression of green fluorescent protein-tagged α-tubulin 6 causes a marked reduction in cell wall synthesis. *J. Integr. Plant Biol.* 48: 85-98.

Harholt, J., Sørensen, I., Fangel, J., Roberts, A., Willats, W.G., Scheller, H.V. et al. (2012) The glycosyltransferase repertoire of the spikemoss Selaginella moellendorffii and a comparative study of its cell wall. *PLoS One* 7: e35846.

Hoebler, C., Barry, J.L., David, A. and Delort-Laval, J. (1989) Rapid acid-hydrolysis of plant cell wall polysaccharides and simplified quantitative determination of their neutral monosaccharides by gas-liquid chromatography. *J. Agr. Food Chem.* 37: 360-367.

Hörnblad, E., Ulfstedt, M., Ronne, H. and Marchant, A. (2013) Partial functional conservation of IRX10 homologs in Physcomitrella patens and Arabidopsis thaliana indicates an evolutionary step contributing to vascular formation in land plants. *BMC Plant Biol.* 13: 3.

Ishikawa, M., Kuroyama, H., Takeuchi, Y. and Tsumuraya, Y. (2000) Characterization of pectin methyltransferase from soybean hypocotyls. *Planta* 210: 782-791.

Jensen, J.K., Johnson, N.R. and Wilkerson, C.G. (2014) Arabidopsis thaliana IRX10 and two related proteins from Psyllium and Physcomitrella patens are xylan xylosyltransferases. *Plant J.* 80: 207-215.

Kuroyama, H. and Tsumuraya, Y. (2001) A xylosyltransferase that synthesizes β-(1-4)-xylans in wheat (Triticum aestivum L.) seedlings. *Planta* 213: 231-240.

Lee, C., O'Neill, M.A., Tsumuraya, Y., Darvill, A.G., and Ye, Z.-H (2007) The irregular xylem9 mutant is deficient in xylan xylosyltransferase activity, *Plant Cell Physiology*, 48: 1624-1634.

Lee, C., Teng, Q., Huang, W., Zhong, R. and Ye, Z.-H. (2010) The *Arabidopsis* family GT43 glycosyltransferases form two functionally nonredundant groups essential for the elongation of glucuronoxylan backbone. *Plant Physiology*, 153: 526–541.

Lee, C., Teng, Q., Zhong, R. and Ye, Z.-H. (2011a) Molecular dissection of xylan biosynthesis during wood formation in poplar. *Molecular Plant*, 4: 730–747.

Lee, C., Teng, Q., Zhong, R. and Ye, Z.-H. (2011b) Molecular dissection of xylan biosynthesis during wood formation in poplar. *Mol. Plant* 4: 730-747.

Peña, M.J., Zhong, R., Zhou, G.-K., Richardson, E.A., O'Neill, M.A., and Darvill, A.G. (2007) *Arabidopsis* irregular xylem8 and irregular xylem9: implications for the complexity of glucuronoxylan biosynthesis. *Plant Cell*. 19: 549–563.

Teleman, A., Lundqvist, J., Tjerneld, F., Stålbrand, H. and Dahlman, O. (2000) Characterization of acetylated 4-O-methylglucuronoxylan isolated from aspen employing 1H and 13C NMR spectroscopy. *Carbohydr. Res.* 329: 807-815.

Teng, Q., Ekman, D.R., Huang, W. and Collette, T.W. (2012) Push-through Direct Injection NMR: an optimized automation method applied to metabolomics. Analyst 137: 2226-2232.

Wu, A-M, Rihouey, C., Seveno, M., Ho¨rnblad, E., Singh, S.K., Matsunaga, T., Ishii, T., Lerouge, P., and Marchant, A. (2009) The *ArabidopsisIRX10* and *IRX10*-LIKE glycosyltransferases are critical for glucuronoxylan biosynthesis during secondary cell wall formation. *Plant Journal*, 57: 718-731.

Wu, A-M., Ho¨rnblad, E., Voxeur, A., Gerber, L., Rihouey, C., and Lerouge, P. (2010) Analysis of the *ArabidopsisIRX9*/*IRX9*-L and *IRX14*/ *IRX14*-L pairs of glycosyltransferase genes reveals critical contributions to biosynthesis of the hemicellulose glucuronoxylan. *Plant Physiology*, 153: 542–554.

Yuan, Y., Teng, Q., Zhong, R. and Ye, Z.-H. (2013) The Arabidopsis DUF231 domain-containing protein ESK1 mediates 2-O- and 3-O-acetylation of xylosyl residues in xylan. *Plant Cell Physiol*. 54: 1186-1199.

Yuan, Y., Teng, Q., Lee, C., Zhong, R. and Ye, Z.-H. (2014a) Modification of the degree of 4-O-methylation of secondary wall glucuronoxylan. *Plant Sci*. 219-220: 42-50.

Zhong, R., Taylor, J.J., and Ye, Z-H (1997) Disruption of interfascicular fiber differentiation in an *Arabidopsis* mutant. *Plant Cell* 9:2159-2170.

Zhong, R., Peña, M.J., Zhou, G.-K., Nairn, C.J., Wood-Jones, A., Richardson, E.A., Morrison, W.H., Darvill, A.G., York, W.S. and Ye, Z.-H. (2005) *Arabidopsis* Fragile Fiber8, which encodes a putative glucuronyltransferase, is essential for normal secondary wall synthesis. *Plant Cell* 17: 3390–3408.

CHAPTER 4

FUNCTIONAL CONSERVATION OF SECONDARY WALL NAC TRANSCRIPTION FACTOR HOMOLOGS IN *SELAGINELLA MOELLENDORFFII* AND *PHYSCOMITRELLA PATENS*[3]

[3] Haghighat, M., Zhong, R., and Ye, Z.H. To be submitted to Plant Cell Physiology.

ABSTRACT

Vascular plants evolved the ability to make secondary cell walls in order to be able to colonize dry land. NAC domain transcription factors are plant-specific transcriptional regulators, and important for plant growth and development and stress responses. Secondary wall-associated NAC (SWN) transcription factors are master switches and capable of activating the secondary wall biosynthetic program. To understand whether the SWN-mediated transcriptional regulation of secondary wall biosynthesis is conserved in non-vascular and vascular plants, we have investigated the functional roles of SWN genes from *Selaginella moellendorffii* and *Physcomitrella patens*. *S. moellendorffii* and *P. patens* SWN genes were able to complement the *Arabidopsis snd1 nst1 nst2* triple mutant defective in secondary wall thickening. When overexpressed in *Arabidopsis*, SmSWNs and PpSWNs were able to activate a number of secondary wall biosynthetic genes, and result in the ectopic deposition of lignin. These results indicate that early vascular plants recruited SWN-like NAC transcription factors as transcriptional activators of secondary wall biosynthesis and that the SWN-mediated regulatory mechanism for secondary wall biosynthesis is conserved in vascular plants.

INTRODUCTION

Several adaptations have been required to make the evolution of plants onto land possible. One of these adaptation mechanisms was acquisition of vascular tissue, allowing plants to colonize almost every terrestrial ecosystem. Water and nutrient are transported by vascular tissues throughout plant bodies and enable the land plants to have more specialized tissues and less need of being immersed in water. Although some nonvascular plants contain water conducting tissue with similar structure to vascular tissue, xylem vessels of vascular plants with lignified secondary cell wall are unique. Therefore, the formation of lignified cell walls in the water conducting xylem vessels of vascular plants allowed them to evolve to a larger size than non-vascular plants which are limited to relatively small sizes due to lack of these specialized conducting tissues and provide structural support to allow plants growing taller and competing for sunlight.

Wood or secondary xylem is mainly made of xylem parenchyma cells and two types of cells with thickened secondary cell wall, fibers and tracheary elements (Demura and Fukuda, 2007). Fibers support the plant bodies, whereas tracheary elements including vessels and tracheids transport water and nutrients. Tracheary elements in the xylem undergo elongation before tubular conducting system is formed. For this reason, the loosening of the cellulose-hemicellulose network is mediated by expansions, cell wall loosening enzymes. Plant hormones such as brassinosteroids are also involved in the regulation of cell elongation. After elongation, tracheary elements undergo secondary wall thickening to create different patterns including scalariform, annular, and pitted. Mechanical strength provided by the thickened secondary walls is important for plants to bear the negative pressure produced through transpiration. Programmed Cell Death (PCD) is the last step of wood formation which produces mature xylem cells. Some hydrolytic enzymes including cystein protease, serine proteases, and nucleases are produced during wood formation (xylogenesis), and they are stored in vacuoles before autolysis initiates. PCD begins with

destroying the vacuoles membrane and releasing these hydrolytic enzymes into cytosol. The enzymes degrade nuclear DNA and remove the cellular contents in order to create hollow tubular columns that are called vessels (Ye, 2002).

Proper wood formation needs a multitude of enzymes in several biosynthetic pathways to synthesize the complex polysaccharides and control proper deposition and assembly of cell wall components in each cell type based on its functional roles. Therefore, a precise regulation of plant cell wall formation is under complex and dynamic genetic control involving a network of transcription factors acting as master regulators of gene expression. Transcription factors typically have two domains in their structure. The DNA binding domain is responsible for binding to specific DNA *cis*-elements in the promotor regions of target genes, whereas the regulatory domain is responsible for regulating transcription of the target genes.

Transcription factors belonging to the NAM, ATAF and CUC (NAC) domain family are one of the largest plant-specific transcription factor gene families with more than 100 members in *Arabidopsis.* NAC transcription factors are involved in plant cell wall biosynthesis and development and response to biotic and abiotic stress (Olsen et al., 2005). NAC proteins contain a conserved N-terminal region with five subdomains (A-E) and C-terminal motifs. Phylogenetic studies have revealed that genomes of higher plants (except for grape) contain between 100 and 200 NAC genes, while genomes of lower plants like moss and *S. moellendorffii* harbor 40 or fewer NAC genes.

Functions of *Arabidopsis XND1, VND6, VND7, NST1, NST2,* and *SND1* have been identified. Overexpression of *AtXND1* had negative impacts on differentiation of tracheary elements, programmed cell death in xylem vessel cells and overall lignocellulose cell wall biosynthesis (Zhao et al., 2005; Zhao et al., 2008). *VND6* and *VND7* are involved in trans

differentiation of various cells into metaxylem- and protoxylem-like vessel element in both *Arabidopsis* and poplar (Kubo et al., 2005). *NST1* and *NST2* act redundantly in secondary wall formation of anther endothecium in *Arabidopsis*, while *NST1* and *SND1* act redundantly in cell wall thickening of the interfascicular fibers and secondary xylem vessels (Mitsuda et al., 2005, 2007; Zhong et al., 2008). Dominant repression or loss of function of *SND2* and *SND3* results in dramatic reduction in the secondary wall thickening of the fibers, indicating that these genes are involved in secondary cell wall thickening in xylem elements and interfascicular fibers. Moreover, the downregulation of *SND2* and *SND3* in *NST1/SND1* RNAi lines suggested that these genes work downstream of *SND1* and *NST1*, and *SND2* was identified as a direct target of *SND1* (Zhong et al., 2006, 2007).

Zhong et al. (2011) showed that the rice and maize secondary wall-associated NACs (*OsSWNs* and *ZmSWNs*) were able to complement the *Arabidopsis snd1 nst1* double mutant with defective secondary wall thickening. Overexpression of *OsSWNs* and *ZmSWNs* in *Arabidopsis* resulted in the ectopic deposition of cellulose, xylan, and lignin, indicating that the overexpression of these NAC transcription factors were sufficient for activating a number of secondary wall-associated transcription factors and biosynthetic genes. Overexpression of *OsMYB46* and *ZmMYB46* caused the activation of the entire secondary wall biosynthetic program in *Arabidopsis*, indicating that the rice and maize MYB transcription factors are functional orthologs of *Arabidopsis* MYB46/83 and their promoters contain secondary wall NAC-binding elements (SNBEs) that can be bound and activated by *OsSWNs* and *ZmSWNs*. These results indicate that the SWN-mediated transcriptional regulation of secondary wall biosynthesis is a conserved mechanism in monocots and dicots. Considering that both nonvascular plants and seedless vascular plants have close homologs of SWNs, further characterization of the SWN-mediated

transcriptional regulation of cell wall biosynthesis in *P. patens* and *S. moellendorffii* may provide us better understanding of the transcription factors network involved in the plant cell wall biosynthesis.

RESULTS

SWN homologs in *Physcomitrella patens* and *Selaginella moellendorffii*

The amino acid sequences of *S. moellendorffii* and *P. patens* secondary wall NACs (SWNs) were analyzed for their phylogenetic relationship with *Arabidopsis* SND1, NSTs and VNDs using the ClustalW program and the phylogenetic tree shown in Figure 4.1 was constructed using the MEGA6 program. *S. moellendorffii* and *P. patens* genomes contain four and eight close homologs of *Arabidopsis* SWNs, respectively. It is currently not known whether the SWN homologs from *S. moellendorffii* are functional orthologs of *Arabidopsis* SWNs. It is the focus of this study to find out roles of *S. moellendorffii* SWN homologs by their genetic complementation of *Arabidopsis snd1 nst1 nst2 triple* mutant and their overexpression analysis.

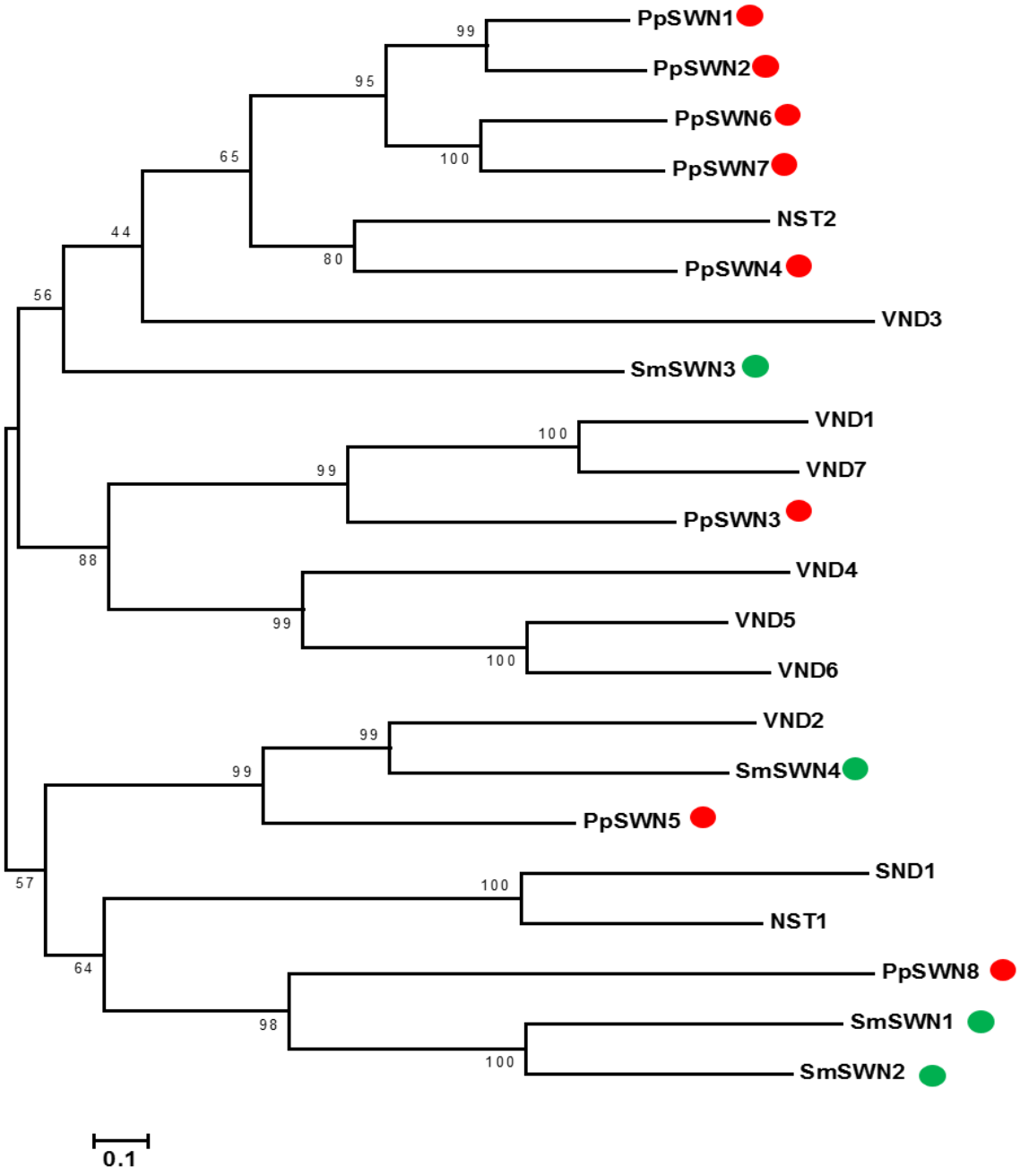

Figure 4.1- Phylogenetic relationship of *S. moellendorffii* (marked with green circles) and *P. patens* SWNs (marked with red circles) to *Arabidopsis SND1, NSTs* and *VNDs* was inferred using the Neighbor-joining methods. The 0.1 scale denotes 10% changes.

***SmSWNs* and *PpSWNs* are able to rescue the secondary wall defects of the *Arabidopsis snd1 nst1 nst2* triple mutants**

The *snd1 nst1 nst2* triple mutant showed the pendent inflorescence stem and reduced stem strength phenotypes due to lack of lignified secondary walls in fibers (Zhong et al., 2007). To test whether the *SmSWN* and *PpSWN* genes are functional orthologs of *Arabidopsis SND1* and *NST1/2*, we employed the complementation approach. Expression of *SmSWN* and *PpSWN* genes driven by *SND1* promoter in the *snd1 nst1 nst2* triple mutant effectively rescued the pendent stem strength (Figure 4.2) due to restoration of the formation of lignified secondary walls in fibers in the *snd1 nst1 nst2* mutant plants (Figure 4.3). Therefore, the complementation analysis demonstrates that the *SmSWN* and *PpSWN* genes are functional orthologs of *SND1* and *NST1/2*, capable of activating the secondary wall biosynthetic program.

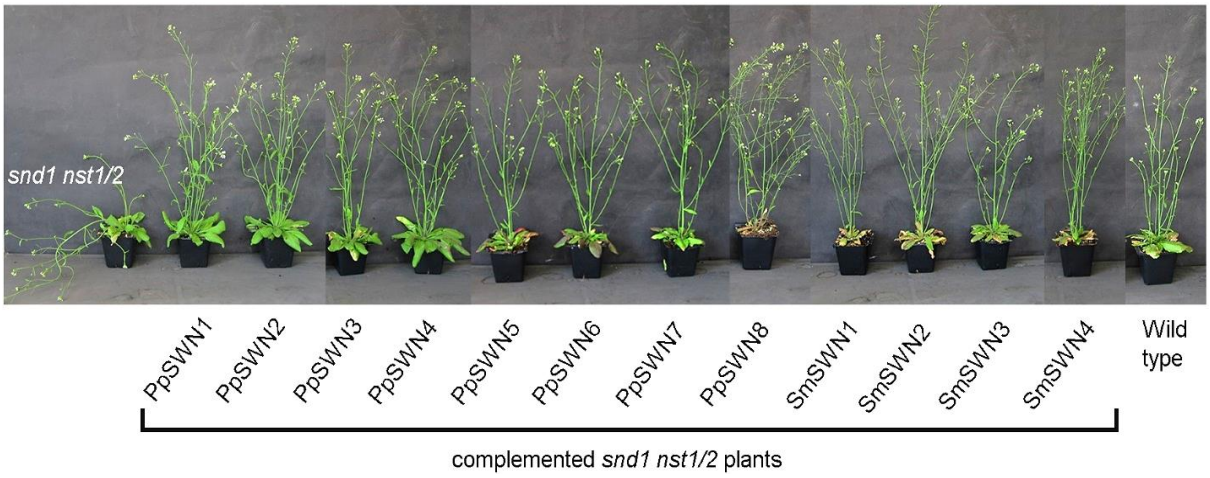

Figure 4. 2- Complementation of the pendent stem phenotype of the *snd1 nst1 nst2* triple mutant plants by expression of *PpSWNs* and *SmSWNs*. The full-length cDNAs of *PpSWNs* and *SmSWNs* driven by the *SND1* promoter were introduced into *snd1 nst1/2* and the first generation of transgenic plants was examined for their morphological phenotypes. Shown are 7-week-old plants.

Overexpression of *SmSWN* and *PpSWN* genes in *Arabidopsis* induces ectopic deposition of secondary walls

To investigate the functional roles of *SmSWNs* and *PpSWNs* in the regulation of secondary wall biosynthesis, we overexpressed their cDNAs in *Arabidopsis*. The full-length *SmSWN* and *PpSWN* cDNAs driven by the CAMV 35S promoter were expressed in the wild-type *Arabidopsis*, and the first generation of transgenic plants was used for analyses. Seedlings of both SmSWN and PpSWN overexpressors showed the reduced rosette sizes and the curly leaf phenotype similar to the SND1 overexpressor (Zhong et al., 2006; Figure 4.4). The ectopic deposition of secondary wall components such as lignin was examined in at least 10 plants with the curly leaves for each construct. Wild-type leaves had jigsaw puzzle-shaped epidermal cells with thin walls and no lignin signals. Epidermal cell walls of PpSWN overexpressors (i.e. PpSWN6-OE) and mesophyll cell walls of SmSWN overexpressors (i.e. SmSWN3-OE) exhibited the lignin signals for the ectopic helical secondary wall thickening (Figure 4.5). All of the other PpSWN and SmSWN overexpressors also exhibited ectopic deposition of lignified secondary walls in leaf epidermal and mesophyll cells (data not shown). Our examination of the stems also revealed the ectopic deposition of lignified secondary walls in the epidermis, cortical cells of the inflorescence stems and pith cells of SmSWN and PpSWN overexpressors compared with the wild-type stems, which show the secondary wall deposition only in the interfascicular fibers and xylem cells (Figure 4.6).

Consistent with the observed ectopic deposition of secondary walls, gene expression analysis showed that the expression of secondary wall biosynthetic genes for cellulose (*CesA4*, *CesA7* and *CesA8*), xylan (*IRX9*, *FRA8* and *PARVUS*) and lignin (*PAL1*, *4CL* and *CCoAOMT1*) was significantly elevated in the SmSWN and PpSWN overexpressors (Figure 4.7). These results

demonstrate that SmSWNs and PpSWNs are capable of activating the biosynthetic pathways for all three major secondary wall components.

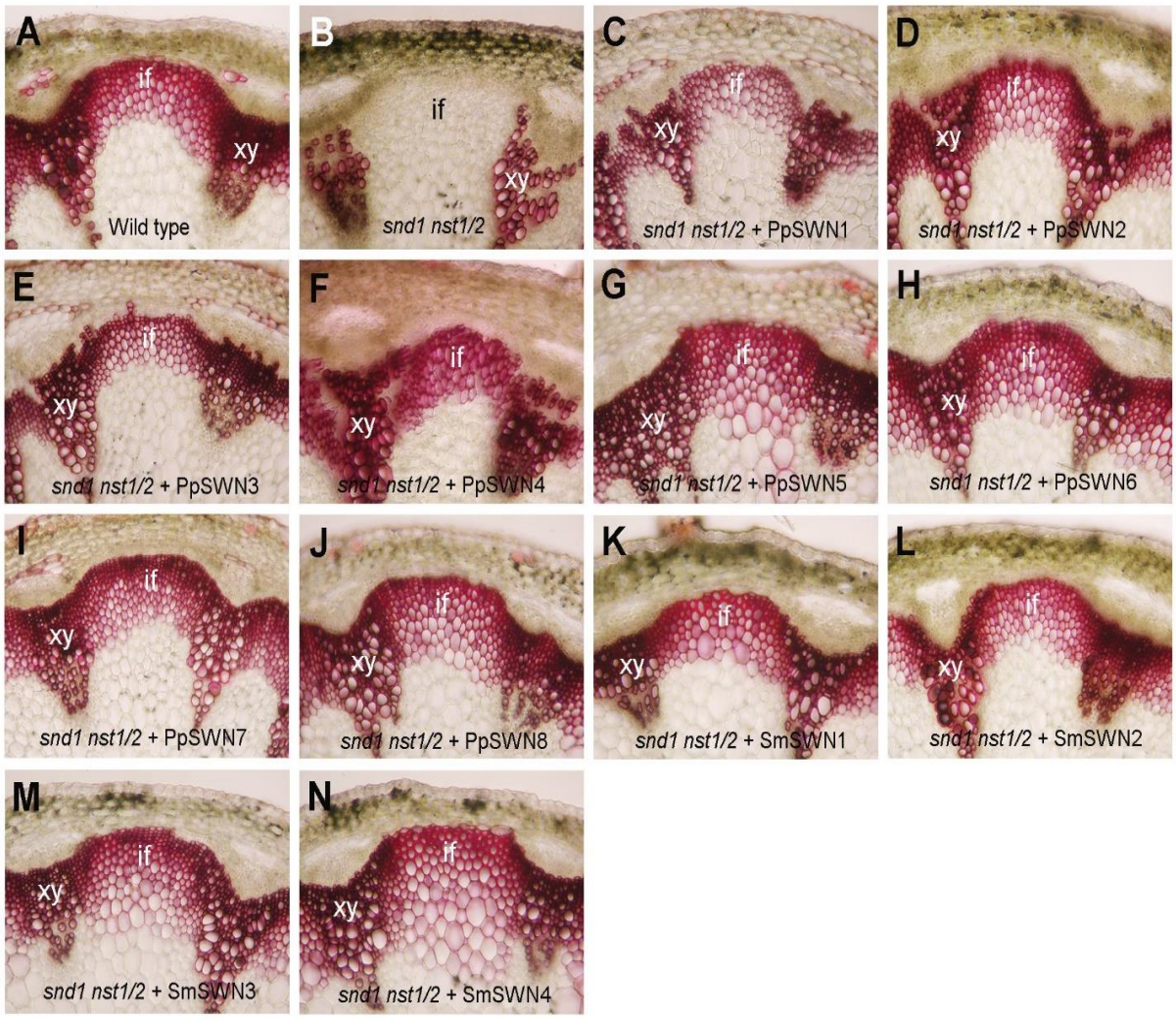

Figure 4. 3- Restoration of lignified secondary walls by expression of PpSWNs and SmSWNs in interfascicular fibers of stems of *snd1 nst1 nst2*. The basal parts of inflorescence stems were sectioned and stained for lignin with phloroglucinol-HCl. Lignified walls were stained red. if, interfascicular fiber; xy, xylem.

Figure 4. 4- Effects of overexpression of PpSWNs and SmSWNs on plant growth. The full-length cDNAs of *PpSWNs* and *SmSWNs* driven by the CaMV 35S promoter were introduced into wild-type *Arabidopsis* and 4-week-old transgenic plants were examined for their morphological phenotypes. Note the reduced rosette size and curly leaves in PpSWN and SmSWN overexpressors (PpSWN-OE and SmSWN-OE).

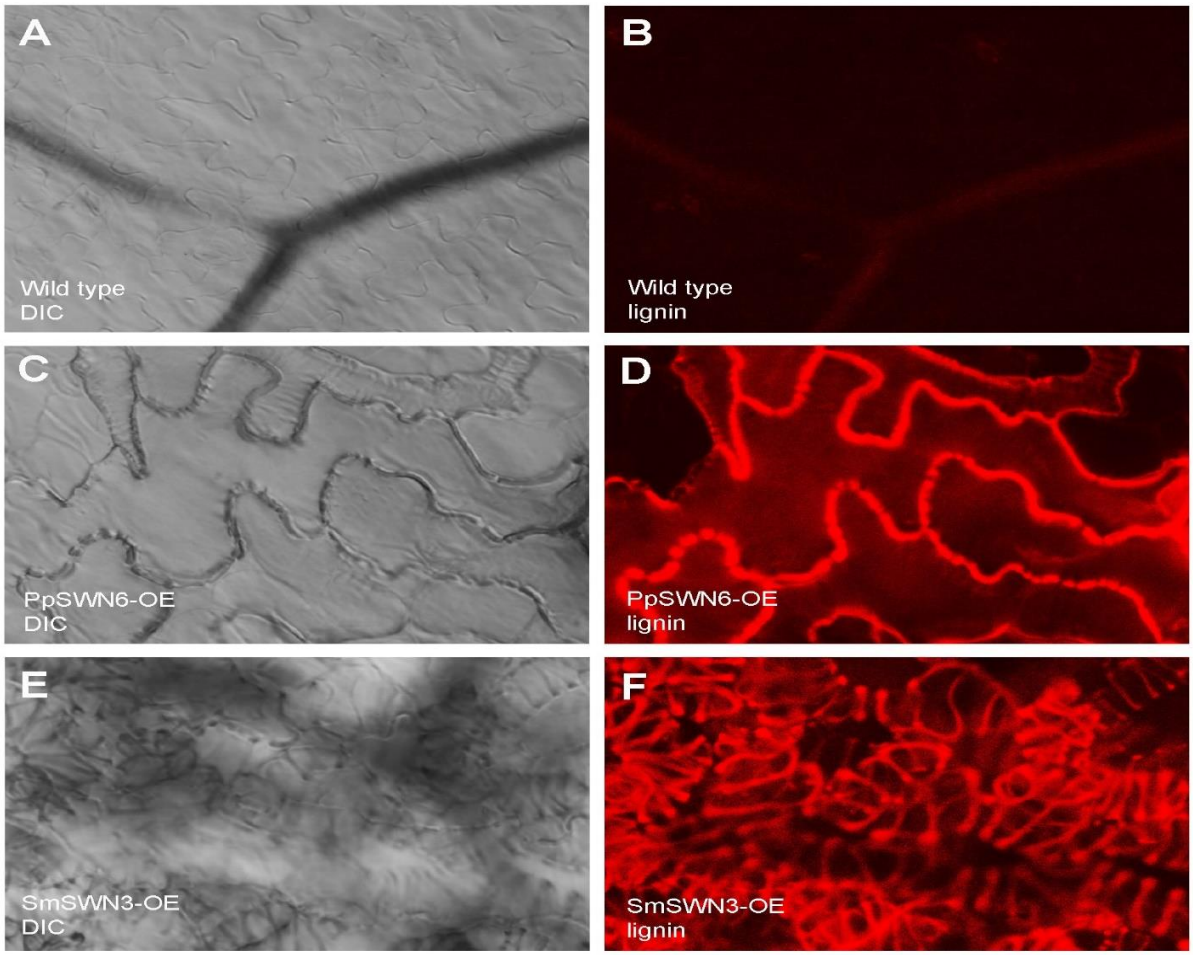

Figure 4. 5- Ectopic deposition of lignified secondary walls in leaf epidermal and mesophyll cells of PpSWN6 and SmSWN3 overexpressors. Leaves of 4-week-old PpSWN6-OE and SmSWN3-OE plants were examined for lignin autofluorescence under a UV light microscope. (A) Differential interference contrast (DIC) of a wild-type leaf showing jigsaw puzzle-shaped epidermal cells with thin walls. The thick gray lines were leaf veins underneath epidermal cells. (B) lignin autofluorescence image of the wild-type leaf in (A) showing the absence of lignin signals in epidermal cell walls. (C) and (D) Epidermal cells of a PpSWN6-OE leaf showing the ectopic secondary wall thickening (C) and lignin autofluorescence signals (D). (E) and (F) Mesophyll cells of a SmSWN3-OE leaf showing the helical secondary wall thickening (E) and lignin autofluorescence signals (F).

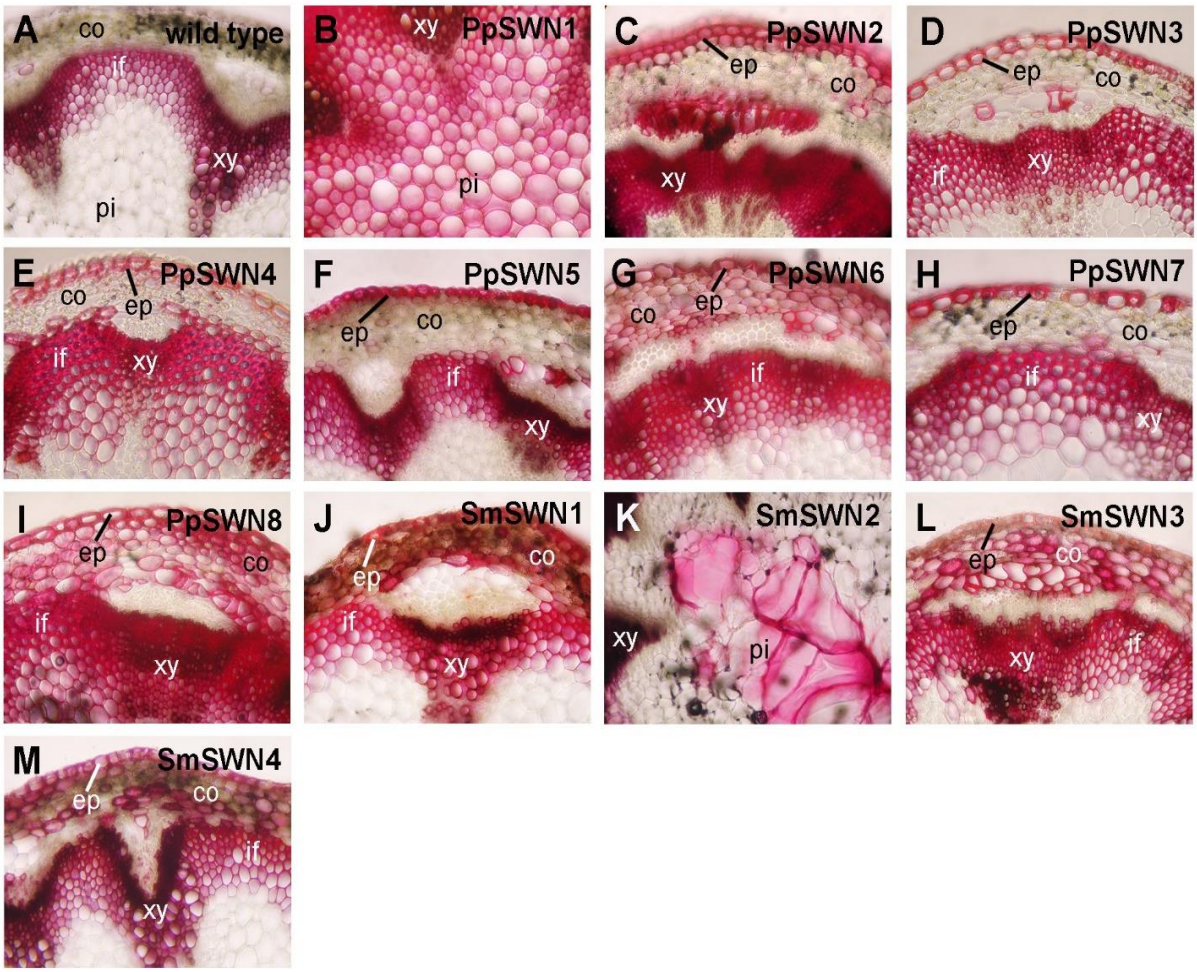

Figure 4. 6- Ectopic deposition of lignified secondary walls in epidermis, cortical and pith cells of PpSWN and SmSWN overexpressors. Inflorescence stems of 7-week-old PpSWN-OE and SmSWN-OE plants were stained for lignin with phloroglucinol-HCl. Lignified walls were only observed in interfascicular fibers and xylem cell walls in the wild type, whereas lignified, thick walls were evident in epidermal, cortical or pith cells in the stems of PpSWN-OE and SmSWN-OE. co, cortex; ep, epidermis; if, interfasciculer fiber; pi, pith; xy, xylem.

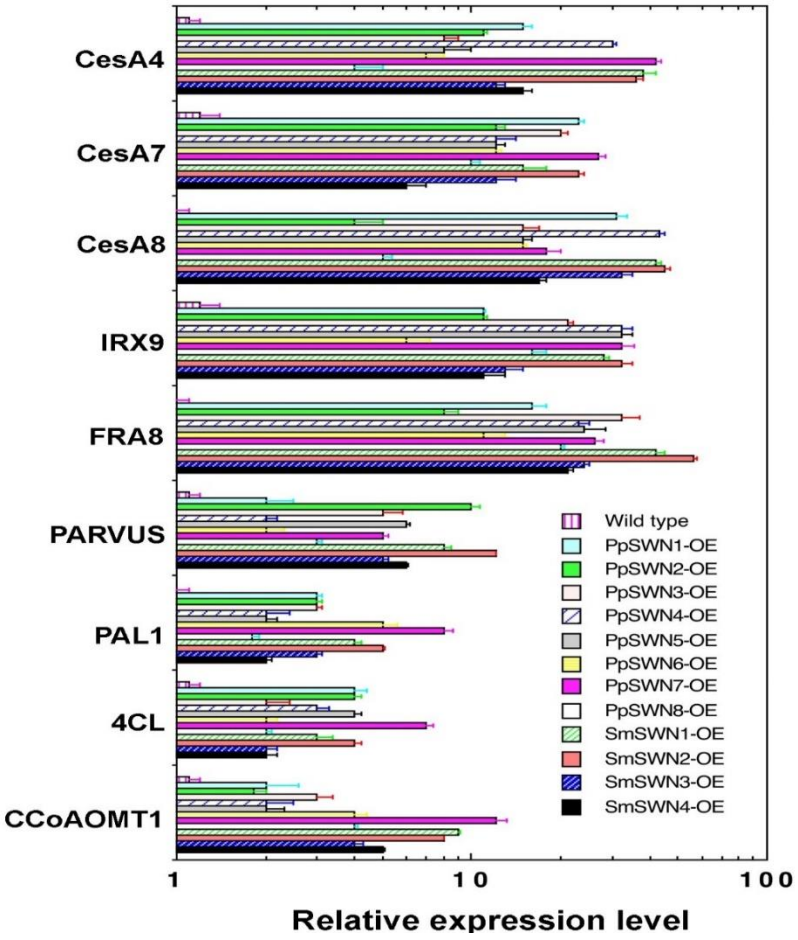

Figure 4. 7- Elevated expression of secondary wall biosynthetic genes for cellulose (*CesA4*, *CesA7* and *CesA8*), xylan (*IRX9*, *FRA8* and *PARVUS*) and lignin (*PAL1*, *4CL* and *CCoAOMT1*) in PpSWN-OE and SmSWN-OE. Total RNA isolated from leaves of 4-week-old plants was subjected to real-tile quantitative PCR for examination of the expression of secondary wall biosynthetic genes. The expression level of gene of interest in the wild type was set to 1. The data were the average of three biological replicates.

DISCUSSION

SND1, NSTs and *VNDs* have been characterized as master switches involved in transcriptional regulation in *Arabidopsis*, poplar and Eucalyptus (Zhong et al., 2010). Recently, a group of rice and maize NAC domain transcription factors (*OsSWNs* and *ZmSWNs*) have been identified as transcriptional master switches required for the activation of the entire secondary wall biosynthesis in grass species. The overexpression of *OsSWNs* and *ZmSWNs* in *Arabidopsis* are able to rescue the *snd1 nst1* double mutant and activate the secondary wall biosynthetic program due to the presence of an imperfect palindromic 19 bp consensus sequence designated as SNBE, (T/ANN(C/T)(T/C/G)TNNNNNNNA(A/C)GN(A/C/T)(A/T), in the promoters of their direct targets (Zhong et al., 2010; McCarthy et al., 2011). These results suggest that the DNA binding specificity of SWNs was conserved between dicots and monocots.

The evolution of vascular tissue was a gradual process in order to adapt to the terrestrial environment. Lacking true vascular tissue with lignified secondary cell walls is one of the most important properties of bryophytes. However, many bryophytes have water conducting cells with a secondary layer of primary cell wall material which undergo programmed cytoplasmic lysis, and can be considered as a precursor to vascular tissue in higher plants (Ligrone et al., 2000). Exploring the transcriptional network regulating secondary cell wall formation may reveal that a similar network is responsible for the vascular cell like formation in the water conducting cells of bryophytes. Previous studies on the evolutionary conservation of SNBE site distribution in the vascular plants demonstrated a significant enrichment of SNBE sites in gene promoters. However, the bryophyte *Physcomitrella patens* exhibited no enrichment, and this distinction may be the key evolutionary changes in vascular plants to form the vascular tissue with lignified secondary cell walls (McCarthy et al., 2011).

Our complementation analysis of *SmSWNs* and *PpSWNs* in *snd1 nst1 nst2* triple mutant plants has demonstrated that SmSWNs and PpSWNs are functional orthologs of *Arabidopsis* NAC transcription factors and are able to activate the secondary wall biosynthetic pathway. Overexpression of *SmSWN* and *PpSWN* genes in *Arabidopsis* has resulted in the ectopic deposition of secondary walls in the epidermis, cortical cells of the inflorescence stems and pith cells compared with the wild-type stems with the deposition of secondary walls only in interfascicular fibers and xylem cells. Our gene expression analysis has also revealed that the overexpression of the *SmSWN* and PpSWN genes is sufficient enough to activate the biosynthetic pathways for all three major components of the secondary walls. Thus, the findings from this study together with those from previous studies may propose that SWN-mediated transcriptional regulation of secondary wall formation evolved as early as land plants appeared.

MATERIALS AND METHODS

Phylogenetic analysis

The amino acid sequences of *S. moellendorffii* and *P. patens* SWNs were analyzed for their phylogenetic relationship with *Arabidopsis* SND1, NSTs and VNDs using the ClustalW program (Thompson et al. 1994), and the phylogenetic tree was shown using the MEGA6 program.

Complementation of Arabidopsis mutants

SmSWN and *PpSWN* full-length cDNAs were ligated into the XbaI site between the *SND1* promoter and the nopaline synthase terminator in the pGPTV binary vector, and introduced into the *Arabidopsis snd1nst1nst2* triple mutant (Zhong et al. 2007b) by *Agrobacterium*-mediated transformation (Bechtold and Bouchez 1994). The basal parts of stems were cut into 50 μm thick sections and then stained for lignin with phloroglucinol-HCl.

Overexpression

The full-length cDNAs of *S. moellendorffii* and *P. patens SWN* genes (the same primer sequences and engineered cloning sites as those used for complementation constructs) were inserted in the *Xba*I site downstream of the CaMV 35S promoter in a modified pBI121 to create the overexpression constructs. The constructs were introduced into wild-type *Arabidopsis* plant (ecotype Columbia) by *Agrobacterium*-mediated transformation. At least 64 transgenic plants were generated for each construct; 10 representative plants exhibiting severe phenotypes were used for phenotypic characterization and the representative results were presented. Leaf and stem tissues were fixed and sectioned for lignin staining. Lignin was examined by staining sections with phloroglucinol-HCl or visualized using a UV fluorescence microscope (Zhong et al. 2006).

Gene expression analysis

Total RNA from *Arabidopsis* tissues was isolated using a Qiagen RNA isolation kit. Quantitative PCR analysis was done using the first-strand cDNA as templates with the QuantiTect SYBR Green PCR Kit (Clontech). The PCR primers for the genes examined were described previously (Zhong et al. 2006, Zhou et al. 2009). The relative mRNA levels were determined by normalizing the PCR threshold cycle number of each gene with that of the *EF1α* reference gene. The expression level of each gene in the wild type was set to 1 and the data were the average of three biological replicates.

Statistical analysis

The experimental data of quantitative PCR measurement was subjected to statistical analysis using the Student's *t*-test program (http://www.graphpad.com/quickcalcs/ttest1.cfm).

REFERENCES

Demura, T. and Fukuda, H. (2007) Transcriptional regulation in wood formation, *TRENDS in Plant Sciences*, 12: 64-70.

Kubo, M., Udagawa, M., Nishikubo, N., Horiguchi, G., Yamaguchi, M., Ito, J., Mimura, T., Fukuda, H. and Demura, T. (2005) Transcription switches for protoxylem and metaxylem vessel formation. *Genes Dev* 19 (16):1855–60.

Ligrone, R., Duckett, J.G., and Renzaglia, K.S. (2000) Conducting tissues and phyletic relationships of bryophytes. *Phil. Trans. R. Soc. Lond. B.* 355:795-813.

McCarthy, R. L., Zhong, R., and Ye, Z.H. (2011) Secondary wall NAC binding element (SNBE), a key cis-acting element required for target gene activation by secondary wall NAC master switches, *Plant Signal Behav.* 6(9):1282-1285.

Mitsuda, N., Seki, M., Shinozaki, K. and Ohme-Takagi, M. (2005) The NAC transcription factors NST1 and NST2 of *Arabidopsis* regulate secondary wall thickenings and are required for anther dehiscence. *Plant Cell* 17:2993–3006 16.

Mitsuda, N., Iwase, A., Yamamoto H, Yoshida M, Seki, M., Shinozaki, K. and Ohme-Takagi, M. (2007) NAC transcription factors, NST1 and NST3, are key regulators of the formation of secondary walls in woody tissues of *Arabidopsis*. *Plant Cell* 19 (1):270–280.

Olsen, A.N., Ernst, H.A., Leggio, L.L. and Skriver, K. (2005) NAC transcription factors: structurally distinct, functionally diverse. *Trends Plant Sci* 10:79–87 7.

Shen, H., Yin, Y., Chen, F., Xu, Y. and Dixon R. A. (2009) A bioinformatics analysis of NAC genes for plant cell wall development in relation to lignocellulosic bioenergy production. *Bioenerg. Res.* 2:217-232.

Ye, Z-H (2002) Vascular tissue differentiation and pattern formation in plants, *Annual Review in Plant Biology*, 53: 183-202.

Zhao, C.S., Craig, J.C., Petzold, H.E., Dickerman, A.W. and Beers, E.P. (2005) The xylem and phloem transcriptomes from secondary tissues of the *Arabidopsis* root-hypocotyl. *Plant Physiol* 138:803–818 13.

Zhao, C., Avci, U., Grant, E.H., Haigler, C.H. and Beers, E.P. (2008) XND1, a member of the NAC domain family in *Arabidopsis* thaliana, negatively regulates lignocellulose synthesis and programmed cell death in xylem. *Plant J* 53:425–436 14.

Zhong, R., Taylor, J.J., and Ye, Z-H (1997) Disruption of interfascicular fiber differentiation in an *Arabidopsis* mutant. *Plant Cell* 9:2159-2170.

Zhong, R., Demura, T., and Ye, Z-H (2006) SND1, a NAC domain transcription factor, is a key regulator of secondary wall synthesis in fibers of *Arabidopsis*. *Plant Cell* 18:3158-3170.

Zhong, R., Richardson, E.A., and Ye, Z-H (2007) Two NAC domain transcription factors, SND1 and NST1, function redundantly in regulation of secondary wall synthesis in fibers of *Arabidopsis*. *Planta*, 225: 1603-1611.

Zhong, R., Lee, .C, Zhou, J., McCarthy, R.L. and Ye, Z.-H. (2008) A battery of transcription factors involved in the regulation of secondary cell wall biosynthesis in *Arabidopsis*. *Plant Cell* 20:2763–2782 12.

Zhong, R., Lee, C., and Ye, Z-H (2010) Evolutionary conservation of the transcriptional network regulating secondary cell wall biosynthesis, *TRENDS in Plant Sciences*, 15: 625-632.

Zhong, R., McCarthy, R.L., Lee, C., Ye, Z.-H. (2011) Dissection of the transcriptional program regulating secondary wall biosynthesis during wood formation in poplar. *Plant Physiol.* 157:1452-1468

Zhou, J., Lee, C., Zhong, R. and Ye, Z.-H. (2009) MYB58 and MYB63 are transcriptional activators of the lignin biosynthetic pathway during secondary cell wall formation in Arabidopsis. Plant Cell 21:248-266.

CHAPTER 5

CONCLUSSION

The plant cell wall is a complex structure that provides shape to individual cell and structural integrity or plasticity to tissues and organs. A thin, pectin-rich primary cell wall can be found in almost all cells whereas a thick secondary cell wall is laid down next to the primary cell wall in sclerenchyma cells. The secondary cell wall is composed of a framework of cellulose microfibrils associated with hemicelluloses such as xylan and lignin, a complex phenolic network (Scheller and Ulvskov, 2010). Xylan is the essential component of the secondary cell walls in *Arabidopsis* because mutations in xylan biosynthetic genes result in the collapsed xylem vessels and stunted plant growth (Wu et al., 2009).

Xylan polysaccharides are composed of a linear backbone of β-1, 4- linked xylosyl residues with a degree of polymerization (DP) of about 150 xyloses in *Arabidopsis* secondary cell walls and 1000-4000 in wheat endosperm (Freeman et al., 2015). It has been proposed that the 180^{o} inversion of each xylosyl residue with respect to each neighboring xylose in the linear structure of xylan backbone could be done either through repetitive addition of disaccharide unites (β-1, 4-linked xylose dimer) or by involvement of at least two enzymes with opposite catalytic sites (Carpita, 2011). Lee et al. (2010) suggested that *IRX9* and *IRX14* are strong candidates for such two glycosyltransferase activities involved in xylan backbone elongation because they are non-redundant in their functions. By the help of transcriptional profiling of genes specifically expressed in cells undergoing secondary cell wall deposition in *Arabidopsis* and poplar, candidate genes involved in xylan biosynthesis have been identified (Brown et al., 2005). Among those genes,

FRA8, IRX8, and PARVUS have been identified as three essential glycosyltransferases required for the reducing end sequence (Pena et al., 2007; Lee et al., 2007; Brown et al., 2007), while GUX1 and GUX2 in family GT8, two functionally redundant glycosyltransferases, are required for the substitution of glucuronic acid (GlcA) (Mortimer et al., 2010).

Previous studies revealed that the four GT43 members in the *Arabidopsis* genome including *IRX9*, *IRX9*L, *IRX14*, and *IRX14*L are essential for xylan backbone elongation. Lee at al. (2010) demonstrated that all these genes are expressed in interfascicular fibers and xylem cells in the inflorescence stems, and their encoded proteins are localized at Golgi where xylan is synthesized. In addition, the mutation of *IRX9* and *IRX14* results in a defect in the GX chain length and a reduction in the xylosyltransferase activity. Thus, *IRX9*/*IRX9*L and *IRX14*/*IRX14*L are two functionally non-redundant glycosyltransferases required for the normal elongation of xylan backbone. Xylan polysaccharides have been detected in non-vascular plants, such as mosses, and vascular plants. *Physcomitrella patens* and *Selaginella moellendorffii* genomes contain close homologs of a number of xylan biosynthetic genes including GT43 and GT47 members. Since the structure of xylan in *P. patens* and *S. moellendorffii* differs from *Arabidopsis* xylan due to lack of the reducing end sequence in both non-vascular and seedless vascular plants as well as no methylation of GlcA side chains in *P. patens* compared with fully methylated GlcA side chains in *S. moellendorffii*, it is necessary to investigate whether xylan biosynthetic genes are functionally conserved across different taxa of land plants.

Xylan structure of *P. patens* has been studied previously; however, it was little known about *S. moellendorffii* xylan structure. As an initial step to address our question, we employed ^{1}H-nuclear magnetic resonance (NMR) spectroscopy to analyze the structure of *S. moellendorffii* xylan. We extracted xylan from *S. moellendorffii* stems using both KOH and dimethyl sulfoxide

(DMSO). The study of KOH-extracted xylan revealed the similar NMR signals for the backbone [branched 4.62 ppm) and unbranched 4.46 ppm) xylosyl residues] and methylated GlcA (5.29 ppm) as *Arabidopsis* xylan, little signals for unmethylated GlcA (5.31 ppm), and no signals for the reducing end tetrasaccharide sequence. ^{1}HNMR analysis of DMSO-extracted xylan from *S. moellendorffii* stems revealed the presence of the characteristic resonances for acetyl groups around 2.2 ppm. Similar to *Arabidopsis* xylan, NMR signals for 2-O- and 3-O- monoacetylated, 2,3-di-O-acetylated, and 3-O-acetylated 2-O-GlcA-substituted xylosyl residues have been detected for *S. moellendorffii* xylan. Therefore, our structural analyses have demonstrated that *S. moellendorffii* xylan is composed of a β-1, 4-xylosyl residues backbone substituted with MeGlcA and acetylated at O-2 and O-3. Based on our studies of DUF579 genes in *S. moellendorffii* and *P. patens*, SmGXM is glucuronoxylan methyltransferase with a K_m value of 0.58 mM toward the (GlcA) Xly_4 acceptors. K_m value of SmGXM is 6.6 times lower than that of *Arabidopsis* GXM3/GXMT1 (3.85mM), that indicates a much higher substrate binding affinity of SmGXM than *Arabidopsis* GXM, which may contribute to the complete methylation of GlcA side chains in *S. moellendorffii* xylan. The only DUF579 gene in *P. patens* encodes a protein with no glucuronoxylan methyltransferase activity which is consistent with the previous observation of unmethylated xylan in *P. patens*. IRX15 and IRX15L are two *Arabidopsis* DUF579 proteins that do not show glucuronoxylan methyltransferase activity, but they are required for normal xylan biosynthesis. Since SmDUF579 in *S. moellendorffii* and PpDUF579 in *P. patens* did not exhibit the glucuronoxylan methyltransferase activity, it will be interesting to investigate whether they have similar functions as *Arabidopsis* IRX15 and IRX15L in xylan biosynthesis.

NMR analysis of DMSO-extracted xylan from *P. patens* revealed that similar to *Arabidopsis* and *S. moellendorffii* xylans, *P. patens* xylan is composed of a backbone of β-1, 4-

linked xylosyl residues substituted with only GlcA side chains and acetylated at O-2 and O-3. It has previously been shown that xylan from gymnosperms are not acetylated. This indicates that the ability to acetylate xylan seems to be evolved as early as land plants appeared, and this ability might be lost in the lineage of gymnosperms. The acetylation of xylan in *Arabidopsis* has been shown to be catalyzed by ESK1 and its close homologs from DUF231 protein family. *S. moellendorffii* and *P. patens* genomes harbor 16 and 17 DUF231 genes, respectively, and they are not phylogenetically grouped together with ESK1. Therefore, it will be interesting to investigate whether any of *S. moellendorffii* DUF231 genes are involved in xylan acetylation in *S. moellendorffii* in order to understand the evolution of xylan acetylation.

We have demonstrated that *Selaginella moellendorffii* and *P. patens* GT43 genes are functional orthologs of *Arabidopsis IRX9* and *IRX14*. Overexpression of *SmGT43A* and *SmGT43B* in *irx9* and *irx14* mutant plants, respectively could restore the rosette size and stem strength to the wild-type level and rescue the collapsed xylem vessels in the stem due to the restoration of GX level and xylosyltransferase activity. NMR and MALDI-TOF analyses revealed that the overexpression of *SmGT43A* and *SmGT43B* in *irx9* and *irx14* mutants, respectively, restored the signals for GlcA side chains in xylan. Because *SmGT43A*, close homolog of *IRX9,* could not complement *irx14* mutant and *SmGT43B*, close homolog of *IRX14*, was not able to rescue the *irx9* mutant phenotypes, we suggested that the involvement of two functionally non-redundant groups of GT43 in xylan biosynthesis is conserved throughout the vascular plants. In addition, only *PpGT43A* is a functional ortholog of *Arabidopsis IRX9*, and *PpGT43B*, another *IRX9* homolog, could partially complement the *irx9* mutant. Overexpression of *PpGT43C/D/E* was not able to complement *irx14* mutant and suggested that moss *IRX14* homologs might have diverged

significantly from *Arabidopsis IRX14* so that they could not interact with the partners of *Arabidopsis* xylan synthase complex and thus unable to rescue the *irx14* mutant phenotypes.

Proper deposition and assembly of cell walls components in each cell based on its function needs a precise regulation of a complex and dynamic genetic control involving a network of transcription factors acting as master switches for gene expression. *SND1, NSTs,* and *VNDs* have been identified as master switches of transcriptional regulation for all three major components of cell walls in *Arabidopsis* (Zhong et al., 2010). SND1 binds to secondary wall NAC binding elements (SNBE), an imperfect palindromic 19 bp consensus sequence (T/A)NN(C/T) (T/C/G)TNNNNNNNA(A/C)GN(A/C/T)(A/T), in the promoters of its direct targets and activates their expression (McCarthy et al., 2011). Close homologs of NAC transcription factors have been found in *P. patens* and *S. moellendorffii* genomes. Because *P. patens* is a non-vascular plant lacking true vascular tissues in its structure and no enrichment of SNBE sites in its gene promoters, we investigated whether *PpSWN* and *SmSWN* genes are functional orthologs of *SND1, NSTS,* and *VNDs*.

Overexpression of PpSWNs and SmSWNs was able to rescue the secondary wall defects in *Arabidopsis snd1 nst1 nst2* triple mutant. The pendent inflorescence stem and reduced stem strength were effectively rescued due to restoration of the formation of lignified secondary walls in fibers in the *snd1 nst1 nst2* mutant. In addition, overexpression of SmSWNs and PpSWNs in *Arabidopsis* resulted in ectopic deposition of lignified secondary walls in epidermis, cortical cells of inflorescence stem and pith cells compared with the wild-type stems in which secondary wall depositions was only seen in interfascicular fibers and xylem cells. Consistent with the ectopic deposition of secondary walls in PpSWN and SmSWN overexpressors, the expression of secondary wall biosynthetic genes for cellulose, xylan, and lignin was significantly elevated. These

results together demonstrate that *SmSWN* and *PpSWN* genes are functional orthologs of *SND1*, *NST1/2* and capable of activating the secondary wall biosynthetic pathways for all three major secondary wall component. Thus, it seems that SWN-mediated transcriptional regulation of secondary wall formation evolved as early as land plants appeared.

CO2 emission due to burning fossil fuels for heat, electricity, and transportation is one of the main factors leading to climate change, which is an increasing problem. To reduce or eliminate CO_2 emission, alternative energy sources are being heavily sought and plant biomass is considered to be a promising avenue to provide an abundant, renewable source for biofuel production. However, the complex structure of xylan because of the addition of different side chains makes it one of the factors contributing to biomass recalcitrance for biofuel production. By forming a physical barrier, xylan blocks cellulolytic enzymes from hydrolyzing cellulose to fermentable sugars. Enzymatic degradation of xylan into xylose, which could be potentially used for fermentation into ethanol, is difficult because the various substitutions in xylan negatively impact the process of digestion. In addition, the acetyl groups released from xylan in form of acetate during pre-treatments of biomass for converting cellulosic biomass into biofuels inhibit microorganisms used for sugar fermentation (Helle et al., 2003). Therefore, deciphering the molecular and biochemical mechanisms controlling secondary wall biosynthesis is crucial and will potentially provide tools for genetic modification of cell wall composition in biofuel crops and design novel strategies to genetically modify wall composition better suited for biofuel production.

REFERENCES

Brown, D.M., Zeef, L.A.H., Ellis, J., Goodacre, R., and Turner, S.R. (2005). Identification of novel genes in *Arabidopsis* involved in secondary cell wall formation using expression profiling and reverse genetics. *Plant Cell* 17: 2281–2295.

Brown, D.M., Goubet, F., Wong, V.W., Goodacre, R., Stephens, E., Dupree, P., and Turner, S.R. (2007). Comparison of five xylan synthesis mutants reveals new insight into the mechanisms of xylan synthesis. *Plant Journal*, 52:1154-1168.

Carpita, N.C. (2011). Update on Mechanisms of Plant Cell Wall Biosynthesis: How Plants Make Cellulose and Other (1→4)-β-d-Glycans. *Plant Physiol*. 155: 171-184.

Freeman, J., Lovegrove, A., Wilkinson, M. D., Saulnier, L., Shewry, P. R., and Mitchell, R. A. (2015) Effect of suppression of arabinoxylan synthetic genes in wheat endosperm on chain length of arabinoxylan and extract viscosity. *Plant Biotechnol. J.* doi:10.1111/pbi.12361.

Helle, S., Cameron, D., Lam, J., White, B., and Duff, S. (2003). Effect of inhibitory compounds found in biomass hydrolysates on growth and xylose fermentation by a genetically engineered strain of S. cerevisiae. *Enzyme Microb. Technol*. 33: 786–792.

Lee, C., Zhong, R., Richardson, E.A., Himmelsbach, D.S., McPhail, B.T. and Ye, Z.-H. (2007) The *PARVUS* gene is expressed in cells undergoing secondary wall thickening and is essential for glucuronoxylan biosynthesis. *Plant Cell Physiol.* 48: 1659-1672.

Lee, C., Teng, Q., Huang, W., Zhong, R. and Ye, Z.-H. (2010) The *Arabidopsis* family GT43 glycosyltransferases form two functionally nonredundant groups essential for the elongation of glucuronoxylan backbone. *Plant Physiology*, 153: 526–541.

McCarthy, R. L., Zhong, R., and Ye, Z.H. (2011) Secondary wall NAC binding element (SNBE), a key cis-acting element required for target gene activation by secondary wall NAC master switches, *Plant Signal Behav.* 6(9):1282-1285.

Mortimer, J.C., Miles, G.P., Brown, D.M., Zhang, Z., Segura, M.P., Weimar, T., Yu, X., Seffen, K.A., Stephens, E., Turner, S.R., and Dupree, P. (2010). Absence of branches from xylan in *Arabidopsis* mutants reveals potential for simplification of lignocellulosic biomass. *Proc Natl Acad Sci U S A.* 107(40):17409-14.

Peña, M.J., Zhong, R., Zhou, G.-K., Richardson, E.A., O'Neill, M.A., and Darvill, A.G. (2007) *Arabidopsis*irregular xylem8 and irregular xylem9: implications for the complexity of glucuronoxylan biosynthesis. *Plant Cell*. 19: 549–563.

Scheller, H.V. and Ulvskov, P. (2010) Hemicelluloses. *Annu. Rev. Plant Biol.*16: 263-289.

Wu, A-M, Rihouey, C., Seveno, M., Ho¨rnblad, E., Singh, S.K., Matsunaga, T., Ishii, T., Lerouge, P., and Marchant, A. (2009) The *ArabidopsisIRX10* and *IRX10*-LIKE glycosyltransferases are critical for glucuronoxylan biosynthesis during secondary cell wall formation. *Plant Journal*, 57: 718-731.

Zhong, R., Lee, C., and Ye, Z-H (2010) Evolutionary conservation of the transcriptional network regulating secondary cell wall biosynthesis, *TRENDS in Plant Sciences*, 15: 625-632.